Control Analysis of Mixed Populations of *Gluconobacter oxydans* and *Saccharomyces cerevisiae*

by
Christiaan Johannes Malherbe

Dissertation presented for the degree of Doctor of Philosophy in the Faculty of Science at the University of Stellenbosch

Promoter: Prof Jacob L. Snoep
Co-promoter: Prof. Johann M. Rohwer
Faculty of Science
Department of Biochemistry

December 2010

Declaration

By submitting this dissertation electronically, I declare that the entirety of the work contained therein is my own, original work, and that I have not previously in its entirety or in part submitted it for obtaining any qualification.

November 17, 2010

Abstract

In the last decade a need arose to find a theoretical framework capable of gaining a quantitative understanding of ecosystems. Control analysis was proposed as a suitable candidate for the analysis of ecosystems with various theoretical applications being developed, i.e. trophic control analysis (TCA) and ecological control analysis (ECA). We set out to test the latter approach through experimental means by applying techniques akin to enzyme kinetics of biochemistry on a simple ecosystem between *Saccharomyces cerevisiae* and *Gluconobacter oxydans*. However, this exercise was far more complex than we originally expected due to the extra metabolic activities presented by both organisms.

Nevertheless, we derived suitable kinetic equations to describe the metabolic behaviour of both organisms, with regards to the activities of interest to us, from pure culture experiments. We developed new techniques to determine ethanol and oxygen sensitivity of *G. oxydans* based on its obligately aerobic nature. These parameters were then used to build a simple kinetic model and a more complex model incorporating oxygen limited metabolism we observed at higher cell densities of *G. oxydans*. Our models could predict both situations satisfactorily for pure cultures and especially the more complex model could describe the lack of linearity observed between metabolic activity and cell density at higher cell densities of *G. oxydans*.

Mixed populations of *S. cerevisiae* and *G. oxydans* reached quasi-steady states in terms of ethanol concentration and acetate flux, which was a positive indication for the application of control analysis on the ecosystem. However, the theoretical models based on parameters derived from pure culture experiments did not predict mixed culture steady states accurately. Careful analysis showed that these parameters were mostly under-estimated for *G. oxydans* and overestimated for *S. cerevisiae*. Hence, we calculated the kinetic parameters for mixed population assays directly from the experimental data obtained from mixed cultures. We could calculate the control coefficients directly from the experimental data of mixed population studies and compare it with those from theoretical models based on 3 different parameter sets. Our analysis showed that the yeast had all the control over the acetate flux while control over the steady-state ethanol was shared.

The strength of our approach lies in designing our experiments with a control analysis approach in mind, but we have also shown that even for simple ecosystems this approach is non-trivial. Despite

the various experimental challenges, this approach was very rewarding due to the extra information obtained especially regarding control structure with regards to the steady-state ethanol concentration.

Uittreksel

In die afgelope dekade het daar ’n behoefte ontstaan na ‘n teoretiese raamwerk om tot ‘n kwantitatiewe begrip van ekosisteme te kom. As kandidaat vir so tipe raamwerk is kontrole analise voorgestel gepaardgaande met die ontwikkeling van verskeie teoretiese toepassings, i.e. trofiese kontrole analise en ekologiese kontrole analise. In hierdie tesis het ons laasgenoemde aanslag eksperimenteel ondersoek op ‘n eenvoudige ekosisteem, tussen *Saccharomyces cerevisiae* en *Gluconobacter oxydans*, deur gebruik te maak van tegnieke vanuit ensiemkinetika van biochemie. Hierdie strategie was egter baie meer kompleks as wat oorspronklik verwag is as gevolg van verdere metabolise aktiwiteite aanwesig in beide organismes.

Ons het egter steeds daarin geslaag om kinetiese vergelykings af te lei, vanuit suiwer kulture, wat die metaboliese gedrag van beide organismes beskryf vir die aktiwiteite van belang vir ons studie. Ons het nuwe tegnieke, gebaseer op die aerobiese natuur van *G. oxydans*, ontwikkel om die sensitiwiteit van *G. oxydans* vir etanol en suurstof te bepaal. Hierdie parameters is gebruik om eers ’n eenvoudige model en toe ‘n meer gevorderde model, wat die suurstof-beperkte metabolisme van *G. oxydans* by hoër biomassa te beskryf, op te stel. Beide modelle was baie effektief in die voorspelling van die situasies waarvoor hulle ontwikkel is vir die suiwer kulture waar veral die meer gevorderde model die gebrek aan ‘n linieêre verband tussen die metabolisme van *G. oxydans* en biomassa by hoër biomassa kon beskryf.

’n Bemoedigende aanduiding dat kontrole analise toegepas kon word op die ekosisteem was dat mengkulture van *S. cerevisiae* en *G. oxydans* het quasi-bestendige toestande bereik het in terme van etanol konsentrasies en asetaat-fluksie. Die teoretiese modelle gebaseer op die parameters afgelei vanaf suiwer kulture kon egter nie die bestendige toestande in mengkulture akkuraat voorspel nie. Nadere ondersoek het aangedui dat die parameters meesal onderskat is vir *G. oxydans* en oorskat is vir *S. cerevisiae*. Gevolglik het ons die kinetiese parameters vir mengkulture direk van eksperimentele data van die mengkulture bereken. Verder kon ons die kontrole koeffisiente ook direk vanaf die eksperimentele data van mengkulture bereken en vergelyk met dié bereken vanuit die teoretiese modelle gebaseer op drie verskillende paremeter-stelle. Ons analise het gewys dat die gis alle beheer op die asetaat-fluksie uitoefen en dat die beheer oor die etanol-konsnetrasie gedeel is tussen die twee organismes.

Die krag van ons aanslag lê daarin dat die eksperimente ontwerp is met ‘n kontrole analise in gedagte, maar ons het ook bewys dat hierdie aanslag selfs vir eenvoudige ekosisteme nie triviaal is nie. Ten spyte van die eksperimentele uitdagings, was die aanslag baie waardevol as gevolg van die ekstra inligting verkry met spesifieke klem op die kontrole-struktuur met betrekking tot die etanol konsentrasie by bestendige toestand.

Dedication

with love to Cornelia and Lira

Acknowledgements

National Research Foundation, the *Harry Crossley Trust* and the *Stellenbosch University merit bursary* for funding.

Department of Biochemistry, Stellenbosch University:
Prof. Jacky Snoep for allowing me to develop into an independent researcher and always challenging me to strive towards a deeper understanding of anything I investigate. A special thanks for your patience during the last long stretch of writing this dissertation.

Prof. Johann Rohwer for most valued critique and assistance during crucial moments of the upgrading process and the final preparation of this dissertation. Your knowledge and insight into the theory of control analysis is a constant inspiration.

Prof Jannie Hofmeyr for your enthusiasm and especially that one very inspirational conversation at the Charles de Gaul international airport. You brought my focus back and your enthusiasm for research is infectious.

Ari Arends for so many motivational conversations and support throughout this project. Your humility, integrity and friendship have always motivated me to better myself.

Arno Hanekom, *Lafras Uys* and *Du Toit Schabort* for discussions, explanations and patience during the time spent in the same laboratory. Your willingness to help, give advice and share made the time memorable.

Riaan Conradie and *Franco du Preez*, the enthusiastic students that became friends and then Ph. D's. Always willing to help and answer questions, always curious and enthusiastic about research. When I needed a boost, your optimism always brought me back onto the right track.

My Infruitec-family:
Prof. Lizette Joubert who believed in me when I did not. I am indebted to you .You have done so much for me. You are always a willing ear with real life-advice, a true scientific spirit and ambition to strive ever higher. You employed me and took me into your team without knowing how it would turn out.

Dr. Dalene de Beer who works so hard and still could find ways of picking up my slack when I had to take study leave. How you get the time to do everything you do and still find time to review articles, supervise students and do your own laboratory work is amazing. I cannot thank you enough.

Dr. Chris Hansman for always encouraging me and whose innovative mind, across a multitude of disciplines, is a constant inspiration.

Dr. Ockert Augustyn for many inspiring conversations and encouraging me with your enthusiasm for research.

My remaining friends:
Norbert and *Gisela Kolar*, a very hard working couple who has shown me that respect for each other is not negotiable. So many conversations during rugby matches, coffee breaks and moderate amounts of the amber fluid can never be repaid. Your friendship has never wavered through some of the most difficult times over the past years.

Maikel Jongsma, my best friend. We started out together in the same laboratory and just clicked. Through the years the humour might have become less, but your loyal friendhips and support remained. A true friend.

Tyrone Genade for being such an example of a Christian researcher, asking questions, having opinions, but always believing and seeing God's hand in everything.

Brylea Slawson, my prayer buddy, for perspective in a dark time. Your faith and prayers has led me back to life when I could not find/trust my own way.

Heidi Winterberg Andersen, my "ghuru". You showed me how to approach research, reports and develop methods. In between all that we became friends, laughed a lot and drank liters and liters of coffee.

Hannelie Naudé, for being a good friend, your loyal support, lifely discussions and taking babysitting in your stride.

My family:

Cornelia, my beloved wife, my friend and lifeline. My constant link with reality, my rock, my love. Thank you for your patience, help, support and always being there. You held on when I needed an anchor – thank you.

Lira, my little warrior princess. You make every day worthwhile with your inquisitive nature and sharp sense of humour. Thank you for loving your old dad no matter what.

My ouers, baie dankie vir alles. Julle het baie opgeoffer om my tot hier te kry en ek waardeer dit opreg.

Cornelia se ouers, baie dankie vir die ondersteuning deur die jare.

Elmien en *Roeloff*, my broer en suster. Julle het deur die jare die voorbeeld geword waarna ek kon streef. Dankie daarvoor.

Content

List of Figures

List of Tables

Abbreviations

Acet	Acetate
ADH	alcohol dehydrogenase
ALDH	acetaldehyde dehydrogenase
ATP	adenosine tri-phosphate
BST	biochemical systems theory
^{13}C	carbon-13 isotope
CDFF	constant depth film fermentor
CO_2	carbon dioxide
C-matrix	control matrix
Cyt c	cytochrome c
Cyt o	cytochrome o
DHA	dihydroxyacetone
ECA	ecological control analysis
e^-	Electron
E-matrix	elasticity matrix
EtOH	Ethanol
FAD-dependant	flavin-dependent
FBA	flux-balance analysis
G3P	glycerol-3-phosphate
Glc	Glucose
G.o.	*Gluconobacter oxydans*
GYC-medium	Glucose, yeast extract, calcium carbonate medium
H^+	hydrogen ion / proton
H^+ ATPase	hydrogen-adenosine tri-phosphatase
H_2O	Water
HCA	hierarchical control analysis
HPLC	High performance liquid chromatography
J	Flux
I-matrix	identity matrix
k_1	specific activity of *S. cerevisiae* for ethanol production
k_2	specific activity of *G. oxydans* for ethanol consumption
k_3	specific activity of *G. oxydans* for acetate production
k_4	specific activity of *G. oxydans* for gluconate production

k_5	specific activity of *S. cerevisiae* for glucose consumption
k_6	specific activity of *S. cerevisiae* for glycerol production
k_7	specific activity of *S. cerevisiae* for oxygen consumption
k_9	specific activity of *G. oxydans* for oxygen consumption
$K_L a$	mass transfer coefficient of aeration funnels
K_M	Michaelis-constant
K_S	Monod-constant
K_x	Monod-constant for ethanol of *G. oxydans*
K_o	Monod-constant for oxygen of *G. oxydans*
MCA	metabolic control analysis
MES	2-[N-morpholino]-ethanesulphonic acid
NAD/H	nicotinamide adenine dinucleotide / reduced
NADP/H	Nicotinamide adenine dinucleotide phosphate / reduced
O_2	oxygen molecule
o(t)	oxygen concentration in formulae
ODE	ordinary differential equation
PQQ	pyrroloquinoline quinone
PVDF	polyvinylidene fluoride
q	metabolic quotient
Q_8	ubiquinone-8
Q_9	ubiquinone-9
Q_{10}	ubiquinone-10
s_1	*Saccharomyces cerevisiae* concentration in formulae
s_2	*Gluconobacter oxydans* concentration in formulae
S.c.	*Saccharomyces cerevisiae*
stst	affix, in subscript, indicating steady-state conditions
TCA	trophic control analysis
TCA-cycle	Tricarboxylic acid cycle
UQH_2	ubiquinol
UV	ultra-violet
v_1	ethanol production rate of *S. cerevisiae*
v_2	ethanol consumption rate of *G. oxydans*
v_3	acetate production rate of *G. oxydans*
v_4	gluconate production rate of *G. oxydans*
v_5	glucose consumption rate of *S. cerevisiae*

v_6	glycerol production rate of *S. cerevisiae*
v_7	respiration rate of *S. cerevisiae*
v_8	oxygen transfer rate of aeration funnels
v_9	respiration rate of *G. oxydans*
v_{10}	oxygen dependent ethanol consumption rate of *G. oxydans*
v_{11}	oxygen dependent acetate production rate of *G. oxydans*
v_{12}	oxygen dependent gluconate production rate of *G. oxydans*
V_{max}	maximal enzymic / organismic rate
YE	yeast extract
YPD-medium	yeast extract, peptone, dextrose medium
x(t)	ethanol concentration in formulae
y(t)	acetate concentration in formulae
z(t)	gluconate concentration in formulae

Prologue

Motivation and aim of research

Modelling of ecological systems and sensitivity analysis of the resulting models are not novel concepts, but a generalised theory for the analysis of these systems and models has been lacking (*1-3*). Recently, a start with the development of such a common theory was made with the publication of three articles probing the possibility of using a theory analogous to Metabolic Control Analysis (MCA) for the investigation of ecosystems, Ecological Control Analysis (ECA) (*4-6*). In these publications it is stressed that the framework of hierarchical control analysis (HCA) is probably more suited as the basis for ecological control analysis. Such a hierarchical analysis makes it possible to include variation in the quantity of the processes, i.e. variation in species densities due to growth and environmental effects, which would typically be modelled as constant in MCA (e.g. constant expression level of enzymes in metabolic system). For an excellent review on HCA, I refer the reader to (*7*), while (*8*) applies HCA to glycolysis in three different species of parasitic protists. Recently, Roling *et al* harvested experimental data from the literature for an ecosystem with constant biomass concentrations under non-growing conditions, and used the much simpler MCA approach for the analysis (*6*). It is unlikely that many ecosystems will have constant biomass concentrations for all species, for instance in trophic chains the interactions between the species will necessarily lead to variations in species densities (*3*).

In this study, our aim was to test the feasibility of experimentally applying the theoretical framework of MCA to a simple ecosystem. Our goal was to quantitify the importance of species in such a simple ecosystem, using a combined experimental, modelling and theoretical approach. We tried to select an ecosystem as simple as possible, such that we could make specific perturbations to the system and quantify the effects on the system behaviour. Therefore we chose a non-growing environment, and focused on two species that interact via a common intermediate. This would allow us to use MCA as the analysis method. Although our aims appear to be modest, it should be realized that such an analysis has never been carried out before.

We chose the acidification of wine as the process on which we would focus. In wine-fermentations, most of the ethanol is produced by *Saccharomyces cerevisiae* during the stationary phase of growth

with a quantitative conversion of glucose to ethanol (*9*). Under aerobic conditions, acetic acid bacteria, such as *Gluconobacter oxydans*, can spoil the wine by converting the ethanol produced by *S. cerevisiae* to acetic acid. Acetic acid bacteria are already present on the grapes when on the vine and it is not unreasonable to assume that interaction between the yeasts and acetic acid bacteria can occur before industrial fermentation commences, so one could consider these two organisms forming a very simple ecosystem (*9-13*). Such a simple ecosystem, also found in orange juice, has many similarities to metabolic pathways found in all living systems (*14, 15*). Whereas in metabolic pathways and in metabolic control analyses of such systems the enzymes are seen as catalysts, for the acidification of wine we could see the microorganisms as catalysts. Whereas in metabolic systems reactions are often grouped together, we could treat a complete organism as a black box and use the same theoretical framework for the analysis (*16-18*).

Structure of thesis

Chapter 1 gives a brief literature review on the major components of the study, i.e. the ecosystem and its constituents, ecological modelling and its development, Control analysis of linear enzymatic pathways and drawing an analogy to ecosystems in more detail.

In Chapter 2 the experimental techniques are discussed that are applied to the research problem with emphasis on fermentation and assay techniques as well as brief discussions on sample analysis.

Chapter 3 details the results for single and mixed population studies and the determination of parameters used in the theoretical models. The theoretical models are described that are used to simulate the interaction between *S. cerevisiae* and *G. oxydans* starting with a simple core model that was developed to incorporate the aerobic nature of *G. oxydans*. This Chapter also includes results showing the fit of the model on the data as derived from mixed population assays. Control analysis of the sample ecosystem is described by presenting several strategies applied to the experimental data directly, as well as the derivation of the control structure from the models presented.

In Chapter 4 the results and theoretical model are discussed and a final viewpoint on the scope of the presented research with regard to ecology and theoretical modelling is given.

Chapter 1

1. Literature Review

1.1. The Ecosystem

The simple ecosystem under investigation is responsible for the spoiling of wine and the production of vinegar, i.e. the interaction between *S. cerevisiae* and *G. oxydans* in Figure 1.1 (*12*). It is appropriate to first discuss each organism with emphasis on physiology and industrial importance.

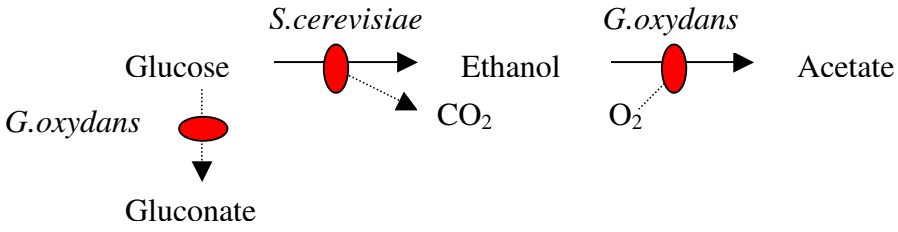

Figure 1.1 Schematic representation of the ecosystem under discussion

1.1.1 *Gluconobacter oxydans*

Gluconobacter, an obligately aerobic Gram-negative bacterium, together with the genus *Acetobacter*, is classified under the family *Acetobacteraceae*. Up to the 1930's *Gluconobacter* was classified within the genus *Acetobacter* and before that as an *Acetomonas* species due to its inability to oxidize acetate (*9, 13, 19*). In 1935, Asai devised a new phylogeny for acetic acid bacteria, and *Acetobacter oxydans* was renamed to *G. oxydans* (*9, 19, 20*). This new classification created clear distinction between the *Gluconobacter*, with a higher affinity for sugar, and its family member *Acetobacter* with its preference for alcohol (*20, 21*). *G. oxydans* has received significant scientific interest; its genome has been sequenced and several patents exist for the isolation of some of its more industrially applicable enzymes (*22-26*). Unlike *Acetobacter* species, *Gluconobacter* does not contain a complete tricarboxylic acid cycle (TCA-cycle) (*11, 27-29*). According to Prust *et al*, the genome of *G. oxydans* contains the complete set of genes for the Entner-Doudoroff pathway, but actual proof of an operating Entner-Doudoroff pathway has not yet been presented (*19, 22, 28, 29*). Furthermore, several transporters for substrates into the cytoplasm have been discovered, e.g. an ABC-transporter for sugars and sugar acids, facilitator proteins for glycerol and several other permeases (*22*).

The industrial interest for *G. oxydans* lies in its incomplete oxidation of sugars and alcohols. Many of the dehydrogenases responsible for these incomplete oxidations are membrane bound, pyrroloquinoline quinone (PQQ)-dependent, containing ubiquinone-10 (Q10) as electron acceptor, unlike other Gram-negative bacteria, e.g. Acetobacter, that utilise Q-8 or Q-9 (*22, 28-32*). They also contain flavin-dependent dehydrogenases (FAD-dependent) which, together with the PQQ-dependent dehydrogenases, are coupled to a membrane-bound respiratory chain exclusively utilizing *cytochromes c* and *o* with oxygen as the final electron acceptor (*28, 30*). Through the direct coupling of the PQQ- and FAD-dependent dehydrogenases with the electron transport chain, a conserved cycle evolved where ubiquinone gets reduced to ubiquinol which is then oxidized to ubiquinone through cytochrome bo_3 ubiquinol oxidases (*9, 19, 21, 22, 28, 29, 32, 33*). These membrane-bound dehydrogenases are seated within the cell membrane with their enzymatic active sites directed into the periplasmic space. Their substrates and products enter and leave the periplasmic space through porins in the cell membrane connecting the periplasm with the extra-cellular media (*22, 23*). Furthermore, the pentose-phosphate pathway, strictly driven towards the production of NADPH with the emphasis on reduction power and not ATP-production, is involved in the oxidation of sugars and alcohols that enter the cytoplasm through the permeases, transporters and facilitator proteins mentioned above (*22, 34*). See Figure 1.2 for a schematic summary of the oxidative metabolism of *G. oxydans* with regard to the sugars and alcohols of interest to the current project and discussed in the following paragraphs.

G. oxydans oxidizes glucose to gluconate through a combination of these two pathways, directly through the membrane-bound PQQ-dependent glucose-oxidases or in combination with its cytoplasmic oxidative pentose-phosphate pathway containing NADP-dependent glucose dehydrogenases (*35*). PQQ-dependent glucose oxidases have reaction rates of about 30 times faster than those of their cytoplasmic counterparts (*29*). Basseguy *et al.* observed a stoichiometry of half a mole of oxygen consumed for every mole of gluconate produced from glucose by these membrane-bound glucose oxidases (*36*). Gluconate is then further converted to either 2-keto-gluconate or 5-keto-gluconate by the flavin-dependent membrane-bound 2-keto-gluconate dehydrogenases and PQQ-dependent 5-keto-gluconate dehydrogenases, respectively (*19, 35*). Eventually, both pathways lead to the production of 2,5-diketo-gluconate as end product. At low pH (< 3.5) and glucose concentrations above 15mM, the pentose phosphate pathway is repressed and only the membrane-bound dehydrogenases are responsible for the oxidation of glucose to its keto-acids (*11, 37*). Furthermore, oxidation of glucose to gluconate is optimal at pH 5.5 while the oxidation of

gluconate to keto-acids is optimal at pH 3.5. This has implications for a buffered system at higher pH, i.e. pH 6, and saturating glucose-concentration, above 300 mM, since an accumulation of gluconate will be observed with a smaller amount of keto-acids accumulating over time due to a markedly slower activity of the gluconate- and keto-gluconate dehydrogenases relative to the glucose dehydrogenases at this pH and glucose concentration above 10 mM (*13, 38*).

In addition, *G. oxydans* contains two membrane-bound dehydrogenases of great importance for the current project, i.e. PQQ-dependent alcohol-dehydrogenase (ADH) and acetaldehyde dehydrogenase (ALDH) that produce acetate from ethanol in two enzymic steps. ADH has also been postulated to mediate electron transfer by the PQQ-dependent glucose dehydrogenases and is linked to the reduction of ubiquinone (*33*). Membrane-bound ADH have been isolated and found to contain three subunits with subunit II being homologous to cytochrome *c* of its electron transport chain (*33, 39*). However, soluble NADP-dependent versions of ADH and ALDH are also present within the cytoplasm (*22, 32*). These cytoplasmic enzymes are believed to be important in the maintenance of cells in stationary phase due to their participation in the synthesis of biosynthetic precursors (*32*). *G. oxydans* does not have the ability to oxidize acetic acid and therefore one expects complete conversion from ethanol to acetic acid by this organism (*11, 20, 32*).

Of minor importance to our current project, due to the involvement of *S. cerevisiae*, glycerol is also metabolized by *G. oxydans*. Membrane-bound glycerol dehydrogenases convert glycerol to dihydroxyacetone with the resultant reduction and oxidation of ubiquinone through their direct links with the electron transport chain (*40, 41*). However, in the cytoplasm glycerol is converted to dihydroxyacetone phosphate by the soluble glycerolkinases and glycerol-3-phosphate dehydrogenases (G3P-dehydrogenases) working in tandem (*27, 42*). In the current study, only small amounts of glycerol are produced by *S. cerevisiae* with estimated dihydroxyacetone levels well below the toxic limits (*43*).

In nature, *G. oxydans* can be found on grapes and will therefore also be present in the wine must since it still contains high sugar levels (*13, 21*). During must fermentation, the presence of *G. oxydans* declines relative to *Acetobacter* species due to its preference for sugar-rich environments, but there is still a considerable level of *G. oxydans* present in wine since the two organisms have similar ethanol tolerance (*11*). Therefore, it is logical that *G. oxydans* will also be present in

unfiltered wine fermentations, where they were shown to be able to grow in the presence of *S. cerevisiae*, and could also infect and acetify filtered wine (*13, 44*).

Even though *G. oxydans* oxidizes ethanol at a slower rate than *Acetobacter*-species, both organisms are suited to vinegar production with the gluconate produced by *G. oxydans* seen as an advantage to the flavour of high quality vinegars (*11, 21, 28, 32*). However, the rate of acetic acid production by acetic acid bacteria in wine is normally relatively low due to lack of aeration and most of the acetate is produced by a thin film of bacteria forming on the surface of the wine (*11, 13, 21*). During a controlled wine fermentation, acetification should not occur due to the thick layer of carbon dioxide (CO_2) forming on top of the surface of the fermentation vessel, but any disturbance of this layer due to pumping will cause aeration and result in acetification (*11-13, 21, 44*).

As mentioned before, the major differences between *Gluconobacter* and *Acetobacter* species are the inability of *Gluconobacter* to oxidize acetate to CO_2 and water, and its preference for sugars above ethanol as carbon source (*11, 19, 29*). Furthermore, due to its "wasteful" process of membrane-bound incomplete oxidations, *G. oxydans* is incapable of rapid growth, or even high cell densities, with its direct oxidase activity often greater in non-growing cells (*28, 32*). Growth is also dependent on certain essential vitamins that can be supplied by including yeast extract in the culture medium (*11, 19*). *G. oxydans* are also highly dependent on dissolved oxygen concentration, thus providing optimal aeration increases the growth densities whilst inducing the membrane-bound PQQ-dependent dehydrogenases (*28*).

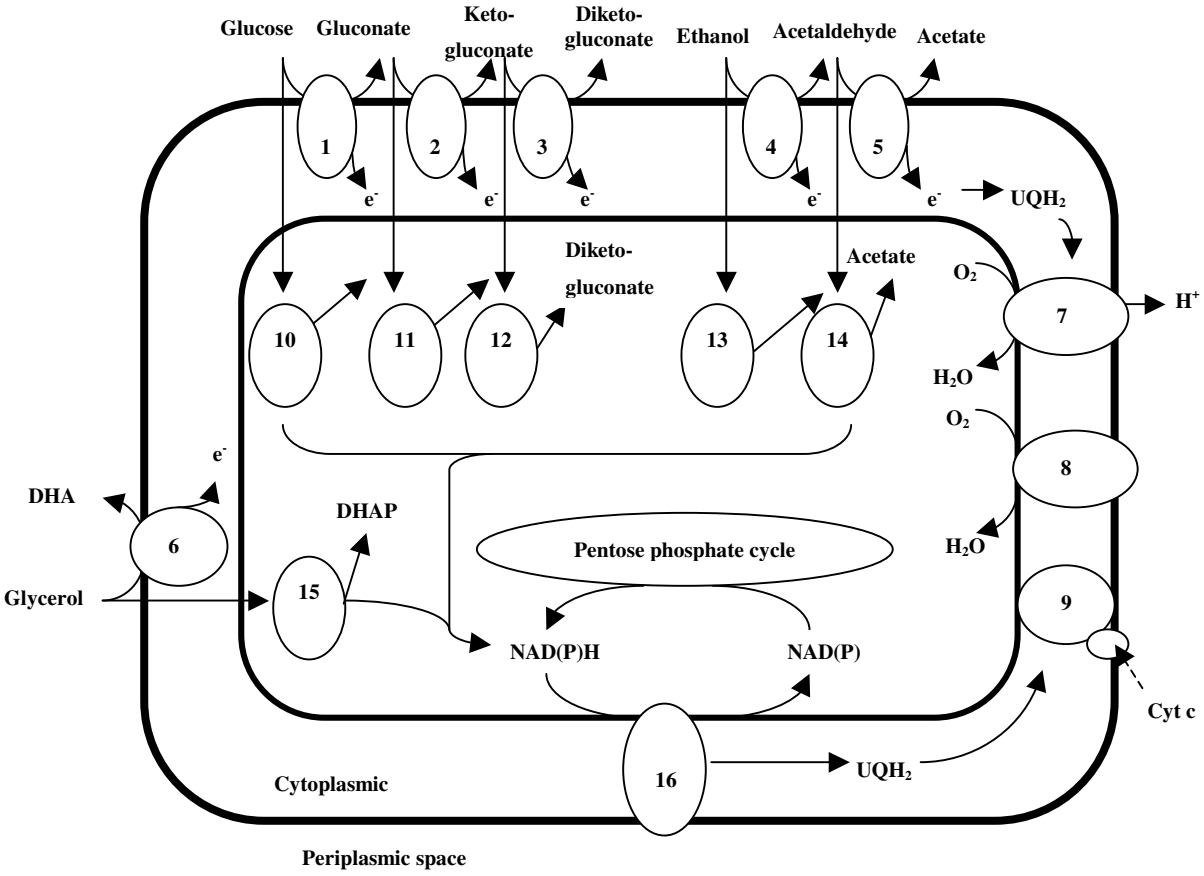

Figure 1.2 Incomplete oxidation-pathways of *Gluconobacter oxydans*.

(based on schemes from (*19, 22, 23, 27, 32, 41, 45, 46*)) Membrane-bound PQQ-dependent dehydrogenases: (1) Glucose dehydrogenase, (2) Gluconate dehydrogenase, (3) Ketogluconate dehydrogenase, (4) Alcohol dehydrogenase, (5) Acetaldehyde dehydrogenase, (6) Glycerol dehydrogenase. Cytosolic NAD(P)-dependent dehydrogenases: (10) Glucose dehydrogenase, (11) Gluconate dehydrogenase, (12) Ketogluconate dehydrogenase, (13) Alcohol dehydrogenase, (14) Acetaldehyde dehydrogenase, (15) Glycerol 3-P dehydrogenase. Respiratory chain: (7) cytochrome bo3 ubiquinol oxidase, (8) cytochrome bd ubiquinol oxidase, (9) ubiquinol:cytochrome c oxidoreductase, (16) nonproton translocating NADH:ubiquinone oxidoreductase.

1.1.2 *Saccharomyces cerevisiae*

Glycolysis in *S. cerevisiae* is one of the best studied metabolic systems; originating with research by Pasteur and Buchner, independently, and currently still receiving a great deal of scientific attention (*9*). *S. cerevisiae* is of great industrial interest, it is used for the baking of bread to the making of beer and wine and possibly will have some role to play in the future production of bio-fuels from organic waste materials. *S. cerevisiae* utilizes the Embden-Meyerhof-Parnas glycolytic pathway, also known as the fructose-1,6-bisphosphate pathway, which yields two moles of ethanol and carbon dioxide for each mole of glucose consumed (*47*). Energetically this metabolic pathway is more efficient than the Entner-Doudoroff-pathway, since two adenosine-tri-phosphate (ATP) molecules are formed per glucose, as opposed to one via the Entner-Doudoroff pathway.

Traditionally the kinases (hexokinase, phosphofructokinase and pyruvate kinase) have been suggested to be rate limiting for glycolysis, but this could never be demonstrated experimentally (*48, 49*). The arguments that control on glycolysis may reside outside of the pathway itself are more convincing (*48-50*), and suggestions for glycolytic flux control by the glucose transporter (*51*) or by the H^+-ATPase have also been postulated on the basis of arguments from supply-demand analysis (*18*) .

Several groups have developed models describing glycolysis in *S. cerevisiae* with many different strategies followed: Curto, Cascante and Sorribas published a three-part series of articles describing how to approach experiments leading to kinetic models and applied the two closely related theoretical frameworks, MCA and biochemical systems theory (BST), for their steady-state analysis (*52-54*). Through this approach they were able to compare the two theories and show how important they could be in future biotechnological applications. They used *in vivo* ^{13}C-data from nuclear magnetic resonance spectroscopy and adapted an existing model. Their modeling strategy showed a strong bias towards the use of *in vivo* data for parameter estimations and BST, for parameter sensitivity analysis, in the study of intact systems. In conclusion, they emphasized that MCA is not equipped to investigate the stability of local steady states, dynamic system behavior and the sensitivity of parameters to metabolite concentrations and reaction rates. However, these arguments against the applicability of MCA to their model are unfounded, since the perceived deficiencies they discussed, especially as far as dynamic behavior are concerned, have been addressed in several publications (*7, 55-57*).

Rizzi *et al* defined a model that incorporated yeast glycolysis, the tricarboxylic acid cycle, the glyoxylate cycle and the electron transport chain (*58-60*). They investigated cellular responses in continuous cultures after glucose addition over 120 second periods in order to investigate glucose transport over the cell membrane. They derived their own rate equations for the facilitated diffusion of glucose over the cell membrane and used published kinetics for the different enzymatic processes in the metabolic pathways involved. Through the use of steady state flux analysis and sensitivity analysis methods they concluded that glucose was taken up via facilitated diffusion, but that glucose-6-phosphate has an inhibitory effect on this process.

Finally, the most complete model of glycolysis in *S. cerevisiae* was developed by Teusink *et al* (*61*). They determined most of the kinetic parameters, based on reversible Michaelis-Menten kinetics, for the enzymatic reactions from non-growing *S. cerevisiae*, and used published parameters for some of the more complex reactions. A comparison was drawn between a model

based on *in vitro* data and the experimental results *in vivo*. Their first attempt using a linear model failed to give a satisfactory prediction of the experimental outcomes, which forced the development of the more detailed model containing branches towards glycogen, trehalose, glycerol and succinate. By adding these branches, the predictive power of the model was considerably improved with the parameters determined *in vitro* of half of the reactions within a two-fold range of the *in vivo* results. Several suggestions are offered for the discrepancy with the other half of the *in vitro* parameters and therefore this model is still a work in progress. However, the promise of such detailed models are immense in their scope of application to a more focused biotechnology.

Several other models on yeast glycolysis exist that are not discussed in detail in this review due to their emphasis being either on detailed mechanistic aspects of glycolytic enzymes, or central nitrogen metabolism or simply due to a lack of application to the current research question (*62-66*).

1.1.3 Mixed population studies

Microbial interactions are classified in two groups, i.e. positive and negative interactions. Each of these two groups is then further subdivided into several subgroups defined by the influences incurred by either of the organisms or both as a result of their interaction (*67, 68*). On this basis, positive interactions are divided into mutualism, commensalism and synergism (*67*). A mutualistic interaction is characterized by mutual benefit to both groups of organisms in the system with a subgroup, protocooperation, where the interaction is beneficial to both and non-obligatory. Commensalism is marked by only one group of microbes benefiting from the collaboration without any effect on the other participant group (*67, 68*). The last of the positive interactions, synergism, is characterized by the effect resulting from the interaction of the two species to be higher than the sum of the two species' individual effects (*67*). Similar to the positive interactions, negative interactions are divided into competition and amensalism. Competition occurs when two species compete for a single resource, both inhibiting each other in an attempt to gain the ascendancy. This interaction is further divided into direct and indirect competition with the latter only occurring when a resource becomes limited (*67, 68*). During an amensalistic interaction, one group of bacteria negatively influences the other with no negative effect to its own functions (*67, 68*). A special kind of amensalism, antagonism, is observed where the one organism excretes a compound to exert a negative influence on its adversary (*67, 68*). Some interactions contains elements of both the positive and negative characteristics, i.e. predation and parasitism (*68*). During predation, which

includes herbivory, the one organism serves as substrate for the other with this having a positive effect on the predator populations and negative effect on prey populations (*67, 68*). Parasitism is the situation where one organism is completely dependent on another species, its host, for its nutrients and with detrimental effects on the host (*67-71*). Neutralism occurs when species co-exist without being dependent or exerting any effects on each other (*68*).

Naturally occurring mixed populations can have major negative implications for the ecosystems they populate if their homeostatic interactions are disturbed, e.g. the host. This is evident in cases of human disease where the ecological balance between populations of micro-organisms co-inhabiting the human oral cavity or gut, are disturbed due to stress or dietary changes leading to periodontal disease or inflammatory bowel disease, respectively (*67, 72*). However, artificial mixed populations are modeled on interactions between two organisms that would lead to some benefit for humankind – either through an understanding of their interaction, e.g. the mechanism of attack by killer yeasts or studying the microbial flora of tubeworms, or through an improvement in some beneficial process, e.g. the curing of camembert cheese or the improvement of the denitrification of waste water (*44, 73-77*).

Several industries incorporate mixed cultures of organisms because there are advantages of having a collection of microorganisms breaking down unwanted compounds, e.g. sewage waste or abattoir effluents, compared to using a single organism (*9*). *G.oxydans* forms part of such an industrially employed mixed culture combined with *Baccillus*-strains in the revised Reichstein-process for the manufacturing of ascorbic acid (*28*). In such defined mixed culture assays, isolated pure cultures can be used, separated by membranes, allowing mixing of the culture media, or the preferred cultures can be mixed before adding them to culture media (*9, 74, 78*). The focus of the current project is on commensalistic mixed cultures where two or more organisms are found together in an ecosystem or culture with the product of one being the substrate for the next organism, creating a processing chain (*79, 80*). Processing chains should not be confused with trophic chains, which are based on predator-prey relationships, i.e. plant-herbivore-carnivore, where the one specie forms the substrate for the next (*5, 81*). Classical ecology has tended towards studies of the second kind where the balance between predator and prey were of the utmost importance and systems consisting of purely commensalistic interaction have largely been ignored (*82-84*).

There are several different strategies followed in studying and setting up kinetic models to describe mixed populations. In the following paragraphs three models are described emphasizing some of these strategies commonly used in combining experimental and theoretical descriptions of microbial interactions. The three models discussed, incorporated different levels of modeling in attempts to describe natural occurring mixed populations with limited success. These particular models were chosen to illustrate the evolution from experimental determination of parameters to simple, semi-descriptive models, i.e. Marazioti *et al.* (*73*), and further on to more complex descriptions, i.e. Pommier *et al.* (*74*), broadening into a general theoretical framework, i.e. Allison *et al.* (*85*). In these descriptions, the focus is not on what types of interactions are modeled, but on model validation and applicability to the systems under study. The main objective in discussing these three models, is to emphasize the importance of having a generalized theoretical framework to gain deeper understanding of the systems that were modeled.

Marazioti *et al* studied defined batch assays of a commensalistic mixed population of *Pseudomonas denitrificans* and *Bacillus subtilis* under various culturing conditions ranging from anoxic to aerobic conditions and using different limiting substrates (*73*). Using Monod-type kinetics to model each organism, they were able to achieve very satisfactory fits to describe the metabolic activity and growth of the organisms in mixed fermentations over all the conditions tested. However, this system still needs to be extended to describe the reality of the "activated sludge" method used in these situations on an industrial level. The behavior of these two organisms within such an undefined mixture will not be easily understood without applying some theoretical framework.

Pommier *et al* followed another strategy to study interactions between two types of yeast, one a killer and the other a sensitive yeast-species, in separate batch fermentations connected by a permeable membrane (*74, 78*). The membrane facilitated more precise biomass estimations by having the two cultures completely separated from each other, but sharing the same medium. Data from these fermentations were used to test a previously published model describing this system through logistical rate equations for growth, inhibition and death rates. By specifying four species of organism, (i.e. viable killer, dead killer, viable sensitive and dead sensitive yeasts) in the model, they gave a more complete description of the interaction. Unfortunately, when the original model was tested against this new set of data, it failed to the extent that new parameters were introduced to improve its incorrect estimations. The new model now predicted viable cell ratios for sensitive/killer yeasts and described a typical enzymatic lag. The original model was not validated over a wide enough range of cellular ratios and left only a small window of application to the

description of the microbial interactions. This stresses the importance of validation of a model under carefully chosen conditions to increase its robustness, e.g.: a wide range of viable/dead yeast ratios, a distinction between dead killer and dead sensitive yeast cells, a wide range of killer/sensitive yeast ratios. The original model made no distinction between dead yeast cells and tested only two ratios of killer/sensitive yeasts.

Finally, Allison *et al* investigated a model based on chemostat-theory for single cultures and extended to describe two interacting species (*85*). This completely theoretical study was not based on any actual microbial interaction in order to create a completely generalized model to apply their theory without any inherent bias. They used Monod-kinetics to describe the growth of both organisms and ordinary differential equations to describe the reaction rates and resultant flux through the system. A further characteristic of their study was the incorporation of a theoretical framework adopted from the MCA of enzymatic systems. Using this rationale, they described the commensalistic interaction in terms of a branched reaction scheme in which the linear chain consists of the limiting substrate being converted to the intermediary metabolite and finally to the system product. Branch-points were created to accommodate the biomass production of each species, defined as products. In order to calculate control coefficients they suggested the use of species-specific inhibitors to perturb the flux of the system under study. They postulated that the control coefficients could be defined in exactly the same way as for enzymatic systems, but I will elaborate on their theory in section 1.2

1.2 Applying Control Analysis on Ecosystems

1.2.1 Metabolic Control Analysis for simple two-enzyme linear systems

Metabolic control analysis (MCA) was developed by Kacser and Burns, with the first fundamental publication in 1973, and independently by Heinrich and Rapaport (*86-88*). Since then, the subject has been reviewed on several occasions and has been significantly expanded to include: e.g. supply-demand analysis, regulation analysis, hierarchical control analysis (HCA) and flux-balance analysis (FBA) (*7, 17, 18, 89-112*). Furthermore, several techniques have been developed to simplify the analysis of metabolic pathways with varying degrees of complexity including systems with branch-points (*113-134*). Detailed descriptions of most of these techniques fall outside the scope of this review and only techniques relevant to this thesis will be discussed below.

When applying MCA it is important to make a clear distinction between parameters and variables in the system description. For instance, when using Michaelis-Menten-kinetics to describe an enzymatic step the parameters would be the K_m and V_{max} of the enzyme, i.e. the constituents that are constant for the enzyme described, while the variables would be the reaction rates and the substrate and product concentrations, i.e. the constituents that can vary over time. MCA is mostly concerned with systems at steady state where it provides a link between local properties, i.e. elasticity coefficients describing the effect of perturbations on single enzymes, and global properties, i.e. control coefficients describing the effects perturbations have on the whole system.

If one considers a simple linear pathway containing two enzymes, linked by a single intermediary metabolite, we can apply the methods of control analysis to derive a clear understanding of the control structure with the pathway. Figure 1.3 will be used as a reference pathway:

$$X_1 \xrightarrow{E_1} S_2 \xrightarrow{E_2} X_3$$

Figure 1.3 Reaction scheme of linear metabolic pathway

The elasticity for Enzyme 1 (E_1) to the intermediary metabolite, S_2, is determined by varying the concentration of S_2 in the presence of isolated E_1 with all other metabolite-concentrations kept at their concentrations found at the reference steady state. In the simplest terms, the elasticity coefficient is the scaled slope of the tangent to the curve of the rate through E_1, symbolized by v_1, against the concentration of S_2 at the normal *in vivo* concentration of S_2. The scaling factor for elasticity coefficients is this *in vivo* metabolite concentration divided by the enzymatic rate at that concentration. Otherwise, the elasticity coefficient can be determined as the tangent to the double logarithmic plot of the corresponding data. Equation 1.1 illustrates these definitions in mathematical form:

$$\varepsilon_{S_2}^{v_1} = \frac{\partial v_1}{\partial S_2} \bullet \frac{S_2}{v_1} = \frac{\partial \ln v_1}{\partial \ln S_2} \quad (1.1)$$

MCA defines two types of control coefficients, i.e. the flux control coefficient ($C_{E_1}^{J}$) and the concentration control coefficient ($C_{E_1}^{S_2}$) quantifying the control a specific enzyme has on the pathway flux (J) or a metabolite concentration, respectively. The flux control coefficient is defined analogously to the elasticity coefficients, but with the emphasis on the system flux and not the local enzymatic rate. Hence, the flux control coefficient is calculated from the scaled tangent to the curve

of J against the activity of E_1 at the enzyme concentration at steady state with the scaling factor being the enzyme activity *in vivo* divided by the corresponding flux at the specific enzyme concentration. As with the elasticity coefficients, the tangent of the curve in log-log space can also be used to calculate the flux control coefficient. Equation 1.2 shows the mathematical formulation of the flux control coefficient with regards to E_1 in Figure 1.3.

$$C^{J}_{v_1} = \frac{\partial J}{\partial v_1} \bullet \frac{v_1}{J} = \frac{\partial \ln J}{\partial \ln v_1} \quad (1.2)$$

The concentration-control coefficient for E_1 on the concentration of the intermediary metabolite S_2 is described by the scaled tangent, at the S_2-concentration at steady state, to the curve of the metabolite concentration against the enzyme activity. Alternatively, the slope of the tangent to the double-logarithmic plot of the same data gives the concentration control coefficient for E_1 on S_2. The mathematical formulation for this concentration control coefficient is given below in Equation 1.3.

$$C^{S_2}_{v_1} = \frac{\partial S_2}{\partial v_1} \bullet \frac{v_1}{S_2} = \frac{\partial \ln S_2}{\partial \ln v_1} \quad (1.3)$$

The power of MCA lies in its foundation of two sets of theorems in which the inter-connections between the elasticity and control coefficients are summarized. One set of theorems describes the relation between the flux-control and elasticity coefficients (*86*) whilst the other is focused on the concentration-control coefficients and their relation to the elasticity coefficients (*87, 111*). Each set consists of a summation theorem for the control coefficients and connectivity theorems describing the relation between the control coefficients and the elasticity coefficients.

Hence, the summation theorem for flux control coefficients states that all the flux control coefficients for enzymes influencing the flux through a particular system add up to one. In short it states that all enzymes in such a system could potentially share control over the flux through the system. For one enzyme to be "rate-limiting" its flux control coefficient will have to be (very close to) one with all the other enzymes having very low flux control coefficients. Equation 1.4 shows the mathematical formulation of this theorem for two enzymes:

$$C^{J}_{v_1} + C^{J}_{v_2} = 1 \quad (1.4)$$

The connectivity theorem that links flux control coefficients to the elasticity coefficients shows that the sum of products of flux control coefficients of enzymes and elasticity coefficients with respect to the same metabolite adds up to zero. This theorem creates the link from local properties to global

properties of systems. Equation 1.5 shows this relation's mathematical formulation for a linear pathway with two enzymes linked by an intermediary metabolite, S_2:

$$C^{J}_{v_1}\varepsilon^{v_1}_{s_2} + C^{J}_{v_2}\varepsilon^{v_2}_{s_2} = 0 \quad (1.5)$$

MCA has one summation theorem for concentration control coefficients, but two connectivity theorems depending on the combinations of metabolite concentrations described within each theorem. The sum of all concentration control coefficients affecting one particular metabolite concentration adds up to zero. Again this places emphasis on control on metabolite concentrations being shared across the enzymes involved. Equation 1.6 is a mathematical description for the summation theorem for concentration control coefficients relating to S_2.

$$C^{s_2}_{v_1} + C^{s_2}_{v_2} = 0 \quad (1.6)$$

The connectivity theorems for concentration control coefficient are divided between concentration control coefficients and elasticity coefficients related to the same metabolite concentration and those related to different metabolite concentrations. When only two enzymes are linked together by a single intermediary metabolite, as in our sample pathway, only one connectivity theorem exists, since both the concentration control coefficients must be related to the same metabolite concentration.

Equation 1.7 shows the connectivity theorem applicable to our sample system:

$$C^{s_2}_{v_1}\varepsilon^{v_1}_{s_2} + C^{s_2}_{v_2}\varepsilon^{v_2}_{s_2} = -1 \quad (1.7)$$

Using the summation and connectivity theorems the control coefficients can be expressed in terms of elasticity coefficients, by combining Equations 1.4 and 1.5 they can be rewritten as Equations 1.8 and 1.9 for the pathway shown in Figure 1.3.

$$C^{J}_{v_1} = \frac{\varepsilon^{v_2}_{s_2}}{\varepsilon^{v_2}_{s_2} - \varepsilon^{v_1}_{s_2}} \quad (1.8)$$

$$C^{J}_{v_2} = \frac{-\varepsilon^{v_1}_{s_2}}{\varepsilon^{v_2}_{s_2} - \varepsilon^{v_1}_{s_2}} \quad (1.9)$$

In the same way Equations 1.6 and 1.7 can be rewritten as Equations 1.10 and 1.11 for the model system in Figure 1.3.

$$C_{v_1}^{s_2} = \frac{1}{\varepsilon_{s_2}^{v_2} - \varepsilon_{s_2}^{v_1}} \quad (1.10)$$

$$C_{v_2}^{s_2} = \frac{-1}{\varepsilon_{s_2}^{v_2} - \varepsilon_{s_2}^{v_1}} \quad (1.11)$$

The mathematics behind MCA has been reviewed since its inception with several different approaches being taken to accommodate more complex systems than the simple two-enzyme system described above (*101, 102, 113, 115, 116, 119-122, 127, 134-141*). The currently preferred method to describe the relation between local and system properties as described in Equations 1.8 – 1.11, is by combining the theorems of MCA within the control-matrix theorem, $\mathbf{C} = \mathbf{E}^{-1}$ (*102, 133, 142*).

In the most general form by Hofmeyr (*102*), the **C**-matrix contains all control coefficients while the **E**-matrix represents the elasticity coefficients as can be seen in the matrix equations below using the sample pathway as reference:

$$E = \begin{pmatrix} 1 & -\varepsilon_{s_2}^{v_1} \\ 1 & -\varepsilon_{s_2}^{v_2} \end{pmatrix} \quad (1.12)$$

$$C = \begin{pmatrix} C_{v_1}^{J} & C_{v_2}^{J} \\ C_{v_1}^{s_2} & C_{v_2}^{s_2} \end{pmatrix} \quad (1.13)$$

The control-matrix theorem can also be described by **E x C = I**, where **I** represents the identity matrix.

1.2.2 Analysis of ecosystems

The idea of performing sensitivity analysis on ecosystems has been discussed in the early to mid 1990's and then again gained interest through several publications since 2002 (*4-6, 83-85, 143*).

In 1991, two articles were published by Giersch in collaboration with Wennekers, discussing the theoretical aspects of a sensitivity analysis for ecosystems (*83, 84*). Giersch performed a sensitivity analysis on a plant-herbivore system at steady state with regards to biomass (*83*). He defined

"relative sensitivities" in much the same way as control coefficients are defined in MCA and then derived summation theorems for these. Thus, summation of the relative sensitivities of population densities and biomass fluxes with respect to a specific parameter add up to 0 and 1, respectively. This result, for a plant-herbivore system, was completely malleable with the summations found in terms of concentration and flux control coefficients of MCA if one regards the concentration and formation of biomass as a metabolic process. Emphasis was put on the fact that rate equations or "laws" were mostly functions containing parameters on which this sensitivity analysis could be performed. For the plant-herbivore system analysed, the model showed clearly that these summation theorems derived by Giersch hold and furthermore some of the more intricate details were brought to light by this analysis, e.g. both the steady-state population densities and biomass fluxes were insensitive to the maximal growth rate of the herbivore, but very sensitive to the maximal growth rate of the plant.

In combination with Wennekers, Giersch applied the abovementioned sensitivity analysis on an unbranched Lotka-Volterra food chain or predator-prey system (*84*). Using this simple predator-prey system as a basis, they derived a similar relation between the matrices of "relative sensitivities" and the community matrix evaluated at steady-state population densities to what can be seen between the **E**- and **C**-matrices of MCA, i.e. they are inverse matrices of each other. Furthermore, they found that each of the species interlinked in the food chain were not necessarily affected by the species nearest to it in the chain as was traditionally thought, e.g. in a three part chain the central species' population density is only determined by the species for which it is prey and not by its own food source at all. However, if species are added to an ecosystem, e.g. through introduction of a predator to an ecosystem, the control on the various population densities in the ecosystem can shift dramatically. For example, adding a predator to Giersch's original ecosystem, as was done in this publication by Wennekers, immediately shifted the control on the herbivore-population density towards this predator and away from the herbivore's food-source, i.e. the plant species (*84*). The control on the predator-population was shared amongst all three inhabitants of the new ecosystem.

In 1995 Schulze published a correspondence speculating on the applicability of control analysis to ecosystems (*143*). He elaborated on the similarities between ecosystems and biochemical systems, but emphasized the individuality of different organisms in contrast to enzymes. However, in terms of their processing capabilities these organisms are indeed very similar to enzymes. Furthermore, he showed the complex hierarchical nature and interconnectedness of ecosystems in terms of resource

flux (e.g. energy, water and carbon) and multitudes of trophic levels. It is this hierarchical nature as well as fluctuating organism populations which makes adopting MCA directly to ecosystems a non-trivial matter, and shows that HCA might be a better option for dynamic ecosystems. Ecosystem steady states are also not perceived to be nearly as unique and stable as their metabolic counterparts are postulated to be, which should encourage the use of caution in approaching such an analysis. The concept of key species limiting the flux through an ecosystem also raises some concerns, since it is alarmingly close to the traditional approaches in biochemistry where MCA has shown that one enzyme is unlikely to have all the control over the flux through a pathway. Nonetheless, this speculative communication did lead to some minor controversy when Giersch commented in a reply to this article that control analysis is not the correct tool for use on ecosystems (*1*). Thomas *et al*, corresponded on the same issue that MCA might be quite a helpful theoretical framework for ecosystem analysis (*144*).

In 2002 Westerhoff *et al* published a theoretical investigation focusing on a system similar to the one that is the subject of the current study, albeit under growing conditions (*4*). Under growing conditions it makes sense to use HCA to describe the ecosystem with growth and decline of biomass for the two species and their metabolic interactions at separate hierarchical levels. Using arbitrary parameter-values for their model interaction the authors could show that the theorems of MCA hold and that the steps in one level of the hierarchy can influence another level while up or down perturbations as a whole does not effect another level, i.e. the same way HCA describes such interaction between levels.

Shortly after the Westerhoff-publication, an article was published by the same group of collaborators that went into an in depth theoretical investigation of trophic chains within the field of ecological modelling (*5*). They focussed on two groups of common rate laws used for the description of trophic chains, i.e. linear and non-linear growth functions. The linear rate laws included Lotka-Volterra-type growth and feeding kinetics as well as the compensatory power function, whereas for non-linear feeding rate laws, equations of the Beddington and Holling-type were tested. Besides the linear Lotka-Volterra growth kinetics, two non-linear kinetic descriptions were used, i.e. hyperbolic growth and metaphysiological growth. The investigation further employed perturbations to the feeding and growth of organisms to derive the control structures of models using the abovementioned rate laws. A new type of control analysis based on these investigations was derived and named trophic control analysis (TCA). Using TCA the authors could establish two sets of control theorems, one set for systems described by linear rate laws and another

for those described by non-linear rate laws. These two different sets of theorems employed two different matrices for their description, the R-matrix for linear and the T-matrix for non-linear systems. TCA appears to be less effective for ecosystems than MCA has been for biochemical systems, since the models used to describe the foodwebs were not as realistic as their counterparts used for metabolic systems modelling. However, this limitation is not so much a limitation of TCA but more of the models used to describe trophic systems and we see great potential in the application of TCA in the analysis of ecological systems.

In a more recent publication on ecological control analysis (ECA), Roling *et al.* focussed on the widespread ecological problem of wastewater treatment. They conducted a literature search for parameter values of microorganisms involved in the process and constructed kinetic models to which they applied control analysis (*6*). They employed Michaelis-Menten type kinetics to two simple ecological scenarios and highlighted the control structure within these systems. The first system was a simple linear system of two groups of organisms under non-growing conditions, linked together by a single intermediary metabolite inhibiting its producing group. Non-growing conditions meant that they could employ the theorems of MCA directly and it showed that both groups shared control over the flux through the system as well as the concentration of the linking metabolite hydrogen. With their study they disproved both the concept of a single rate-limiting organism as well as the concept that only consumer organisms determine the concentrations of intermediary metabolites. The second system they studied was branched with one group of organisms producing two products forming the intermediary metabolites for the two branches. Both intermediary metabolites again inhibited their producers. Applying MCA to this system now showed that the two branches could affect the fluxes flowing through each other as well as the concentrations of their intermediary metabolites. They showed further that environmental conditions as well as redox processes have considerable influence on the control structures of the ecosystem. Although hampered by several discrepancies in the parameter sets they obtained from the literature, they managed to show how ECA could be an effective tool in terms of industrial processes driven by ecosystems.

In a recent review Tollner *et al.* applies control theory to ecological systems (*145*). Although the title would appear to make the study very relevant for our work, it should be stressed here that the control theory that Tollner uses is a different type of control than the control analysis framework we used in this thesis. Control theory stems for the engineering and mathematics field and literally refers to the control of a system to obtain a desired effect. Whereas there are overlaps between the

two fields, for instance in optimization studies one could investigate for what function a biological system is optimized and use the metabolic control coefficient distribution as a guideline to test for optimized performance in control theory terms, such a study would be interesting but falls outside the scope of this thesis.

1.3 Conclusion

In many ecological studies complex theoretical models are used to describe large and intricate ecosystems, but the common assumption still exists that specific organisms or groups of organisms in such systems would determine the rates of product formation through these systems (68, 82). This is very similar to the state of classical biochemistry up to the 1970's with the concept of rate-limiting enzymes being commonplace in textbooks and scientific publications regarding metabolic systems. Since then researchers employing MCA have convincingly disproved this concept and replaced it with a quantifiable degree of control using control coefficients, and showed that in many systems control is shared over the processes in a system.

In several recent publications, as mentioned in this chapter, a movement has started from within the MCA-community to analyze ecological systems in terms of a control analysis based theoretical framework, ECA. As was the case with classical biochemistry with the advent of MCA, experimental data available from ecological studies are not necessarily suited for application of ECA. Even though Roling et al. have applied ECA using previously published experimental data with reasonable success, some of the parameters found in their data-mining could differ up to a 1000-fold (6). Validation of a model system derived from several independent datasets is difficult since no single independent experimental data set exists with which the model outcomes could be compared.

We started this study with the aim to experimentally test the feasibility of an ecological control analysis. Ideally, in such a study one would want to use a simple ecosystem, consisting of organisms that can be cultured in isolation such that kinetic parameters for each of the organisms can be determined independent of the system. Such a system should reach steady states with regard to its intermediary metabolites when the species are cultured together, and it should be possible to make specific perturbations to the system. We have chosen the acetification of wine by acetic acid

bacteria as a model system, and we have shown that in a core model for such an ecosystem, S. cerevisiae and G. oxydans can be linked together by the intermediary metabolite, ethanol. However, even under aerobic conditions the growth of G. oxydans is too slow to make co-culturing of the two species under growing conditions possible. We have therefore chosen to perform all assays under aerobic, non-growing conditions. Single culture assays were performed to determine parameters for both organisms as well as their sensitivities for all compounds present in the reaction mixtures. These parameters could then be used to create a kinetic model describing mixed population assays under similar conditions. Mixed population assays were used to validate the model and calculate control coefficients for flux and the concentration of the intermediary metabolite.

We developed two models based on linear kinetics for S. cerevisiae and Michaelis-Menten type kinetics for G. oxydans. Linear kinetics was used for the yeast since it was not sensitive to the ethanol at the concentrations achieved in our experiments and glucose was present at saturating concentrations throughout. The first of the two models only took the sensitivity of both organisms towards ethanol into account, but the second more complex model also incorporated oxygen as both organisms were found to use oxygen under our experimental conditions. The details on experimental conditions and analysis are presented in Chapter 2 whilst the results and model fitting procedures are discussed in Chapter 3. Our findings regarding the control structure and applicability of control analysis on the sample ecosystem are discussed in Chapter 4. Details on the strategies employed to overcome some of the experimental and analytical pitfalls encountered during this project are also discussed in Chapter 4.

Chapter 2

2. Materials and Methods

2.1 Microbial culturing methods

2.1.1 Microbial strains and their maintenance

Both *Gluconobacter oxydans* 7145DSM and *Saccharomyces cerevisiae* VIN13 were kindly provided by the Institute for Wine Biotechnology (IWBT) at Stellenbosch University.

Stock cultures for *G. oxydans* were prepared by mixing 200µl of pure overnight culture with 800µl of a sterile 65% (v/v) glycerol solution in cryogenic vials and "snap"-freezing the mixture in liquid nitrogen before storage at –80^{o}C. These frozen "glycerol-stocks" were used for one inoculation each and discarded to decrease the propagation of contaminant organisms and to ensure the vitality of stocks. GYC-agar plates (2% (w/v) Glucose (Sigma-Aldrich), 1% (w/v) Yeast Extract (BioLab, Merck), 30% (w/v) Calcium Carbonate (Saarchem, Merck), 25% (w/v) Bacto-Agar (BioLab, Merck)) were inoculated from overnight liquid-medium cultures of *G. oxydans*, used as a bridge between frozen stocks and solid medium to increase culture viability, and incubated at 30^{o}C for 48h. The resultant agar plates were stored at 4^{o}C and replaced weekly to ensure strain integrity.

Stock cultures for *S. cerevisiae* were prepared similar to those for *G. oxydans*, with the exception that a sterile 50% (v/v) glycerol solution was used. For the same reasons as mentioned above, frozen "glycerol"-stocks were used for only one inoculation each and then discarded. YPD-agar plates (2% (w/v) Glucose (Sigma-Aldrich), 1% (w/v) Yeast Extract (BioLab, Merck), 2% (w/v) Bacteriological Peptone (BioLab, Merck), 15% Bacto-Agar (BioLab,Merck), 20mM Na-Phosphate buffer, at pH 6, from corresponding salts (Saarchem, Merck)) were "streaked" directly from frozen stocks and incubated for 48 h at 30^{o}C. New agar plates were prepared on a weekly basis.

2.1.2 Culturing media and conditions

Pre-cultures of *G. oxydans* were inoculated from GYC-agar plates and cultivated in 100ml Erlenmeyer flasks containing 50ml of the ½% YE-Ethanol medium (0.5%(w/v) Yeast Extract

(BioLab, Merck), 1% Ethanol (pro analysi GR, Merck), 20mM Na-Phosphate buffer at pH 6.0 from corresponding salts (Saarchem, Merck)) at 30°C in a gyrotary water bath shaker at 200rpm (New Brunswick model G76D) for 19h. After visual checks for purity of cultures by microscope, 9L fermentation-vessels were inoculated with 20ml of culture. These large-scale fermentations consisted of 10L glass medium-vessels containing 9L of ½% YE-Ethanol medium (50mM Na-Phosphate buffer, pH 6.0) being aerated with compressed air at 10L/hr, kept at 30°C by temperature finger from a circulating water bath and stirred at 1200rpm using a magnetic stirrer bar (50mm × 10mm) and electric stirrer (Framo-Gerätetechnik M20/1).

After 42h the bacterial cells were harvested by centrifugation (Beckman J2-21 centrifuge with JA10-rotor and 470ml polypropylene tubes) after the culture purity was determined by microscope (Carl Zeiss Axiostar) and the optical density at 600nm (OD_{600}) was around 0.3 as determined by spectrophotometer (Jenway 6100). The prolonged fermentation time was to ensure optimal development of the capability of *G. oxydans* to utilize ethanol for the production of acetate. The fermentation duration was comparable to published fermentations of *G. oxydans* by Villa *et al*.(*146*) and Albin *et al*.(*147*).

Single colonies of *S. cerevisiae* were inoculated from YPD-agar plates into 100ml Erlenmeyer flasks containing 50ml of YPD-liquid medium (20mM Na-Phosphate buffer, pH 6.0), containing no agar, and cultured at 30°C in a gyrotary water bath shaker at 100 rpm for 11h. After visual purity checks by microscope, 5L large-scale fermentation-vessels were inoculated with 10mL of exponentially growing culture. The culture-vessels were 10L glass medium-vessels containing 5L of liquid YPD-medium (50mM Na-Phosphate buffer, pH 6.0) kept under anaerobic conditions by sparging with nitrogen at 6L/h, kept at 30°C by circulating water bath and stirred at 300rpm using a magnetic stirrer bar (50mm × 10mm) and electric stirrer (IKAMAG RET). *S.cerevisiae*–cells were harvested after 12 h in early exponential growth phase and the culture purity was verified via visual inspection with a microscope.

2.2 Bioconversion assays

2.2.1 Design of aeration funnel

Aeration funnels were designed similar to the bubble columns described by Adlercreutz *et al.*, but on a smaller scale, 100ml as compared to their 500ml columns, and with a cylindrical shape that was not tapered at the bottom (*148*). Incorporated into each cylindrical aeration funnel, was a glass

sinter, adjustable air-valve connected to an airflow-meter, a head-port onto which a condenser could be placed as well as an outlet-port to which a 5ml disposable syringe could be connected. The condenser was cooled down by a circulating cryostat at 0.4^{o}C to ensure that none of the volatile fermentation compounds could evaporate. (See Figure 2.1)

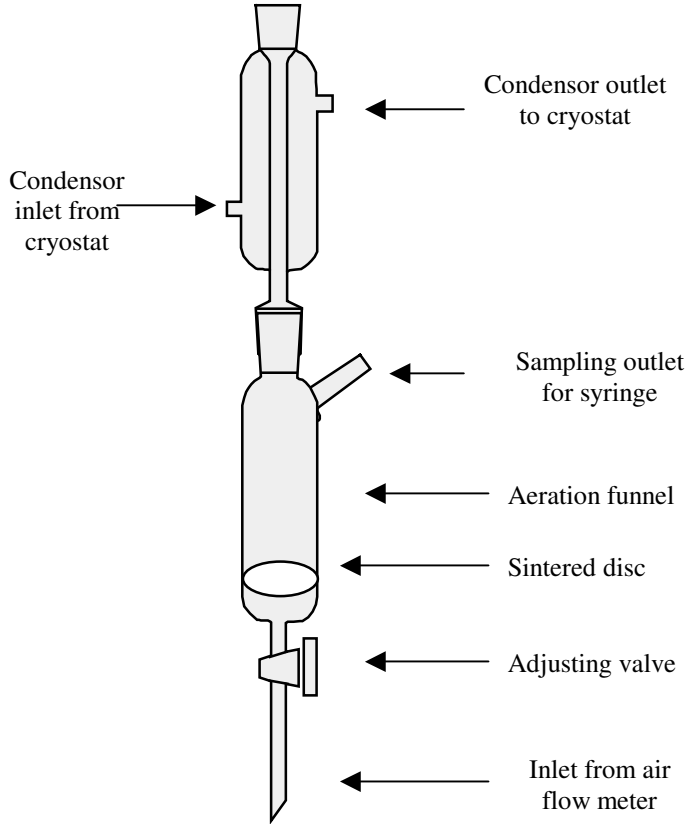

Figure 2.1: Diagrammatic representation of Aeration funnel

2.2.2 Single culture experiments

Cells of *G. oxydans* or *S. cerevisiae* that were harvested from the macro-fermentations, were pooled and washed by repetitive centrifugation (4500 × g) and re-suspension in 100mM MES-buffer (2-[N-morpholino]-ethanesulphonic acid, monohydrate, USB), pH 6.0 by NaOH, until all remnants of culture media were removed. Re-suspension was done by vortex (Gemmy Industrial K VM-300), decanting the supernatant after centrifugation and replenishing with 30ml of fresh MES-buffer between each wash step. After three wash steps, cells were concentrated by centrifugation, resuspended in 100mM MES-buffer and the cell density measured by OD_{600} and Coulter counter (Beckman Multisizer 3) using a counting probe with 30µm aperture. *G. oxydans* were measured between 0.77 to 2.86µm whilst *S. cerevisiae* were measured between 2.862 and 8.78µm (boundaries were chosen from cell counts obtained from pure cultures). Cell-densities thus measured were used

to calculate the volumes of cells to be added for the desired biomass concentrations in the 100ml bioconversion assays.

The working volume of the culture in the aeration funnel was 100 ml, and the funnel was placed in a heating water bath at 30^{o}C, with air or nitrogen flow through the funnel regulated at 6L/hr depending on whether assay conditions were aerobic or anaerobic. Cells from either *S. cerevisiae* or *G. oxydans* were inoculated into this mixture at the correct volumes needed to ensure the correct biomass concentrations in the final volume of 100ml.

For assays with *S. cerevisiae*, glucose (final concentration of 222mM) was added as substrate whilst in assays with *G. oxydans*, the substrates were glucose (222mM and ethanol (final concentration of 85.5mM). Both organisms were tested against different concentrations of acetate, gluconate, ethanol and glucose to determine their sensitivities for these compounds under concentrations reached in mixed culture assays. The time of substrate addition was defined as the start of each assay and was accompanied by the taking of the first set of 2ml samples, into 2ml reagent vials (Eppendorf), after which samples were taken every 20 minutes until 2h had passed. The pH at the start and end of each experiment was noted to ensure that buffering capacity was sufficient to prevent acidification during the assays. Duplicate biomass estimations were made half-way through the incubation, by spectrophotometer and Coulter counts.

Samples were centrifuged, for 1 minute (20 800 × g) and 1.8 ml of the supernatant were transferred to new 2ml reagent vials on ice. Perchloric acid was added to quench any remnant enzymatic activity. The supernatant were neutralised by adding potassium hydroxide and the samples were stored at –20^{o}C for analysis by high performance liquid chromatography (HPLC) at a later stage. See Section 2.3 for more detail on the quenching process and sample preparation.

2.2.3 Mixed population studies

Mixed population assays were performed in similar fashion to the single culture experiments. Cells of both species were harvested through centrifugation on the mornings of experiments. After cells were washed, following the same procedure as in Section 2.2.2, the biomass concentrations were determined by coulter counter and the desired biomass of both organism were added to the funnels. For each mixed culture experiment two control experiments with pure cultures of *G. oxydans* and *S. cerevisiae* were used to test for variability in the specific activity of the organisms. Biomass

concentrations were verified for each aeration funnel to ensure that the precise ratios of *S. cerevisiae* to *G. oxydans* were known for each experiment.

Incubations were started by the addition of glucose and samples were taken every 20 minutes for 5h. The samples were treated in the same fashion as the samples from single culture experiments and stored at –20^{o}C until HPLC-analysis could be performed. The pH of each assay was measured at the beginning, midpoint and end of the experiment with biomass determined in duplicate by Coulter counter after 1h had passed.

2.2.4 Oxygraph assays

Oxygraph assays were employed to determine the kinetic parameters for *G. oxydans* with respect to ethanol and oxygen sensitivity, and to determine the respiration rate for *S. cerevisiae*. The oxygraph consisted of a 4-port, 750ml jacketed flask (Glas Instrument Makerij, De Dreijen, Wageningen) connected to a circulating water bath at 30^{o}C and a Clark-type oxygen electrode from a New Brunswick Bioflo 110 bioreactor. Calibration of the oxygen probe was performed according to the instructions as stipulated within the user manual supplied by New Brunswick for the Bioflo 110 bioreactors.

During the determination of the kinetic parameters for ethanol and oxygen, 100mM MES-buffer was added to the jacketed flask and inoculated with low densities of *G. oxydans* (OD_{600} = 0.1). The reaction mixture was oxygenated, using compressed air, and the basal respiration rates were measured after which ethanol was added at varying concentrations per experiment. Initial respiration rates, in response to the ethanol added, were measured after re-oxygenation of the culture. Basal respiration rates were subtracted from the ethanol-enhanced rates to determine the respiration rate specific to each ethanol concentration after normalisation. Respiration rates were determined for 0.5mM, 2.5mM, 10mM, 20mM and 50mM ethanol in the presence and absence of 222mM glucose. Using nonlinear fitting procedures in Mathematica 6 we fitted the initial respiration rates versus ethanol concentrations to Michaelis-Menten kinetics and calculated the K_s and V_{max} values of *G. oxydans* for ethanol. Ethanol consumption rates could be calculated directly from the oxygen consumption rates on the assumption that 1 mol of oxygen is consumed per mol of ethanol converted to acetate (*9, 20*).

The oxygen-dependence of *G. oxydans* was calculated under saturating concentrations of glucose and ethanol, and measuring the oxygen consumption until depletion. Data originating from these "runout-assays" were fed into Mathematica and an interpolating function was derived to describe the changes in oxygen-concentration with time. The differential of this function was used to calculate the rate of oxygen consumption as a function of the dissolved oxygen concentration. Using non-linear fitting of Michaelis-Menten kinetics to the relation between the rates of oxygen consumption versus the corresponding oxygen concentrations, the K_s and V_{max} for *G. oxydans* for oxygen were determined.

During bioconversion assays with *S. cerevisiae* it was noted that not all of the glucose consumed was converted to ethanol even though the *S. cerevisiae* harvested for the assays were grown under anaerobic conditions. It was postulated that some of the glucose was completely oxidised to carbon dioxide suggesting that the respirative machinery in the yeast were switched on during the aerobic assays. The oxygraph was used to determine the rates of oxygen consumption on freshly harvested yeast cells and on cells already used in the bioconversion assays. Determination of the respiration rates from freshly harvested yeast cells, was done using exactly the same method as used in determining the ethanol consumption rates for *G. oxydans*. The respiration rates of yeast cells that underwent aerobic incubations were measured by pooling the reaction mixtures from six single culture experiments after the 2h were completed. These pooled cells were analyzed in oxygraphs as described before.

2.3 HPLC analysis of assay samples

2.3.1 HPLC-apparatus

The HPLC-system, employed in the analysis of our assay-samples, was kindly made available to us by the Central Analytical Facility at Stellenbosch University. It consisted of an Agilent 1100 series quaternary pump, a Waters 410 Refractive Index detector, a Waters 996 photodiode array detector, a Waters 717 Wisp autosampler and a Waters column oven controlled by a Waters TCM temperature controller. We used a BioRad Aminex AH87H-column with Phenomenex SecurityGuard precolumn for the separation of metabolites. Millenium software was used to control the Wisp and photodiode array detector as well as processing the chromatographic data.

2.3.2 Sample and calibration standard preparation

Directly after samples were drawn from bioconversion assays, centrifugation was used to pellet the cell mass and the supernatant was transferred into new 2 ml Eppendorf reagent vials. The supernatant was kept on ice and 35% perchloric acid (NT-laboratories, Merck) was added to a final concentration of 2%(v/v) to precipitate any proteins present in the mixture. After all samples were taken and the last sample-set was left to quench for at least 10 minutes, 7 M potassium hydroxide (Saarchem, Merck) was added to the sample at a final concentration of 0.35M to neutralize the mixture. Samples sets were kept at –20^{o}C until HPLC analysis when the precipitant matter were removed by centrifugation (20 800 × g) (Eppendorf 5804R with F-45-30-11 rotor) and the supernatant filtered using 0.45µm pore size PVDF-filters (30mm Durapore filters, Milipore)

Calibration standards were prepared on the days of HPLC analysis from earlier prepared 200mM stocks of glucose (Sigma-Aldrich), sodium gluconate (Sigma-Aldrich), glycerol (Synthon Fine Chemicals), sodium acetate (Saarchem, Merck) and ethanol (pro analysi GR, Merck). Two stock standard-mixtures were created, one containing glucose and ethanol whilst the other contained gluconate, acetate, glycerol and ethanol. Before HPLC analysis, these stocks were diluted to create two calibration-sets of 20 and 200mM, respectively. The same procedure for quenching and neutralization was followed as with the sample sets to ensure that both samples and standards were diluted in the same fashion. By changing the injection-volumes of each stock using the auto-sampler on the HPLC, calibration-curves ranging from 2 to 200mM, were created to cover the range of experimental concentrations expected from bioconversion assays.

2.3.3 Sample analysis and HPLC-program

Samples were analysed on the BioRad Aminex AH87H-column kept at 55^{o}C at an isocratic flow-rate of 0.5ml/min of 0.05mM sulphuric acid (AnalaR, BDH) for 30 minutes. The duration of each solvent run was determined by the time the last compound in the separation eluted, i.e. ethanol eluting after 26 minutes.

Two different injection volumes, 5µl and 20µl, from each sample were loaded onto the HPLC-column using the autosampler, thereby effectively diluting the sample four times to accommodate for higher concentrations than those contained in the calibration curve. The concentrations were derived from the areas of chromatographic peaks formed by each compound. Two detectors were

used to distinguish between some co-eluting compounds, i.e. glucose and gluconate as well as MES-buffer and acetate, and due to higher sensitivity of some of the compounds for UV at 210nm, i.e. the organic acids, and others only visible by refractive index, i.e. the sugars and alcohols.

2.4. Data Analysis

Data derived from these analyses were used to calculate all the different production and consumption rates used in the calculations of kinetic parameters as well as the sensitivities to different compounds. Mathematica 6 and Microsoft Excel were used to perform data analysis and fitting of data on Hanes-Woolf-graphs, non-linear Michaelis-Menten curves as well as trends through datasets.

2.4.1 Symbolic solution for the simple model

One of the strengths of Mathematica is that it can solve sets of differential equations (ODEs) symbolically, as long as the equations are not too complicated. This was particularly useful when we needed to fit kinetic parameters of the model to a large number of mixed culture experimental data sets. With the symbolic solution for the ODEs we could directly fit the parameters to the experimental data, which was much faster than finding an optimized parameter set for the fitting of a numerical integration to the individual data sets.

We first set out the definitions on which the symbolic solution for the differential equations were based:

$x(t) = \text{Ethanol} - \text{concentration}$

$y(t) = \text{Acetate} - \text{concentration}$

$s_1 = \text{fixed concentration of } S.\ cerevisiae$

$s_2 = \text{fixed concentration of } G.\ oxydans$

$k_1 = \text{specific acitivity of } S.\ cerevisiae \text{ in } \mu\text{mol EtOH/cell/min}$

$k_2 = \text{specific acitivity of } G.\ oxydans \text{ in } \mu\text{mol EtOH/cell/min}$

$K_x = \text{Ethanol affinity constant (Monod - constant) of } G.\ oxydans$

From these definitions we could now write the ODEs:

$$\frac{dx}{dt} = k_1 s_1 - k_2 s_2 \left(\frac{x(t)}{K_x + x(t)} \right)$$

$$\frac{dy}{dt} = 0.516 k_2 s_2 \left(\frac{x(t)}{K_x + x(t)} \right)$$

Hence, the symbolic solution for ethanol,

$$x(t) = \frac{1}{k_1 s_1 - k_2 s_2} \bullet K_x \bullet \left(k_2 s_2 \bullet W \left(\begin{array}{l} \dfrac{1}{k_2 s_2} \bullet k_1 s_1 \bullet 2.71828^{\frac{t\left(-1 \bullet k_2^{\,4} s_2^{\,4} + 4 \bullet k_2^{\,3} s_2^{\,3} k_1 s_1 - 6 \bullet k_2^{\,2} s_2^{\,2} k_1^{\,2} s_1^{\,2} + 4 \bullet k_2 s_2 k_1^{\,3} s_1^{\,3} - 1 \bullet k_1^{\,4} s_1^{\,4}\right)}{k_2 s_2 K_x \left(k_2 s_2 - 1 \bullet k_1 s_1\right)^2}} \\ \bullet \left(1 \bullet \sinh\left(\dfrac{k_1 s_1}{k_2 s_2} \right) - 1 \bullet \cosh\left(\dfrac{k_1 s_1}{k_2 s_2} \right) \right) \end{array} \right) + k_1 s_1 \right)$$

and for acetate,

$$y(t) =$$

$$\frac{\left(k_2 s_2 K_x \left(\begin{array}{l}\left(\begin{array}{l}-0.56 \bullet {s_2}^4 {k_2}^4 + 2.24 \bullet {k_2}^3 {s_2}^3 k_1 s_1 \\ -3.36 \bullet {k_2}^2 {s_2}^2 {k_1}^2 {s_1}^2 + 2.24 \bullet k_2 s_2 {k_1}^3 {s_1}^3 - 0.56 \bullet {k_1}^4 {s_1}^4\end{array}\right) \\ \bullet W\left(-\frac{k_1 s_1 e^{-\frac{k_1 s_1}{k_2 s_2}}}{k_2 s_2}\right) + k_2 s_2 \left(\begin{array}{l}0.56 \bullet {k_2}^3 {s_2}^3 - 1.68 \bullet {k_2}^2 {s_2}^2 k_1 s_1 \\ +1.68 \bullet k_2 s_2 {k_1}^2 {s_1}^2 - 0.56 \bullet {k_1}^3 {s_1}^3\end{array}\right) \\ \bullet W\left(\begin{array}{l}\frac{1}{k_2 s_2} k_1 s_1 \\ \bullet 2.71828^{\frac{t\left(-{k_2}^5 {s_2}^5 + 5 \bullet {k_2}^4 {s_2}^4 k_1 s_1 - 10 \bullet {k_2}^3 {s_2}^3 {k_1}^2 {s_1}^2 + 10 \bullet {k_2}^2 {s_2}^2 {k_1}^3 {s_1}^3 - 5 \bullet k_2 s_2 {k_1}^4 {s_1}^4 + {k_1}^5 {s_1}^5\right)}{k_2 s_2 K_x \left(k_2 s_2 - k_1 s_1\right)^3}} \\ \bullet \left(1 \bullet \sinh\left(\frac{k_1 s_1}{k_2 s_2}\right) - 1 \bullet \cosh\left(\frac{k_1 s_1}{k_2 s_2}\right)\right)\end{array}\right) \\ + k_1 s_1 \left(\begin{array}{l}\left(\begin{array}{l}-0.56 \bullet {k_2}^3 {s_2}^3 + 1.68 \bullet {k_2}^2 {s_2}^2 k_1 s_1 \\ -1.68 \bullet k_2 s_2 {k_1}^2 {s_1}^2 + 0.56 \bullet {k_1}^3 {s_1}^3\end{array}\right) \bullet \log\left(-\frac{k_1 s_1 e^{-\frac{k_1 s_1}{k_2 s_2}}}{k_2 s_2}\right) \\ + \left(\begin{array}{l}0.56 \bullet {k_2}^3 {s_2}^3 - 1.68 \bullet {k_2}^2 {s_2}^2 k_1 s_1 \\ +1.68 \bullet k_2 s_2 {k_1}^2 {s_1}^2 - 0.56 \bullet {k_1}^3 {s_1}^3\end{array}\right) \\ \bullet \log\left(W\left(\begin{array}{l}\frac{1}{k_2 s_2} k_1 s_1 \\ \bullet 2.71828^{\frac{t\left(-{k_2}^5 {s_2}^5 + 5 \bullet {k_2}^4 {s_2}^4 k_1 s_1 - 10 \bullet {k_2}^3 {s_2}^3 {k_1}^2 {s_1}^2 + 10 \bullet {k_2}^2 {s_2}^2 {k_1}^3 {s_1}^3 - 5 \bullet k_2 s_2 {k_1}^4 {s_1}^4 + {k_1}^5 {s_1}^5\right)}{k_2 s_2 K_x \left(k_2 s_2 - k_1 s_1\right)^3}} \\ \bullet \left(1 \bullet \sinh\left(\frac{k_1 s_1}{k_2 s_2}\right) - 1 \bullet \cosh\left(\frac{k_1 s_1}{k_2 s_2}\right)\right)\end{array}\right)\right)\end{array}\right)\right)\right)}{\left(\left(k_2 s_2 - k_1 s_1\right)^2 \bullet \left(-{k_2}^3 {s_2}^3 + 3 \bullet {k_2}^2 {s_2}^2 k_1 s_1 - 3 \bullet k_2 s_2 {k_1}^2 {s_1}^2 + {k_1}^3 {s_1}^3\right)\right)}$$

Clearly, these algebraic equations are rather unwieldy, but they proved to be very useful for the parameter optimization routines.

Chapter 3

3. Experimental Results

3.1 Introduction

In this Chapter the results and techniques applied on the experimental data are presented. We focus on a description of the results and give only a limited interpretation and discussion to enhance understanding and flow between subsections; we refer to Chapter 4 for a detailed discussion of the experimental and theoretical results. Ultimately, our aim is to use a detailed kinetic model for a quantitative analysis of mixed populations of *S. cerevisiae* and *G. oxydans*. To construct such a detailed kinetic model we started with core models for which parameters were estimated on the basis of pure culture experiments for the two organisms. These models included the non-zero sensitivities for the external metabolites that were present in the complete system. Subsequently, the kinetic models for the pure cultures were tested in their ability to describe mixed cultures. A sensitivity analysis for the parameters derived from pure cultures was performed. On the basis of this sensitivity analysis different strategies were followed to find an optimal parameter set for the mixed culture experiments. Finally we tried to quantify the importance of both organisms for the steady state behaviour of the system using ecological control analysis (ECA). ECA analyses were performed directly on the experimental data set, and indirectly, calculated from the rate equations derived for the kinetic models.

The chapter is divided into sub-sections, starting from parameter estimations for the core models describing pure cultures followed by parameter estimations incorporating oxygen into a further model for the description of oxygen limitation in *G. oxydans*. Furthermore, the results obtained from mixed population experiments are presented leading to the validation of the model and sensitivity analysis of the parameters derived in the previous sections. Finally, control analysis is presented and applied on our model ecosystem through direct elucidation of control structure from experimental data as well as from the theoretical models.

3.2 Parameter estimations for the core models describing pure cultures

3.2.1. Metabolic activity of *Saccharomyces cerevisiae*

In our approach to model a simple ecosystem consisting of two organisms linked via an intermediate we used a black box approach and described the catalytic activity of the organisms with a single rate equation. At high glucose concentrations *S. cerevisiae* is expected to convert glucose to ethanol and under aerobic conditions a relatively low percentage of glucose is expected to be completely oxidized to CO_2 (*9*). We incubated *S. cerevisiae*, under non-growing conditions, with a saturating glucose concentration at different biomass concentrations to estimate the specific rates of ethanol production and glucose consumption. In Figure 3.1(a) the concentrations of ethanol against time are plotted for three representative biomass concentrations. Figure 3.1(b) shows the concentrations of glucose over time for three representative biomass concentrations

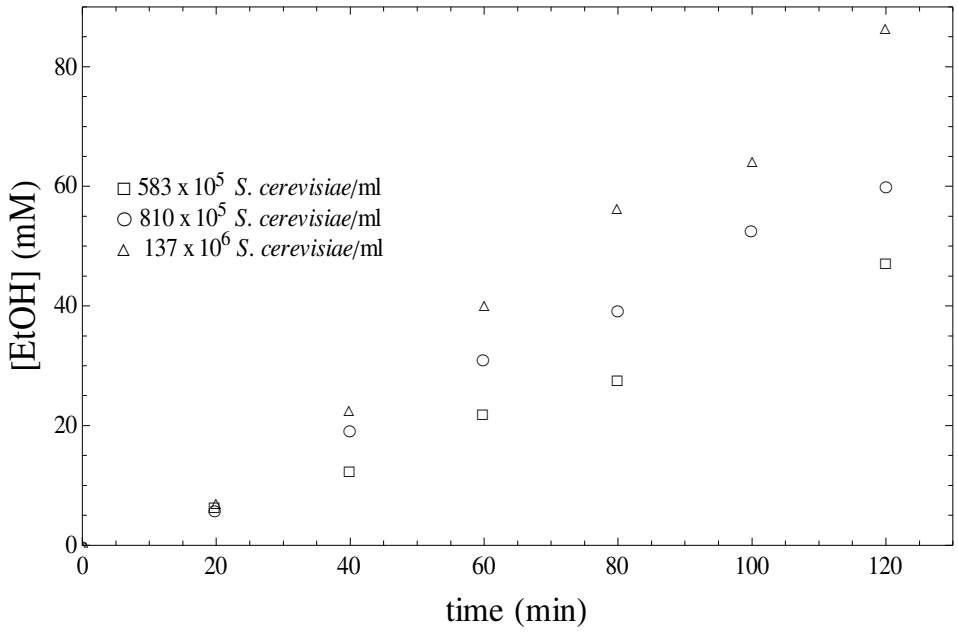

Figure 3.1(a): Ethanol production by *Saccharomyces cerevisiae*.

The plot shows the increase in ethanol over time in bioconversion assays with *S. cerevisiae* used for the determination of its metabolic activity in terms of ethanol production rate. The slopes from these plots, at saturating oxygen and glucose concentrations, were calculated and normalised for biomass (three representative biomass concentrations are shown – see legend) to calculate thespecific activity of *S. cerevisiae*.

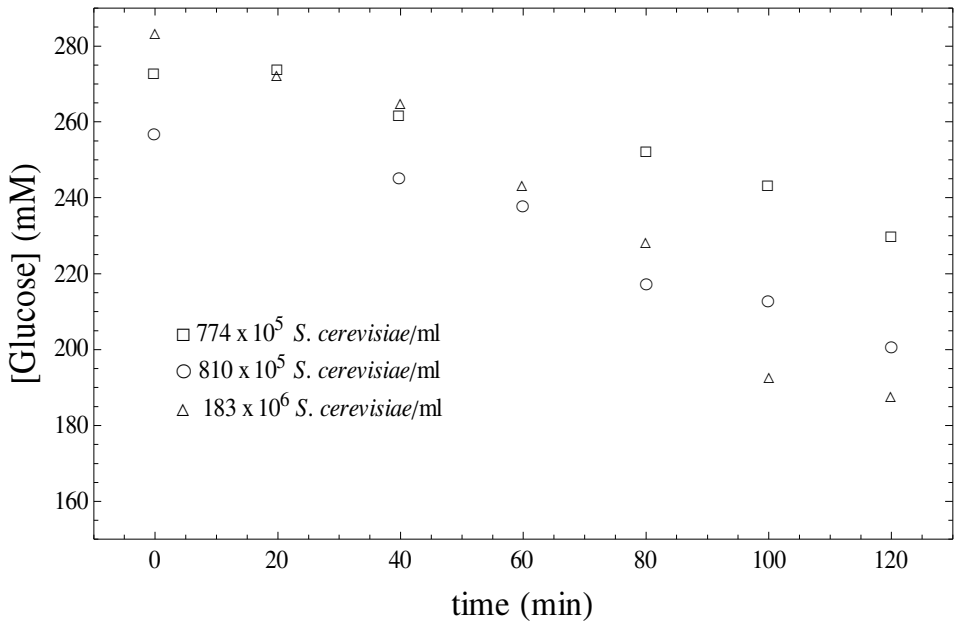

Figure 3.1(b): Glucose consumption by *Saccharomyces cerevisiae*.

The plot shows the decrease in glucose concentration over time in bioconversions assays with *S. cerevisiae* used for the determination of its metabolic activity as in Figure 3.1 (a)

The increase in ethanol was linear over time and production rates could be calculated from the slopes. As expected the rates were dependent on biomass concentration and when tested for a large number of incubations the ethanol production rate and glucose consumption rate were observed to be proportional with biomass concentration (Figure 3.2). From the slopes in Figure 3.2 a specific ethanol production rate (k_1) for *S. cerevisiae* of 1.16×10^{-8} µmol ethanol/cell/min and a specific glucose consumption rate (k_5) of 7.52×10^{-9} µmol glucose/cell/min were determined, respectively.

Since we did not observe a decrease in ethanol production rate at higher ethanol concentrations we decided to use the simplest possible rate equation for the ethanol production activity of *S. cerevisiae*:

$$v_1 = k_1 \bullet s_1 \quad (3.1)$$

(v_1 = the ethanol production rate of *S. cerevisiae*, k_1 = specific ethanol production rate of *S. cerevisiae*, s_1 = cell density of *S. cerevisiae* in cells/ml)

Glucose was always used at saturating concentrations in all further incubations in this thesis and treated as a constant external variable in the model.

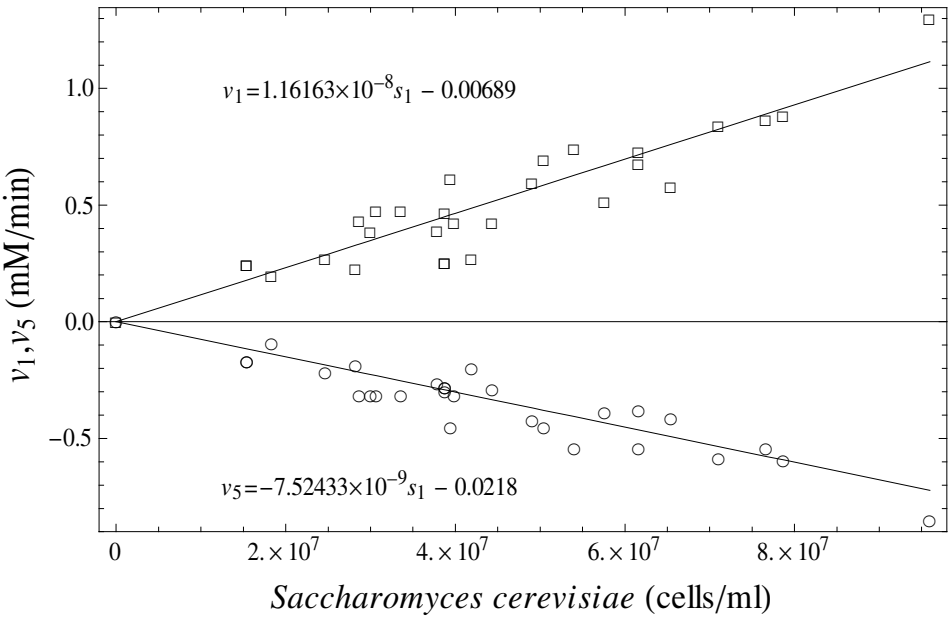

Figure 3.2: Specific glucose consumption and ethanol production rates for *Saccharomyces cerevisiae*.

(○) Glucose consumption- (v_5)and (□) ethanol production-(v_1) rates are shown as functions of cell density in pure culture bioconversion assays of *S. cerevisiae* under aerobic conditions. The slopes from these graphs were calculated as the specific activity for glucose consumption and ethanol production of *S. cerevisiae*, respectively. The fitted equations for each activity are included within the graphs.

3.2.2 Metabolic activity of *Gluconobacter oxydans*

G. oxydans converts ethanol to acetate and in addition the organism also oxidizes glucose to gluconate. We were specifically interested in the conversion of ethanol to acetate, as this is part of the "metabolic pathway" formed by *S. cerevisiae* and *G. oxydans*. Ethanol is a free variable of the system that in principle can vary from 0 to very high concentrations. Thus, in addition to a maximal ethanol consumption rate and the *G. oxydans* biomass concentration, we also needed to include an affinity constant of *G. oxydans* for ethanol to the rate equation describing the ethanol conversion rate.

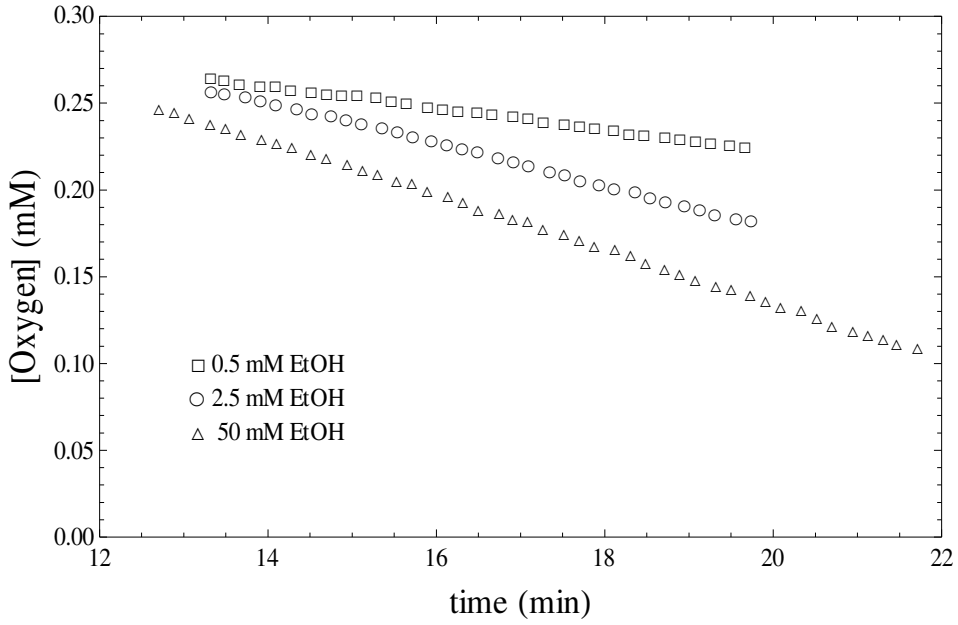

Figure 3.3: Oxygen consumption rate of *Gluconobacter oxydans*.

The decrease in oxygen contration over time in oxygraph assays used for the determination of ethanol sensitivity of *G. oxydans* at varying ethanol concentrations. The respiration rates at varying ethanol concentrations were calculated from the slopes of these plots and normalised with the biomass concentrations measured in each experiment (different symbols are used for each ethanol concentration as shown in the plot legend).

We used oxygraph experiments to determine oxygen consumption rates at a range of ethanol concentrations. In such experiments dissolved oxygen concentrations are followed over time and from the initial slope the oxygen consumption rates can be determined (see Figure 3.3). The oxygraph experiments were performed at low biomass concentration such that the ethanol concentrations did not vary significantly during the experiment. It is important to estimate the initial oxygen consumption rate before the ethanol concentration changes significantly. Oxygen consumption rates were estimated within 10 - 15 minutes, never resulting in a greater than 10 % concentration change in the ethanol concentration. The specific oxygen consumption rates at different ethanol concentrations are plotted in Figure 3.4 (for incubations without added glucose). On the premise that one mol of oxygen is consumed during the metabolism of one mol of ethanol to acetate, see Equation 3.2, one can calculate the specific ethanol consumption rate from the oxygen consumption rate (*20*).

$$\mathbf{1\ Ethanol + O_2 \rightarrow 1\ Acetate + 2\ H_2O} \quad (3.2)$$

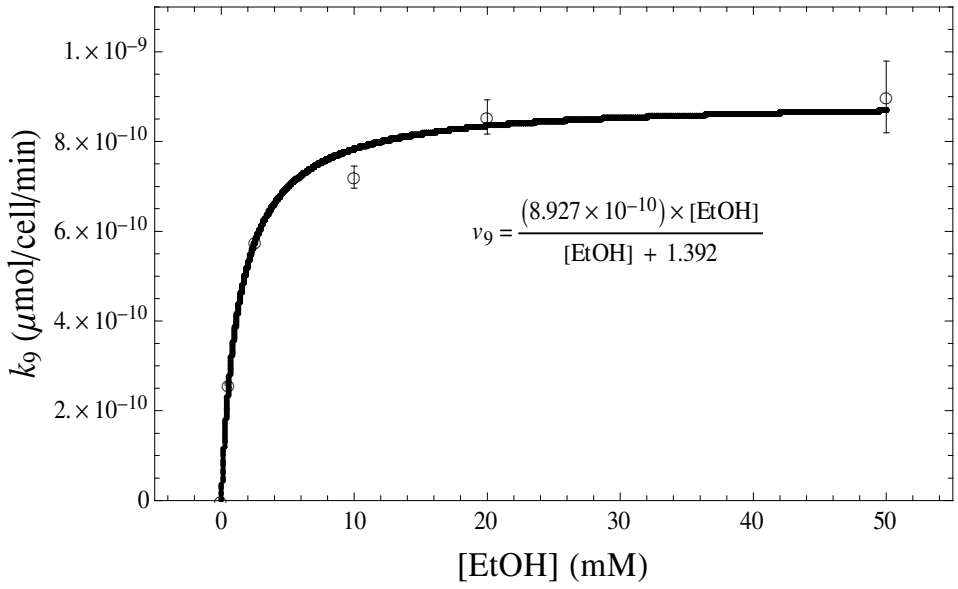

Figure 3.4: Specific oxygen consumption rate of *Gluconobacter oxydans*.

Specific respiration rates of *G. oxydans* are shown as a function of ethanol concentration (error bars represent the Standard error of the Mean for several experiments). The K_x of *G. oxydans* was calculated from non-linear fit of the Monod equation to the experimental values (shown as •) and the best fit was represented by the solid line through the data (the equation for this fit is included in the graph).

Using a non-linear fitting procedure in Mathematica 6, we fitted a hyperbolic function to the experimental data set. We used Equation 3.3 (a Monod or Michaelis Menten type equation) to describe the activity of *G. oxydans* as a function of the ethanol concentration (the resulting fit is shown in Figure 3.4).

$$v_2 = \frac{k_2 \bullet x(t)}{K_x + x(t)} \bullet s_2 \quad (3.3)$$

(x(t) = ethanol concentration, k2 = the specific activity of *G. oxydans* for ethanol, v2 = the rate of ethanol production by *G. oxydans*, K_x = the Monod (or Michaelis) constant for ethanol of *G. oxydans* and s2 = the cell density of *G. oxydans* in cells/mL)

The affinity of the organism for ethanol, expressed as a Monod (or Michaelis) constant was 1.39 mM. These measurements were performed in the absence of glucose. In the mixed culture incubations glucose was present, so we tried to estimate the affinity of *G. oxydans* for ethanol in the presence of saturating glucose concentrations. Due to a high respiratory activity of *G. oxydans* in the presence of glucose, it was not possible to measure a significant increase in oxygen consumption rate upon addition of ethanol. Therefore it was impossible to estimate the K_x of *G. oxydans* in the presence of glucose in these oxygraph experiments. Maximal oxygen consumption rates were 8.93×10^{-10} and 1.40×10^{-9} μmoles O_2/cell/min in absence or presence of glucose, respectively.

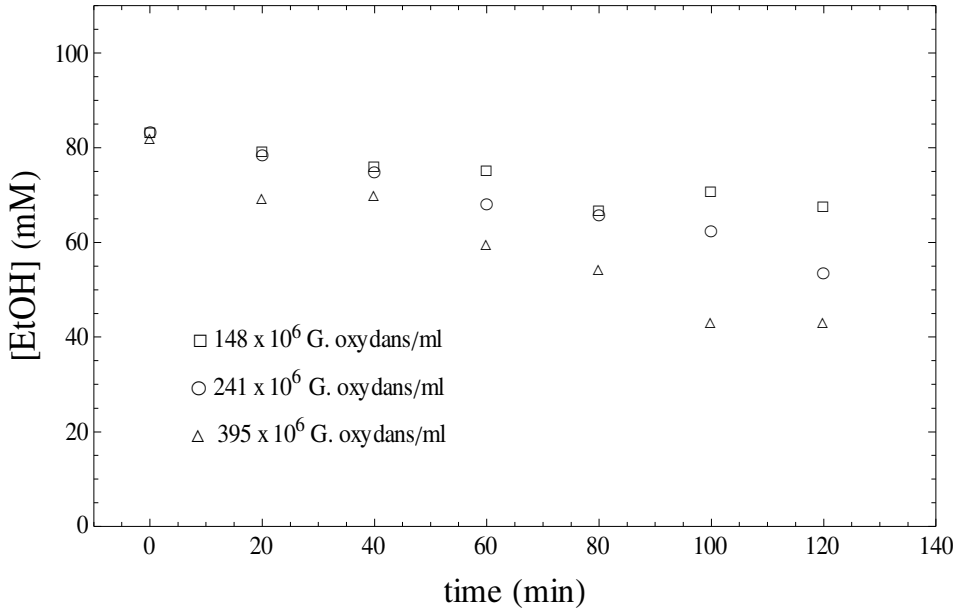

Figure 3.5 (a): The decrease in ethanol concentrations over time in bioconversion assays with *G. oxydans* used for the determination of its metabolic activity for ethanol at varying cell densities.

(each biomass is presented by a different symbol as can be seen from the legend of the graph).The slopes from these assays, at saturating oxygen, glucose and ethanol concentrations, were calculated and plotted against the biomass concentrations to derive the specific activity of G. oxydans for ethanol consumption (see Figure 3.6).

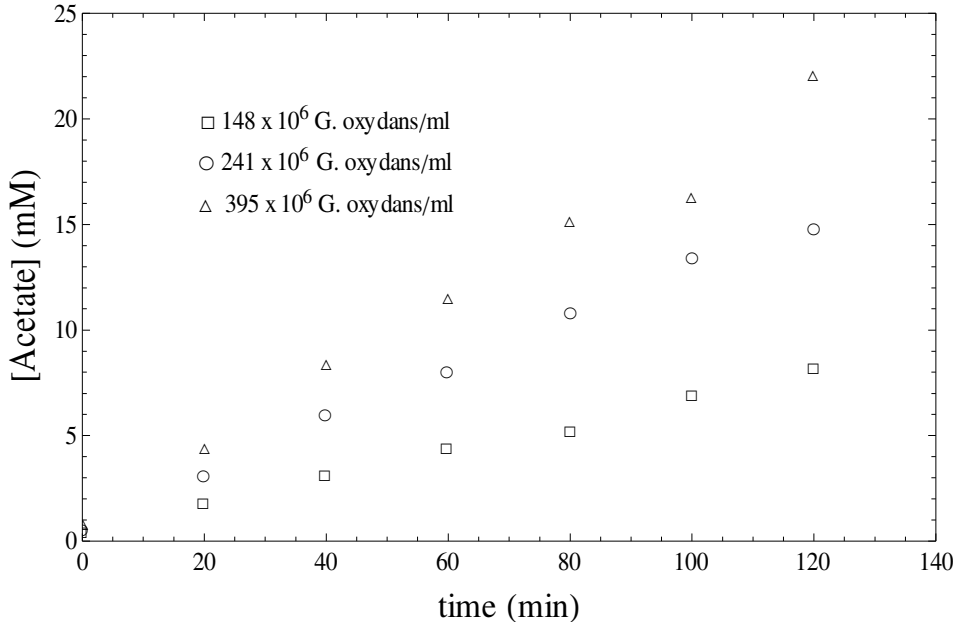

Figure 3.5 (b): The increase in acetate over time in bioconversion assays with *G. oxydans* used for the determination of its metabolic activity for acetate at varying cell densities.

(each biomass is presented by a different symbol as can be seen from the legend of the graph). The slopes from these assays, at saturating oxygen, glucose and ethanol concentrations, were calculated and plotted against the biomass concentrations to derive the specific activity of *G. oxydans* for acetate production (see Figure 3.6).

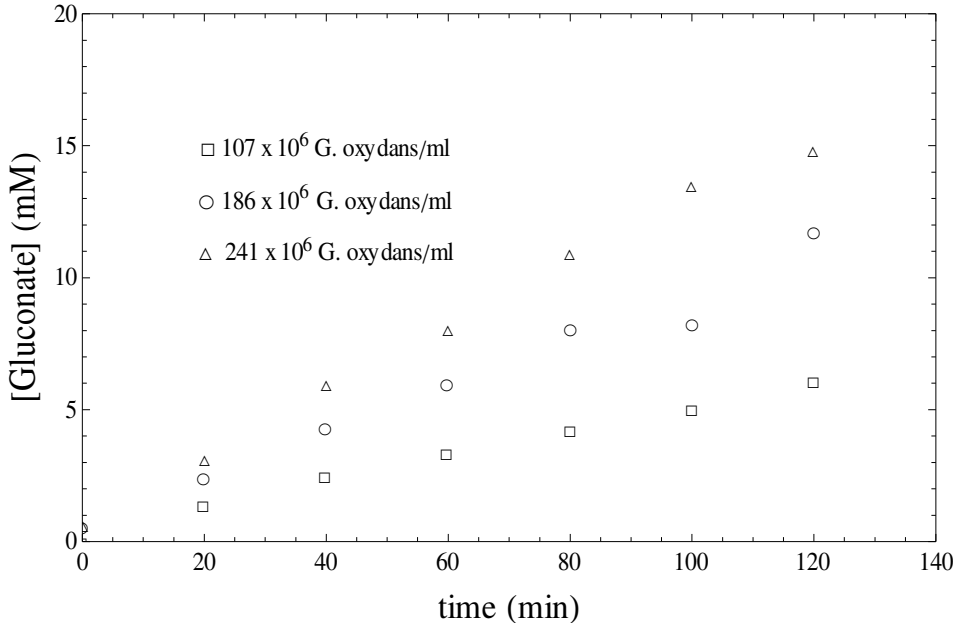

Figure 3.5 (c): The increase in gluconate concentration over time in bioconversion assays with *G. oxydans* used for the determination of its metabolic activity for gluconate at varying cell densities.

(each biomass is presented by a different symbol as can be seen from the legend of the graph). The slopes from these assays, at saturating oxygen, glucose and ethanol concentrations, were calculated and plotted against the biomass concentrations to derive the specific activity of *G. oxydans* for gluconate production (see Figure 3.6).

In addition to the conversion of ethanol to acetate *G. oxydans* also oxidized the available glucose to gluconate. In Figure 3.5 (a), (b) and (c), we show the ethanol consumption, acetate accumulation and gluconate accumulation against time for a number of relevant biomass concentrations. The substrate decrease and the product accumulation were linear with time over the 2-h experiment and the consumption/production rates were determined from the slopes of these graphs. Figure 3.6 shows the linear relation between ethanol consumption and acetate production as functions of the biomass concentration in cells/ml. The specific ethanol consumption rate (k_2) and gluconate (k_4) and acetate (k_3) production rates of *G. oxydans* were obtained by calculating the slope of the respective plots in Figure 3.6. Under these conditions the k_2 was 9.48×10^{-10} µmol ethanol/cell/min, k_3 was 4.89×10^{-10} µmol acetate/cell/min and the k_4 was 3.40×10^{-10} µmol gluconate/cell/min. By dividing k_3 with the k_2, an incomplete conversion of ethanol to acetate was observed with a stoichiometry of 0.516 mole acetate produced from one mole of ethanol consumed by *G. oxydans*. For the gluconate production rate we could use a linear rate equation as the glucose concentration was always maintained at saturating levels, and gluconate showed no inhibitory effects at the concentrations reached in our incubations. Equation 3.4 shows the kinetics used to describe gluconate production rate of *G. oxydans* in cells/ml.

$$v_4 = k_4 \bullet s_2 \quad (3.4)$$

(v_4 = gluconate production rate of *G. oxydans*, k_4 = specific gluconate production rate, s_2 = cell density of *G. oxydans* in cells/ml)

For the ethanol consumption rate we used equation 3.3, with the K_x value as determined in the oxygraph experiment and the k_2 value from the experiments presented in Figure 3.6. Note that we obtained comparable values for maximal ethanol consumption rates in the oxygraph experiment (8.93×10^{-10} µmol ethanol/cell/min) and for the specific ethanol consumption rate in the aeration funnel (conversion assay), 9.48×10^{-10} µmol ethanol/cell/min. In the conversion assay the cells were incubated with 85.5 mM ethanol which is saturating (and therefore the specific activity should be close to the V_{max}. We use the specific activity as determined in the bioconversion assay because these experiments were performed in the presence of saturating glucose concentrations that are closer to the conditions of mixed culture incubations. The good agreement between the specific activities, as determined in the oxygraph and the bioconversion assay, indicate that the assumption for ethanol to acetate conversion in the oxygraph (with the concomitant relation of 1 mol oxygen per mol of ethanol consumed) is valid.

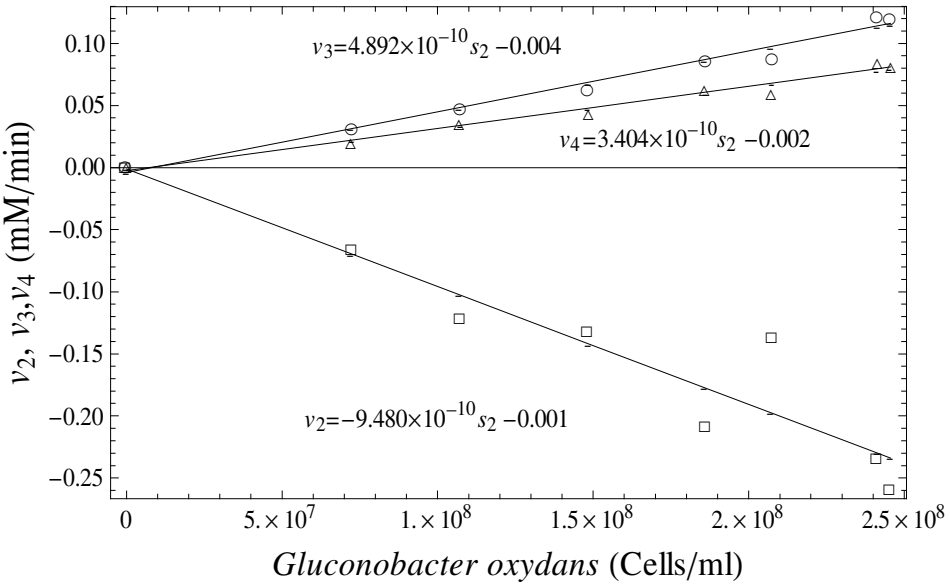

Figure 3.6: Metabolism of *G. oxydans* in bioconversion assays.

(□) Ethanol consumption rate, (○) acetate- and (Δ) gluconate production rates of *G. oxydans*, in bioconversion assays, as a function of cell-density in cells/ml. The slopes from these plots yielded the specific metabolic activities of *G. oxydans* for ethanol consumption, actetate and gluconate production, respectively.

3.2.3 Sensitivity of *S. cerevisiae* and *G. oxydans* for the metabolites present in mixed population experiments

Ultimately we wanted to use the models for the pure cultures to describe the mixed cultures and therefore we tested the sensitivity of yeast and *Gluconobacter* for all metabolites that we had observed in mixed cultures (at the typical concentrations that we observed during these incubations).

Both organisms were cultured in the standard buffer at varying starting concentrations of each tested metabolite. Initial ethanol-production and -consumption rates were then measured for *S. cerevisiae* and *G. oxydans*, respectively.

S. cerevisiae was tested for the effects of acetate at concentrations up to 80mM (Figure 3.7 (a) iii). Around 20mM of acetate, which is above the highest end-of-assay concentration (18 mM) for defined mixed population assays, we found the resulting inhibitory effect on the ethanol production rate to be below 5%.

S. cerevisiae was incubated with varying ethanol concentrations to measure the effect of this product on its metabolic activity. Up to 100 mM ethanol no significant inhibition of its production rate was observed. The highest ethanol concentration that was observed in the mixed incubations was below 25 mM.

Gluconate, which is a by-product of *G. oxydans* showed a small inhibitory effect (20 mM of gluconate caused a 3% reduction in the ethanol production rate). However the gluconate concentrations in mixed populations never reached such high values and were normally below 10mM.

In addition we also varied the substrate concentration (glucose) between 111 and 444 mM and it had a negligible effect on the metabolic activity of *S. cerevisiae* .

In summary, we observed the strongest inhibitory effect of acetate (at 50 and 80 mM) as is evident from Figure 3.7 (a)iii. However, at the concentrations observed in the mixed incubations (20 mM), none of the metabolites had a significant effect on the metabolic activity of *S. cerevisiae*. The inhibitory effects of the tested metabolites are summarized in Table 3.1

Table 3.1: Summary of sensitivity of *S. cerevisiae* for metabolites observed in mixed populations

Metabolites were tested at a range of concentrations (see Figure 3.7(a)), we here list the effect at the maximal concentration that was observed in mixed culture experiments

Metabolite	% Δk_1(experimental concentrations) μmol EtOH/cell/min
Ethanol (100 mM)	-3.1
Acetate (20 mM)	-3.6
Gluconate (20 mM)	-3.2
Glucose (111mM to 444mM)	0.2 to 0.5

Similarly, we measured the sensitivity of *G. oxydans* for acetate, gluconate and glucose. The effect of ethanol was already studied in section 3.2.2. As for *S. cerevisiae* we found very small effects on the metabolic activity of *G. oxydans* upon addition of 20 mM acetate (- 2%), or 50 mM gluconate (+ 7%). Higher concentrations of glucose, around 444 mM, inhibited the acetate production rate by 8.2%.

Table 3.2 summarizes the sensitivity of *G. oxydans* for metabolites present in mixed population experiments, at typical maximal concentrations observed in the mixed culture experiments

Table 3.2: Sensitivity of *G. oxydans* for metabolites observed in mixed populations

Metabolites were tested at a range of concentrations (see Figure 3.7(b)), we here list the effect at the maximal concentration that was observed in mixed culture experiments

Metabolite	% Δk_2 (experimental concentrations) μmol EtOH/cell/min
Acetate (20 mM)	1.815
Gluconate (50mM)	7
Glucose (111mM to 444mM)	0 to -8.2

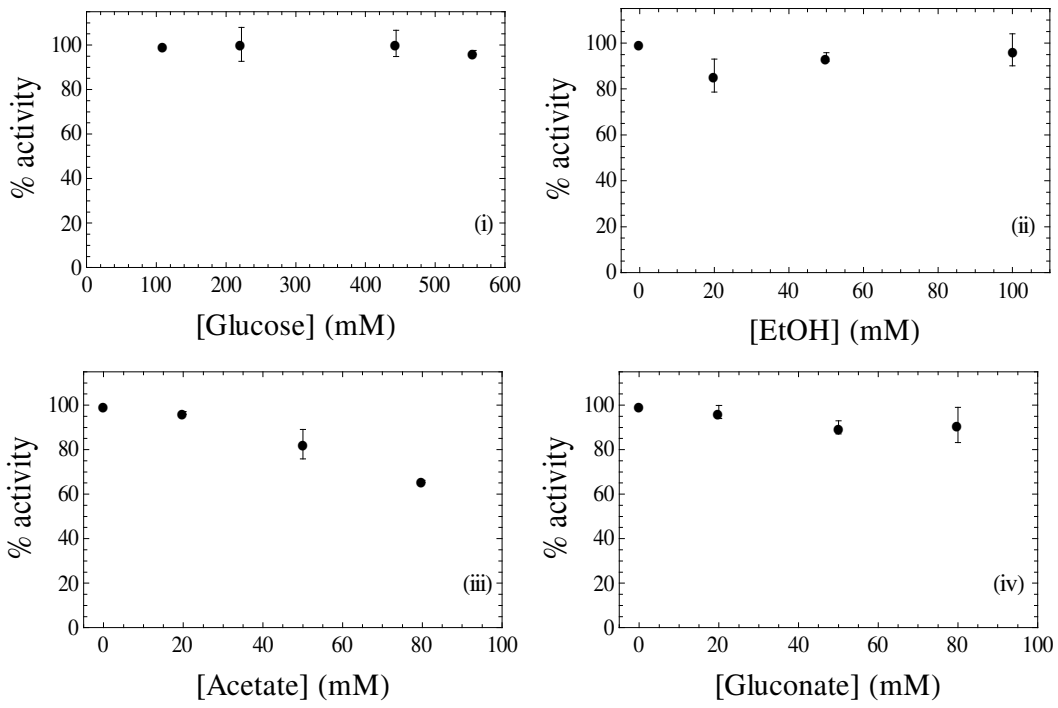

Figure 3.7 (a): Sensitivity of *S. cerevisiae* for (i) glucose, (ii) ethanol, (iii) acetate and (iv) gluconate.

The effect on metabolic activity is measured as % activity relative to the standard buffer conditions concentration (error bars represent the Standard error of the Mean for several experiments).

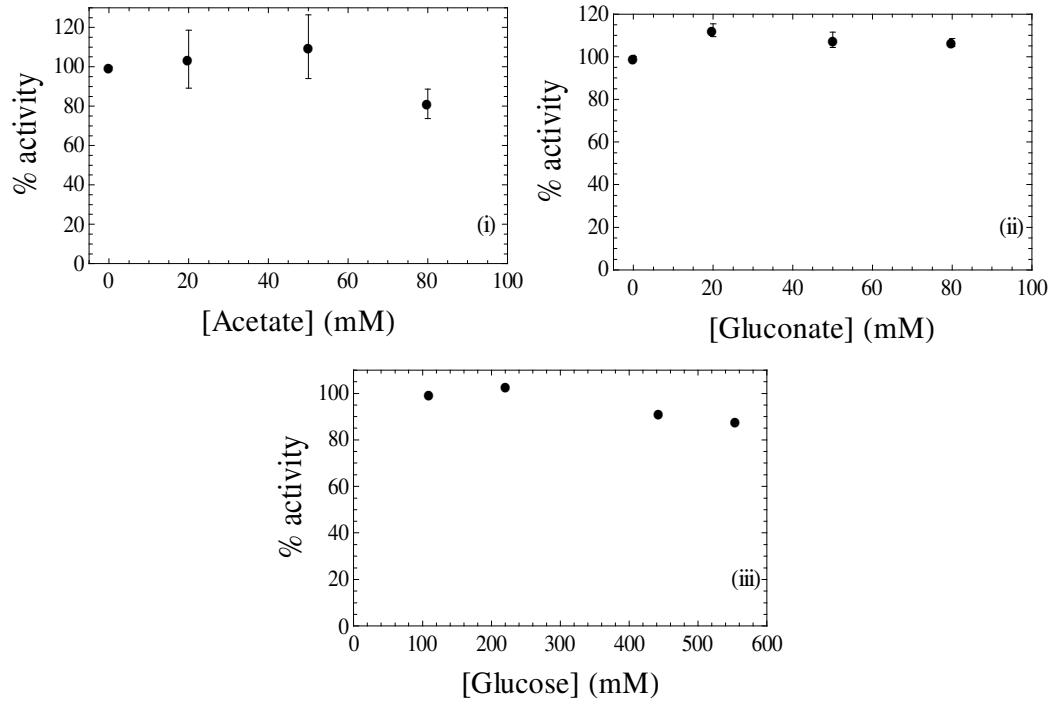

Figure 3.7 (b): Sensitivity of *G. oxydans* for (i) acetate, (ii) gluconate and (iii) glucose.

The effect on metabolic activity is measured as % activity relative to the standard buffer conditions concentration (error bars represent the Standard error of the Mean for several experiments).

3.3 Parameter estimations for the model description including oxygen

For the simplest model we did not include oxygen as a variable, i.e. we assumed its concentration to be saturating. At low biomass concentrations such an assumption is valid if sufficient oxygen is supplied to the cultures, but at higher biomass concentrations the oxygen transfer rate might become limiting. To be able to extend the simple model to include oxygen as a free variable, we needed to measure the kinetic constants for oxygen metabolism in yeast, *G. oxydans* and the oxygen supply by the aeration funnels.

3.3.1 Ethanol production and oxygen consumption of *S. cerevisiae*

At high glucose concentrations *S. cerevisiae* is not very responsive to oxygen; it converts glucose almost exclusively to ethanol, via fermentative pathways. For the simple model we estimated the specific ethanol production rate at saturating oxygen concentrations (section 3.2.1) and although a large fraction (77%) of the glucose consumed (k_5, 7.52×10^{-9} µmoles glucose/cell/min) was converted to ethanol (k_1, 1.16×10^{-8}µmoles ethanol/cell/min) this conversion was clearly not complete and we therefore looked into the effect of oxygen on glucose metabolism of *S. cerevisiae*. We first incubated *S. cerevisiae* under anaerobic conditions (cultures sparged with nitrogen instead of air), and measured the specific glucose consumption and ethanol/glycerol production rates. We tested the dependency of substrate consumption and product formation rates on biomass concentrations under anaerobic conditions. As under aerobic conditions we observed the metabolic activities to be proportional with biomass (Figure 3.8), but what was different from the aerobic incubations ($k_5 = 4.36 \times 10^{-9}$ µmol glucose/cell/min, $k_1 = 7.0 \times 10^{-9}$ µmol ethanol/cell/min, $k_6 = 8.28 \times 10^{-10}$ µmol glycerol/cell/min) was the completely fermentative metabolism. Thus, an almost complete (80% to ethanol and 19% to glycerol) conversion of glucose to ethanol and glycerol was observed, indicative that the incomplete conversion observed under aerobic conditions is due to oxidative metabolism of glucose since no glycerol was observed.

To include oxygen as a free variable in our kinetic model we needed to include the oxygen consumption rate of *S. cerevisiae* in addition to the ethanol production rate. We used the equations 3.1 and 3.5 respectively for the ethanol production and oxygen consumption, i.e. assuming a constant specific rate which was experimentally measured.

$$v_7 = k_7 \bullet s_1 \quad (3.5)$$

(v_7 = oxygen consumption rate of *S. cerevisiae*, k_7 = specific oxygen consumption rate of *S. cerevisiae*, s_1 = cell deinsity of *S. cerevisiae* in cells/ml)

The specific oxygen consumption rate of *S. cerevisiae*, was determined in an oxygraph as 5.20×10^{-10} µmol oxygen/cell/min. As the glucose consumption and ethanol production rates were linear to the concentration of *S. cerevisiae* even at high biomass (Figure 3.2), we felt justified in assuming that the oxygen, at the much lower biomass concentrations in mixed populations, was consumed at a constant specific rate.

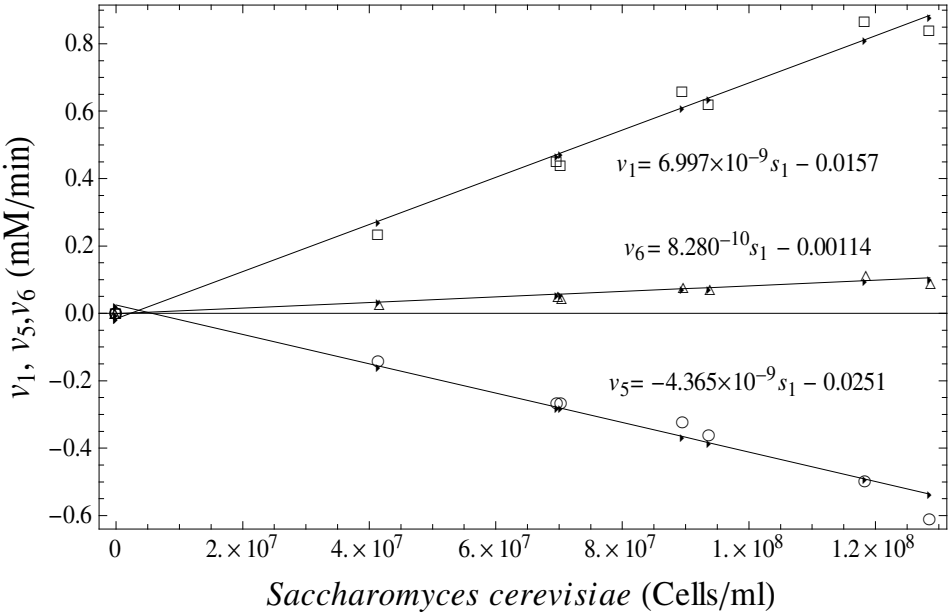

Figure 3.8:Metabolism of *S. cerevisiae* in anaerobic bioconversion assays.

(○)Glucose consumption-, (□) ethanol production- and (Δ) glycerol production rates as functions of cell density in anaerobic fermentations of *S. cerevisiae* performed in bioconversion assays. These values were calculated similar to those in Figure 3.2, but under anaerobic conditions, by sparging with nitrogen gas.

3.3.2 Ethanol and Oxygen consumption by *G. oxydans*

The oxygen dependence of *G. oxydans*, a strictly aerobic organism, was determined by measuring oxygen consumption during an oxygen run-out experiment in an oxygraph (with saturating glucose and ethanol concentrations). Figure 3.9 shows an example of such an oxygen run-out experiment (oxygen concentration is defined as o(t)). The respiration rate was calculated from the gradient in Figure 3.9 and Michaelis-Menten kinetics were fitted on the results using a direct non-linear fit with Mathematica 6 (Figure 3.10). The affinity for oxygen, K_o, and specific respiration rate, k_9, were estimated to be 0.0114 mM +/- 0.0013 (SEM) (for 3 experimental dates the values were: 0.0101 mM, 0.0139 mM, 0.0101 mM) and 1.08×10^{-9} µmol oxygen/cell/min +/- 1.6×10^{-10} (SEM)(for 3

experimental dates the initial respiration rates were: 1.42×10^{-9}, 1.0×10^{-9}, 8.14×10^{-10} µmol oxygen/cell/min), respectively

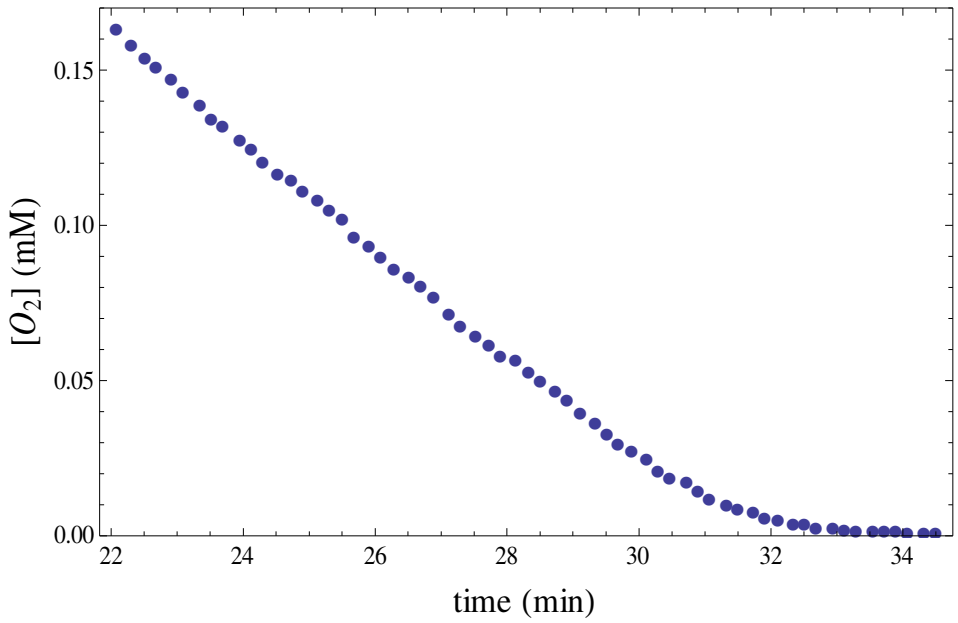

Figure 3.9: An example of an oxygen run out experiment by *G. oxydans* running from saturating to complete oxygen depletion over time.

(The initial respiration rates were calculated as the slope over the initial linear range of these types of data sets)

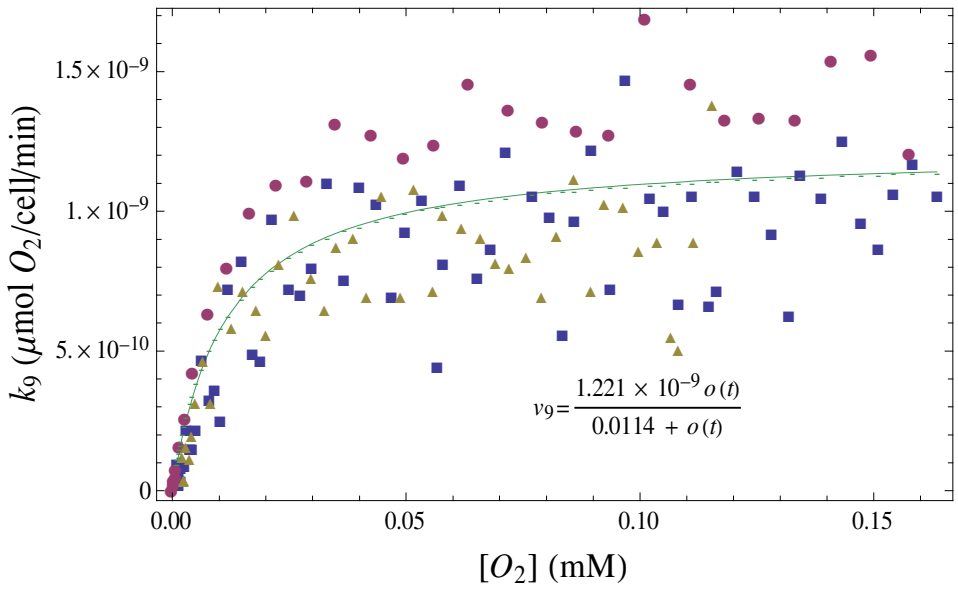

Figure 3.10: Respiration rate of *G. oxydans* as a function of oxygen concentration.

The K_o was calculated from the non-linear fit through all data sets indicated by the solid line and described by the equation included.

For yeast a proportional relation between substrate consumption / product formation rates and biomass was observed, under aerobic as well as anaerobic conditions. For *G. oxydans* we observed

a similar proportional relation between specific substrate consumption and product formation rates at low biomass concentration (Figure 3.6), but at higher biomass concentrations (> 2.5×10^8 cells/ml) no further increase in volumetric consumption / production rates were observed with increasing biomass concentrations (Figure 3.11). A possible reason for the decrease in specific activity of *G. oxydans* at higher biomass concentrations could be that the cells become oxygen limited. Oxygen consumption by *G. oxydans* can be calculated from the specific product formation rates of gluconate and acetate.

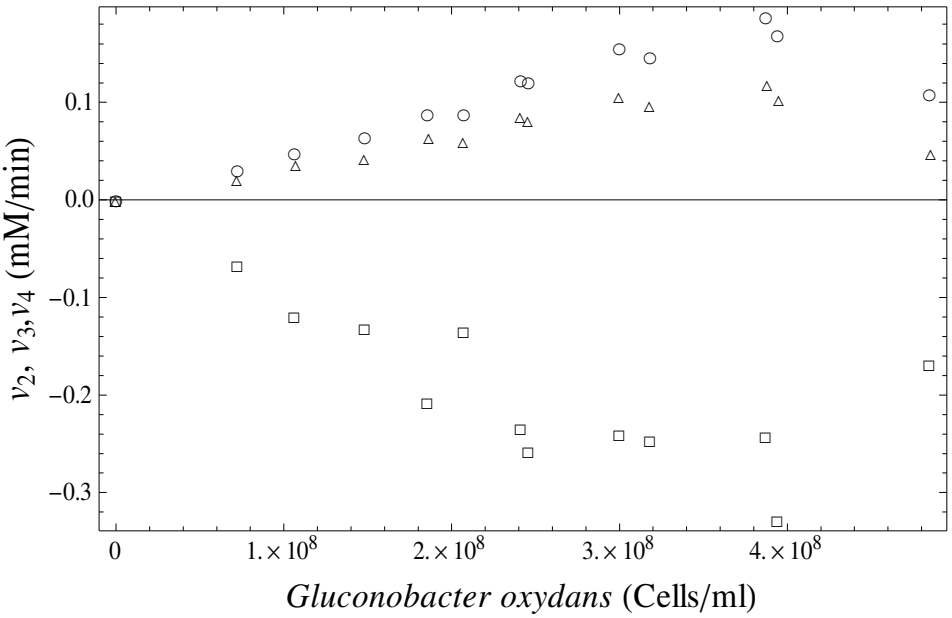

Figure 3.11: Metabolic activity of *G. oxydans* at higher biomass concentrations.

The lack of a linear relation between (□) v_2, (○) v_3 and (Δ) v_4 against cell density at higher biomass concentrations of *G. oxydans* when compared to Figure 3.7 are clearly exhibited

Per mole of gluconate formed, half a mole of oxygen (O_2) is consumed (see Section 1.1.1 and Figure 1.2 in Chapter 1 based on the work of Basseguy *et al.* (*36*)) and thus we could calculate the specific rate of oxygen consumption, k_9 ,through glucose oxidation pathway as 1.7×10^{-10} μmoles O_2/cell/min (50% of the v_4).We assumed this value as a constant at saturating oxygen concentrations as found in the mixed population assays because the concentrations of *G. oxydans* was kept well below the level where oxygen limitation was observed in pure cultures (highest mixed population biomass = 1.1×10^8 cells/ml compared to the oxygen limited concentration of above 2.5×10^8 cells/ml). The oxygen dependent ethanol consumption (v_{10}), acetate production (v_{11}) and gluconate production (v_{12}) rates are presented by equations 3.6 and 3.7, respectively. These equations are extensions of Equation. 3.3 and 3.4, respectively, which described the same process under oxygen saturation conditions.

$$v_{10} = \frac{k_2 \bullet x(t) \bullet o(t) \bullet s_2}{K_x \bullet K_o + K_o \bullet x(t) + K_x \bullet o(t) + x(t) \bullet o(t)} \quad (3.6)$$

$$v_{12} = \frac{k_4 \bullet o(t) \bullet s_2}{K_o + o(t)} \quad (3.7)$$

(x(t) = Ethanol concentration, o(t) = oxygen concentration, v_{10} = oxygen dependent ethanol consumption rate of *G. oxydans*, k_2 =specific ethanol consumption rate of *G. oxydans*, v_{12} = oxygen dependent gluconate production rate of *G. oxydans*,
k_4 =specific gluconate production rate of *G. oxydans*, K_x = Monod constant of *G. oxydans* for ethanol, K_o = Monod constant of *G. oxydans* for oxygen, s_2 =cell density of *G. oxydans* in cells/ml)

3.3.3 Oxygen transfer in the aeration funnels

To fully describe the changes in concentration of dissolved oxygen in the aeration funnel, we must not only take the oxygen consumption by the micro-organisms but also the oxygen influx through aeration into account. Oxygen influx in the system can be described by the oxygen transfer coefficient (K_La) and the difference between the actual oxygen concentration, o(t), and the oxygen concentration at saturation, $o(t)_{sat}$ (e.g. Pirt (*80*)); $do/dt = K_L a\ (o(t)_{sat} - o(t))$. The saturating oxygen concentration, $o(t)_{sat}$, at our working temperature, 30°C, was calculated to be 0.235 mM O_2, using Truesdale's empirically derived equation (*80*)

Under steady state conditions the oxygen influx rate must be equal to the oxygen consumption rate, i.e. $do/dt = 0$. Thus, under such conditions $K_L a\ (o(t)_{sat} - o(t))$ must be equal to the oxygen consumption rate by the micro-organisms. We measured specific oxygen consumption rates (q_{O2}) for *G. oxydans* in oxygraph-assays (see Section 3.3.2). Using the above steady state constraint we could calculate the $K_L a$ for our experimental set-up by measuring the steady state dissolved oxygen concentration at different biomass concentrations. Note that the assumption is made that the q_{O2} remains constant and this is reliant on high enough oxygen concentrations to prevent the oxygen concentration to become limiting to the respiration rate of *G. oxydans*. For this reason the $K_L a$ was determined from values above $10 \times K_o$ of *G. oxydans*, i.e. where the oxygen concentration was above 0.1 mM. In Figure 3.13 we show dissolved oxygen concentrations (o(t)), as measured with an oxygen electrode during the incubation, at different oxygen consumption rates (J_{O2}) (i.e. specific oxygen consumption rate times biomass), where these oxygen consumption rates were varied by varying the biomass concentration. From Equation 3.8 a linear relation is expected between o(t) and J_{O2}, with a slope equal to $-1/K_L a$ and a y-axis intercept equal to $o(t)_{sat}$.

$$o(t) = \frac{-1}{K_L a}(q_{O2} \bullet s_2) + o(t)_{sat} \quad (3.8)$$

(o(t) = oxygen concentration, $K_L a$ = oxygen transfer coefficient in aeration funnels, s_2 =cell density of *G. oxydans* in cells/ml, q_{O2} = specific oxygen consumption rate of *G. oxydans*)

The y-axis intercept, as estimated from the experimental data points (0.237), is very close to the calculated value of 0.235 mM. From Figure 3.13 a $K_L a$ value of 2.139 L/min was calculated.

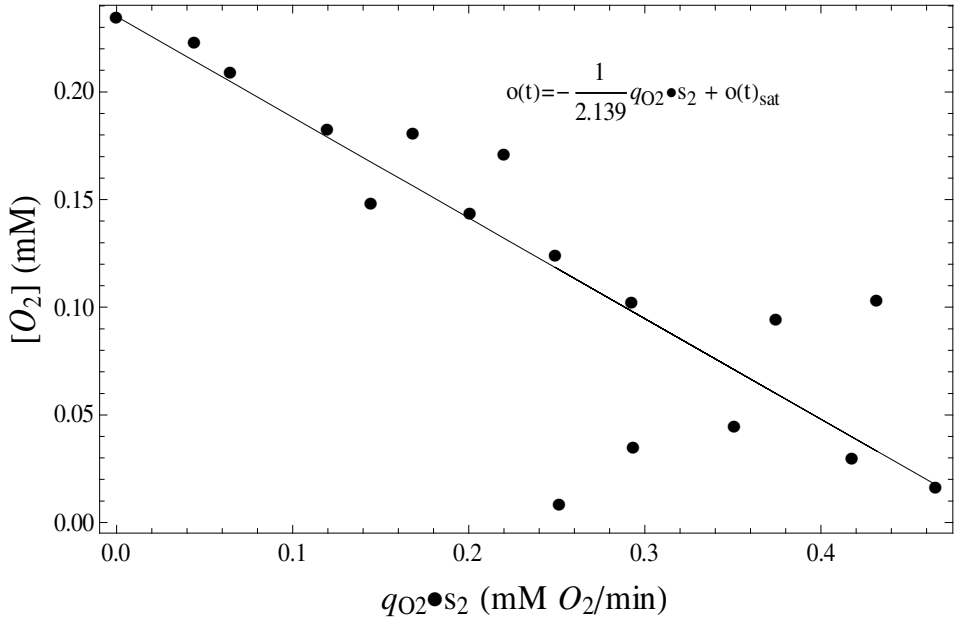

Figure 3.12: Dissolved oxygen concentration as a function of the oxygen consumption rate used in the characterization of the aeration funnels in terms of oxygen supply.

The oxygen consumption rate of *G. oxydans* was varied by changing the biomass concentration. The dissolved oxygen concentration o(t) was measured with an oxygen electrode. A line was fitted to the data points, with as y-axis intercept the o(t) at zero biomass, i.e. $o(t)_{sat}$, and as slope $-1/K_L a$ (see Equation 3.8).

The inclusion of oxygen in the model is essential when oxygen becomes limiting for the micro-organisms, e.g. at high biomass concentrations. With the extended model it should be possible to predict at what biomass concentration the oxygen concentration will become limiting and where the proportionality between biomass and product formation rate should no longer hold (i.e. Figure 3.11). In Figure 3.13 we have plotted the same data points as shown in Figure 3.11, but now included the model prediction, using the parameter values as listed in Table 3.3 and the set of differential equations for the model were (Equations 3.9 to 3.12):

$$\frac{dx}{dt} = -v_{10} \quad (3.9)$$

$$\frac{dy}{dt} = 0.516 \bullet v_{10} = v_{11} \quad (3.10)$$

$$\frac{dz}{dt} = v_{12} \quad (3.11)$$

$$\frac{do}{dt} = v_8 - v_{10} - 0.5 \bullet v_{12} \quad (3.12)$$

(x(t) = ethanol concentration, y(t) = acetate concentration, z(t) = gluconate concentration, v_8 = rate of oxygen supply by aeration funnels, v_{10} = oxygen dependent ethanol consumption of *G. oxydans*, v_{11} = oxygen dependent acetate production rate of *G. oxydans*, v_{12} = oxygen dependent gluconate production rate of *G. oxydans*)

The stoichiometry of 0.516 in Equation 3.10 reflects the incomplete conversion of ethanol to acetate by *G. oxydans* as observed in pure culture experiments (Section 3.2.2). Furthermore, *G. oxydans* consumes half a mole of oxygen per mole gluconate, z(t), produced and that stoichiometry is reflected in Equation 3.12 (see Sections 1.1.1 and 3.3.2). With the metabolic rates for ethanol and gluconate represented by Equations 3.6 and 3.7, respectively.

The rate of oxygen supply is defined by Equation 3.13:

$$v_8 = K_L a\left(o(t)_{sat} - o(t)\right) \quad (3.13)$$

(o(t) = oxygen concentration, v_8 = rate of oxygen supply by aeration funnels, $K_L a$ = oxygen transfer coefficient of aeration funnels)

The model predicts the levelling off of the specific substrate consumption rate and product formation rates with a good accuracy (Figure 3.13). Here it should be realized that the model parameters were not fitted to this experiment but were determined independently. The experiment and model simulation are in excellent agreement with the hypothesis that the deviation from a proportional relation between biomass and product formation rates at higher biomass concentrations is due to oxygen limitation.

Table 3.3 lists the parameters that were measured for the pure culture metabolic activities and aeration funnel characteristics.

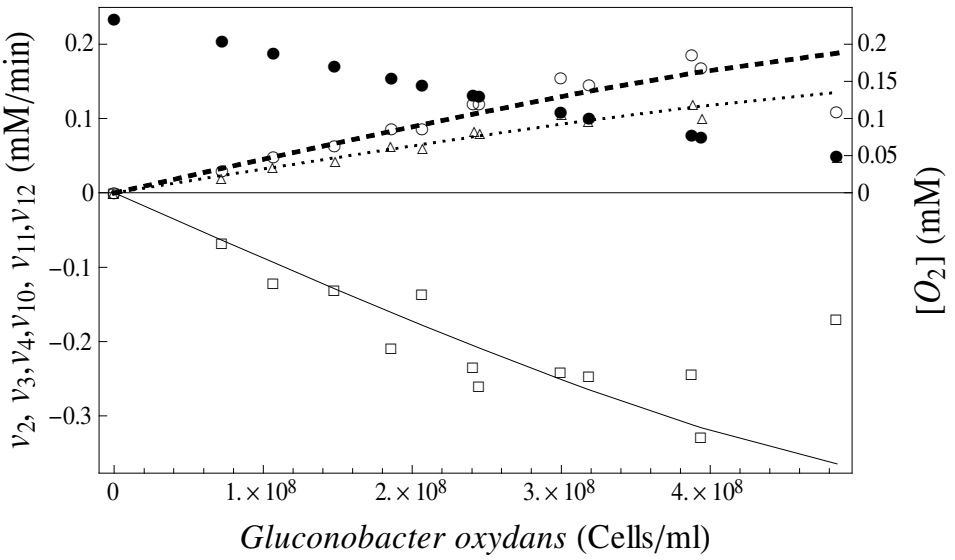

Figure 3.13:Metabolic activity of *G. oxydans* at high biomass concentration, including the model prediction.

The model prediction of oxygen limited metabolism of *G. oxydans* is validated by the experimental data. (□) experimental ethanol consumption rates (v_2), solid line for model predicted ethanol consumption rates (v_{10}), (○) experimental acetate production rates (v_3), dashed line for model predicted acetate production rates (v_{11}), (Δ) experimental gluconate production rates (v_4), dotted lines for model predicted gluconate production rates (v_{12}). The model (●) predicted oxygen concentrations are shown for reference.

Table 3.3: Parameters derived, from pure culture assays, for the more complex description of mixed populations of *S. cerevisiae* and *G. oxydans* including oxygen.

Aeration funnels	
$o(t)_{sat}$	0.23686 mM
K_La	2.33622 L/min^{-1}
S. cerevisiae	
k_1	1.162×10^{-8}µmol ethanol/cell/min
k_7	5.195×10^{-10}µmol oxygen/cell/min
G. oxydans	
k_2	9.480×10^{-10}µmol ethanol/cell/min
K_x	1.392 mM
K_o	0.0114 mM
$k_{.4}$	3.404×10^{-10} µmol gluconate/cell/min

3.4 Results obtained from mixed population studies

3.4.1 Obtaining a steady state

The basic assumption in our mixed population studies was that *S. cerevisiae* and *G. oxydans* interact only via ethanol and that the sensitivity of the two organisms for the intermediate would result in a quasi steady-state condition where the product concentrations, acetate and gluconate will increase with time but the intermediate ethanol concentration would reach a constant level, where its synthesis by *S. cerevisiae* is balanced by the consumption through *G. oxydans*. This was tested by incubating the two strains under aerobic conditions at saturating glucose concentrations and measuring all external metabolite concentrations over time. The results of a typical experiment are shown in Figure 3.14, where a steady state in ethanol concentration was reached after ca 200 minutes.

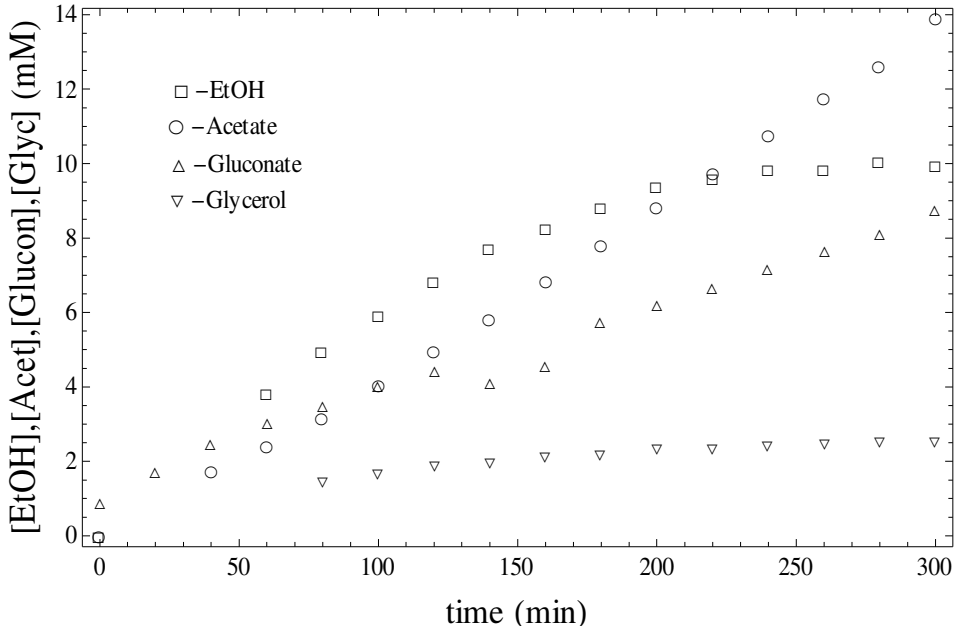

Figure 3.14: A typical mixed culture experiment where *S. cerevisiae* and *G. oxydans* reached a quasi steady state with respect to ethanol concentration and acetate flux.

The variations in all metabolites except glucose over time are shown with different symbols depicting each of the metabolites (see plot legend).

After testing the system for reaching a steady state, we were interested in whether we could experimentally determine the control of both organisms on the steady state ethanol concentration and steady state flux.

3.4.2 Influence of *S. cerevisiae: G. oxydans* ratios on the concentration of the intermediary metabolite, ethanol.

S. cerevisiae and *G. oxydans* were incubated at different relative biomass and the ethanol and acetate concentrations were followed over time until a steady state was reached. Note that the total microbial concentrations between experiments also varied. In Figure 3.15 the ethanol accumulation over time was plotted with the yeast over G*luconobacter* ratio detailed in the legends of each plot. Each plot represented the data for a specific experimental day, henceforth defined as an experimental group. With increasing ratios an increase in the steady state ethanol concentration was observed, together with an increase in time before steady state was reached. For incubations that had not reached a steady state during the experiment, but that showed a clear curvature in ethanol accumulation, an estimation of the steady-state ethanol concentration was made by using a second order polynomial.

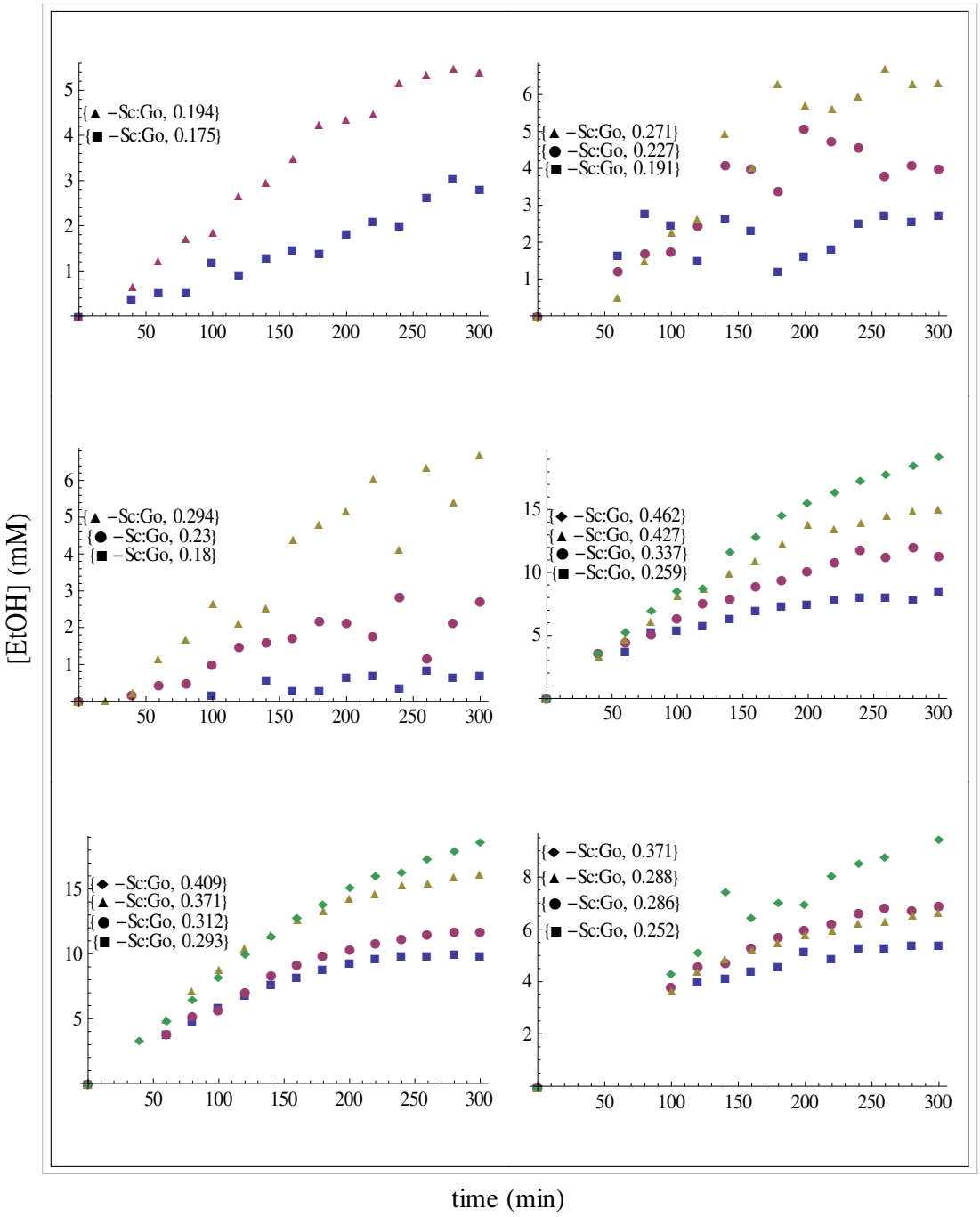

Figure 3.15: Increase in ethanol concentration over time up to a quasi-steady state in mixed population studies. Each experimental group are plotted separately with the *S. cerevisiae*:*G. oxydans* ratios represented by different symbols (included in the legend of each plot). Within experimental groups, due to an increase in the ratio of *S. cerevisiae* to *G. oxydans*, an increase in the ethanol concentration at this steady state can be observed.

In Figure 3.16 we plotted the steady state ethanol concentration as a function of the *Saccharomyces* to *Gluconobacter* ratio. The equation used for the data fit was derived on the assumption that yeast was not sensitive for ethanol and for *Gluconobacter* we assumed a hyperbolic saturation curve for ethanol. At steady state the ethanol production rate by yeast must equal the ethanol consumption by *Gluconobacter*. Using a product insensitive equation for yeast, Equation 3.1, and a Monod equation for *Gluconobacter*, Equation 3.3, we can solve for the steady state ethanol concentration ($[EtOH]_{stst}$)

by following the logical steps from Equation 3.14 to 3.16. Equation 3.14 shows the ordinary differential equations for the change in ethanol concentration:

$$\frac{dx}{dt} = k_1 \bullet s_1 - \frac{k_2 \bullet x(t)}{K_x + x(t)} \bullet s_2 \quad (3.14)$$

(k_1 = specific ethanol production rate of *S. cerevisiae*, s_1 = cell density of *S. cerevisiae* in cells/ml, k_2 = specific ethanol consumption rate of *G. oxydans*, s_1 = cell density of *G. oxydans* in cells/ml,x(t) = ethanol concentration, K_x = Monod constant of *G. oxydans* for ethanol)

However, at steady state the ethanol concentration remains constant and yields Equation 3.15:

$$\frac{dx}{dt} = 0 \left(\text{steady state}\right) \quad (3.15)$$

From Equations 3.14 and 3.15 one can now solve for the steady state ethanol concentration, Equation 3.16:

$$x(t)_{\text{stst}} = \frac{\frac{k_1}{k_2} \bullet \frac{s_1}{s_2} \bullet K_x}{1 - \frac{k_1}{k_2} \bullet \frac{s_1}{s_2}} \quad (3.16)$$

(k_1 = specific ethanol production rate of *S. cerevisiae*, s_1 = cell density of *S. cerevisiae* in cells/ml, k_2 = specific ethanol consumption rate of *G. oxydans*, s_1 = cell density of *G. oxydans* in cells/ml,x(t) = ethanol concentration, K_x = Monod constant of *G. oxydans* for ethanol)

Fitting Equation 3.16 on the experimental data points yields the following parameters k_1/k_2 = 1.5 and K_x = 10.06 mM. Thus to obtain a good fit to the experimental data points with the above assumptions for ethanol production and consumption rates for yeast and *Gluconobacter*, the ratio of proportionality between k_1 and k_2 was 1.5 and the Monod constant for ethanol of *Gluconobacter* was 10 mM. These values were significantly different from the values obtained for the pure cultures where yeast had a 10 fold higher specific activity than *Gluconobacter* and the latter species had a 7 fold higher affinity for ethanol (Section 3.2.2).

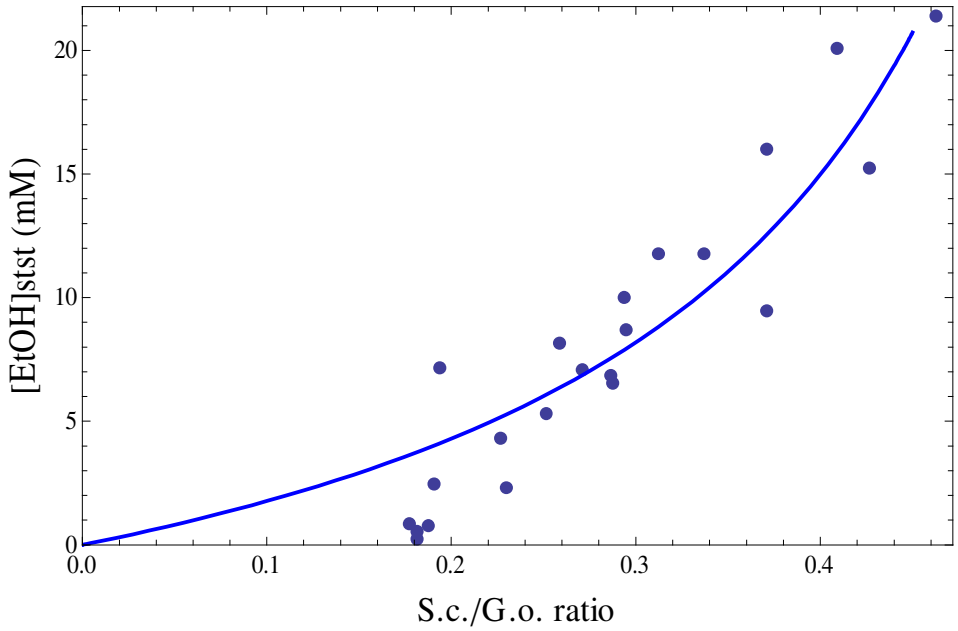

Figure 3.16: Steady-state ethanol concentrations as a function of the ratio between *S. cerevisiae* and *G. oxydans*. The fitted Equation 3.16 is shown as a solid line through the data, with $k_1/k_2 = 1.5$ and $K_x = 10$

3.4.3 Correlation of acetate production rate with *Saccharomyces cerevisiae* biomass.

In the same incubations for which we measured the steady state ethanol concentrations we also determined the acetate production rate. Since we determined in pure cultures that yeast was insensitive for ethanol concentrations well above the ones we obtained in the mixed cultures it follows that yeast will have full flux control. We tested this in our incubations by keeping the *Gluconobacter* concentration relatively constant and making the larger perturbations in the yeast concentration. Figure 3.17 shows the acetate production in mixed population assays over time for all mixed population assays.

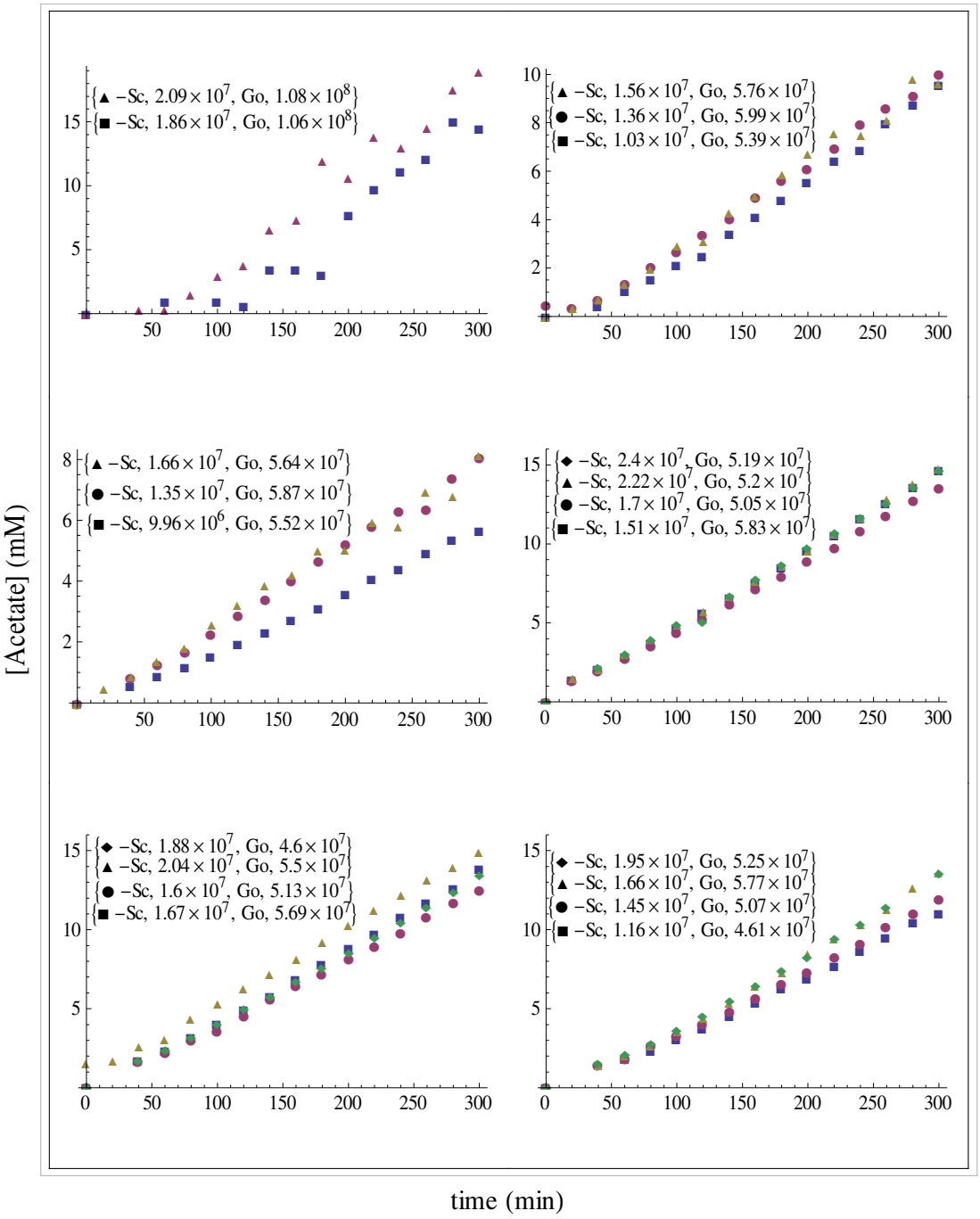

Figure 3.17 Increase in Acetate concentrations as measured over time in mixed population assays.

Each experimental group is presented separately with biomass concentrations of *S. cerevisiae* and *G. oxydans* included for reference (see legend in each graph).

In Figure 3.18 we plot the acetate production rate against yeast (Figure 3.18a) and *Gluconobacter* (Figure 3.18b) concentrations. Clearly the fit in Figure 3.18a is much better ($R^2 = 0.6$) than the fit in Figure 3.18b ($R^2 = 0.15$). Whereas the flux is proportional with the yeast concentration there appears to be no significant increase in acetate flux upon doubling the *Gluconobacter* concentration.

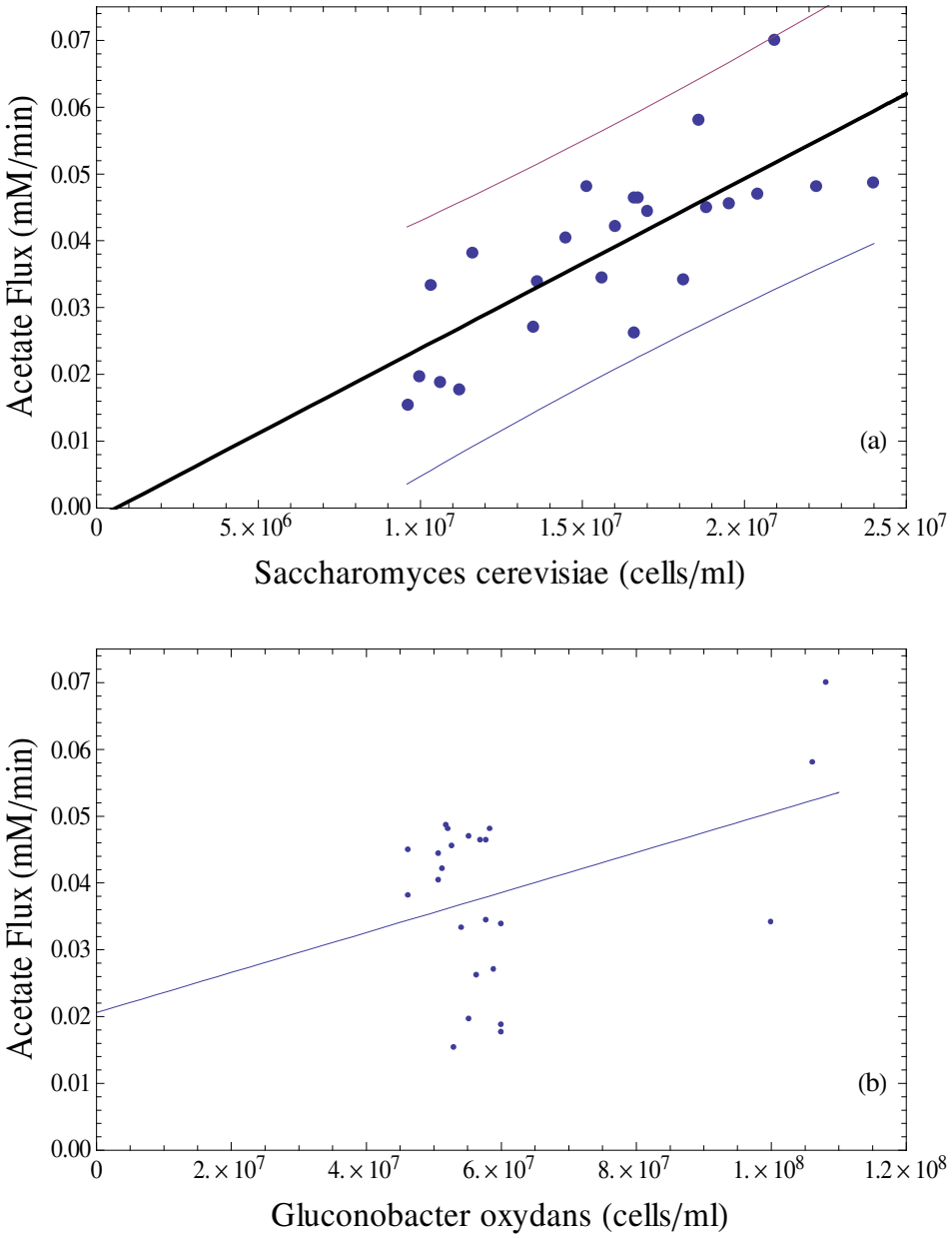

Figure 3.18: Acetate production as a function of *S. cerevisiae* (a) and *G. oxydans* (b) concentrations.

Linear regressions were made for the acetate production rate against the *S. cerevisiae* concentration (a) and the *G. oxydans* concentrations (b). The flux was proportional to the yeast concentration ($J_{Acetate} = 2.54 \times 10\text{-}9 \times$ [S. cerevisiae] - 0.0016, R2 = 0.6) while a very weak correlation was observed for *G. oxydans* ($J_{Acetate} = 3 \times 10^{-10} \times$ [*G. oxydans*] + 0.02, R2 = 0.15). The dashed lines parallel to the regression trendline in (a) illustrates the 95% confidence levels.

From the correlation between the *S. cerevisiae* concentration and the acetate production rate it appears as if yeast has full flux control. This can be understood from the insensitivity of the organism for ethanol, which allows yeast to set the pace, which *Gluconobacter* must follow. The communication between the two organisms is via ethanol, and the concentration of this intermediate will attain such a value that *G. oxydans* has the same activity as yeast, i.e. if *G. oxydans* has a higher activity than yeast ethanol will decrease until *G. oxydans* reaches the same activity as yeast.

From this reasoning one would expect a good correlation between the steady state acetate production and the ethanol concentration. Indeed in Figure 3.19 we have plotted such a relation and obtain a typical hyperbolic saturation curve of *G. oxydans* activity (measured as specific acetate production rate) with the steady state ethanol concentration. From this data set a K_x of 1.7mM could be estimated.

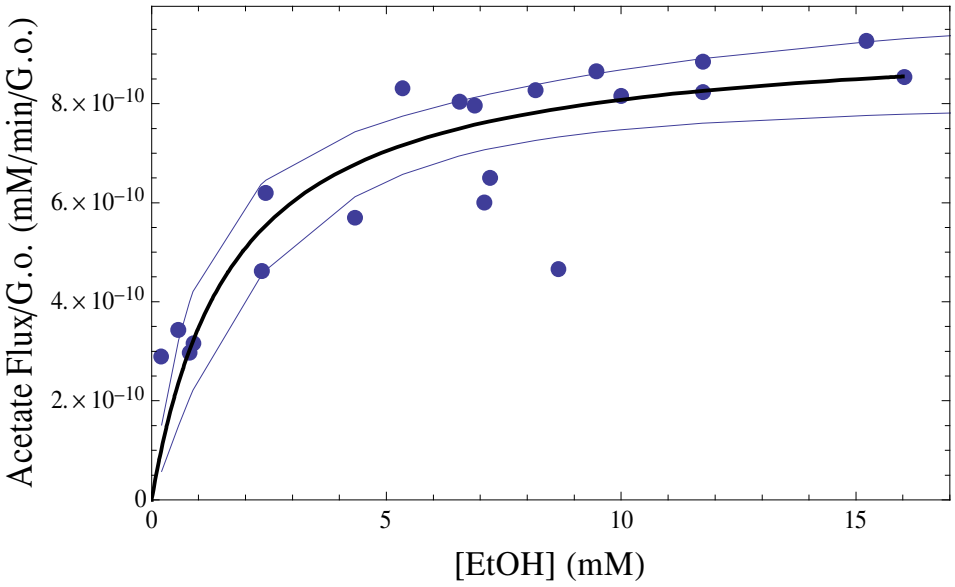

Figure 3.19: Correlation between acetate flux normalised with *G. oxydans* and ethanol concentration as measured in mixed populaion studies.

The Monod-type curve observed was used to estimate a K_x for *G. oxydans* in mixed population assays, of 1.7 mM.

3.4.4 Comparing kinetic parameters for pure and mixed cultures

From the pure cultures we estimated kinetic parameters for yeast in the conversion of glucose to ethanol (k_1= 1.16× 10^{-8} µmol EtOH/cell/min) (Section 3.2.1, Figure 3.2) and for *Gluconobacter* in the conversion of ethanol to acetate (k_2= - 9.48 × 10^{-10} µmol EtOH/cell/min and K_x = 1.392 mM EtOH) (Section 3.2.2, Figure 3.6).

From the mixed cultures we could estimate from the steady state ethanol data the ratio of k_1/ k_2= 1.5, and the K_x for *Gluconobacter* = 10 mM (Section 3.4.2). In addition from the $J_{Acetate}$ we could estimate a kinetic rate constant for yeast of 2.54 × 10^{-9} µmol Acetate/cell/min and K_x for *Gluconobacter* of 1.7 mM (Section 3.4.3)

In the pure cultures we observed a stoichiometry of 0.516 in the conversion of ethanol to acetate by *Gluconobacter oxydans* (Section 3.2.2). Assuming the same stoichiometry in the mixed cultures, the observed acetate production rate is equivalent to an ethanol production rate by yeast of 2.54×10^{-9} / $0.516 = 4.93 \times 10^{-9}$ μmol EtOH/cell/min. Using the ratio between the specific activities of yeast and *Gluconobacter* of 1.5, we can calculate a specific activity for *Gluconobacter* of 4.54×10^{-9} / 1.5 = 3.28×10^{-9} μmol EtOH/cell/min. Thus, for yeast we measure a 2 fold lower activity in the mixed cultures, while *Gluconobacter* is roughly 3 times more active, albeit with a lower affinity for ethanol. When steady-state ethanol concentrations are used this difference is significant, i.e. K_x of 10 mM compared to 1.4 mM.

In the next section we will compare model simulations for the mixed cultures with both parameter sets, and test the sensitivity for model parameter values on the simulation result. First we need to extend the model from the pure culture to the mixed culture set up.

3.5 Model validation and sensitivity analysis

Our working hypothesis, i.e. the only interaction between *S. cerevisiae* and *G. oxydans* is via ethanol, can be tested by comparing model predictions of mixed cultures with experimental data. Before (Section 3.4.4) we already noticed that the parameters obtained by a direct fit to experimental data on the mixed cultures differed from the values obtained with pure cultures, indicating that the predictive power of models based on pure culture experiments might not be very good. Here we test the simple model developed in Section 3.2 (excluding oxygen), which can be used since we kept biomass concentrations sufficiently low such that oxygen will not become limiting. We will use parameter values obtained on the pure cultures and parameter values obtained with the steady state mixed cultures to describe the dynamics of the interaction between *S. cerevisae* and *G. oxydans*.

The model needed to be extended to combine the activity of both organisms, leading to the following set of differential equations:

$$\frac{dx}{dt} = v_1 - v_2 \quad (3.17)$$

$$\frac{dy}{dt} = 0.516 \bullet v_2 \quad (3.18)$$

(v_1 = ethanol production rate of *S. cerevisiae*, v_2 = ethanol consumption rate of *G. oxydans*)

The rate equations for ethanol production by *S. cerevisiae*, v_1, and its consumption by *G. oxydans*, v_2, are defined by Equations 3.1 and 3.3, respectively. The stoichiometry of 0.516, in Equation 3.18, again reflects the incomplete conversion of ethanol to acetate by *G. oxydans*. The parameters k_1, k_2 and K_x have been measured in pure cultures (Section 3.2) and estimated from steady state mixed culture experiments (Section 3.4).

When using the parameter values as measured for the pure cultures in model simulations for the mixed cultures no steady state is obtained, with ethanol continuously increasing in concentration. This is not in agreement with the experimental observations where a steady state ethanol concentration was obtained after circa 5 hours. The absence of a steady state in the model simulations can be understood from the ODEs for the mixed cultures and the kinetic constants for ethanol production and consumption together with the ratios of *S. cerevisiae* and *G. oxydans*. With the estimated values for the pure cultures of $k_1 = 1.16 \times 10^{-8}$, $k_2 = 9.48 \times 10^{-10}$, it is not possible to get a steady state ethanol concentrations at ratios of *S. cerevisiae*/*G. oxydans* above 0.081 (k_2/k_1). The ratios used in the mixed culture experiments ranged between 0.175 and 0.462, and would thus not lead to steady state in the model simulations.

The parameters estimated from the steady state ethanol concentration and acetate production did lead to steady state when used in model simulations, as was to be expected due to the nature of the experimental data set (i.e. steady state data). The test whether these parameters would give a good description of the mixed cultures is still important as it is a validation for the capabilities of the model to describe the dynamics of the experimental system. Thus, whereas the parameters were fitted for the steady state ethanol concentration and acetate production rate, they were not fitted for the dynamics.

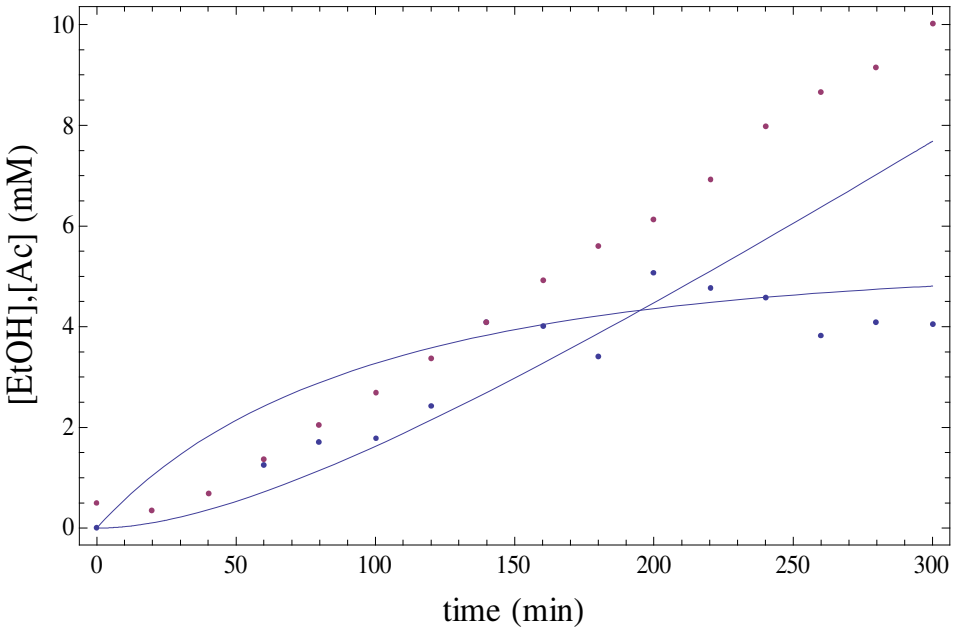

Figure 3.20: Model description of a representative mixed population study, based on parameters calculated from steady-state ethanol data from mixed cultures, accompanied by its corresponding experimental data.

The solid line represents the model description, the blue dots represent measured ethanol concentrations and the purple dots represent the measured acetate concentrations.

Figure 3.20 shows a typical example of a model simulation using the parameter values that were obtained on fitting to the steady state ethanol concentration and acetate production rate (Section 3.4). Typically the ethanol concentrations are overestimated in the beginning of the time simulation and the acetate concentrations are underestimated. The characteristics to which the parameters were fitted were the steady state ethanol concentration, and the acetate production rate. This was evident from most of the simulations; i.e. correct description of ethanol at the end of the simulation and a correct description of the change in acetate concentration with time (slope, not necessarily the absolute concentration). But even when using the parameter values fitted to the steady state data, this did not always lead to a good description of the data sets, and we were interested in testing the sensitivity of the model simulations for changes in the parameter set.

We started with fitting the model parameters to each of the experimental incubations to determine what the variance in these values would be. With this we tested whether the model could describe the experimental data set, not whether the model could predict the data. The fitted parameters of all experiments are summarised in Table 3.4.

Table 3.4 Parameters calculated from each mixed population experiment, separately

S. cerevisiae (cells/mL)	*G. oxydans* (cells/mL)	k_1 (μmol EtOH/cell/min)	k_2 (μmol EtOH/cell/min)	K_x (mM)
1.86×10^{7}	1.06×10^{8}	4.43369×10^{-9}	1.279×10^{-9}	1.38308
2.09×10^{7}	1.08×10^{8}	5.79227×10^{-9}	1.23771×10^{-9}	0.834827
9.59×10^{6}	5.28×10^{7}	2.31768×10^{-9}	2.02451×10^{-8}	12.9218
1.81×10^{7}	9.99×10^{7}	2.64747×10^{-9}	1.93357×10^{-8}	19.7504
1.06×10^{7}	5.98×10^{7}	3.07604×10^{-9}	3.18049×10^{-9}	4.14115
1.12×10^{7}	5.98×10^{7}	2.81872×10^{-9}	1.18624×10^{-9}	0.963161
1.03×10^{7}	5.39×10^{7}	6.0684×10^{-9}	1.11183×10^{-8}	20
1.36×10^{7}	5.99×10^{7}	5.53761×10^{-9}	1.35131×10^{-9}	0.901288
1.56×10^{7}	5.76×10^{7}	5.1911×10^{-9}	1.40923×10^{-9}	1.24003
9.96×10^{6}	5.52×10^{7}	3.53782×10^{-9}	7.37768×10^{-10}	0.1
1.35×10^{7}	5.87×10^{7}	4.02034×10^{-9}	9.27072×10^{-10}	0.185596
1.66×10^{7}	5.64×10^{7}	4.38606×10^{-9}	1.2935×10^{-9}	1.24053
1.51×10^{7}	5.83×10^{7}	8.04323×10^{-9}	2.36887×10^{-9}	2.52268
2.22×10^{7}	5.20×10^{7}	6.50784×10^{-9}	2.78548×10^{-9}	4.62245
1.67×10^{7}	5.69×10^{7}	7.27362×10^{-9}	2.44328×10^{-9}	3.7419
1.60×10^{7}	5.13×10^{7}	7.55305×10^{-9}	2.36223×10^{-9}	3.47042
2.04×10^{7}	5.50×10^{7}	7.64014×10^{-9}	2.83909×10^{-9}	5.17668
1.16×10^{7}	4.61×10^{7}	7.46045×10^{-9}	2.356×10^{-9}	2.05071
1.45×10^{7}	5.07×10^{7}	6.61349×10^{-9}	2.02554×10^{-9}	1.66507
1.66×10^{7}	5.77×10^{7}	6.25932×10^{-9}	2.05342×10^{-9}	1.78883
	Average	5.36×10^{-9}	4.13×10^{-9}	4.44
	SEM	3.73×10^{-10}	1.1×10^{-9}	1.4

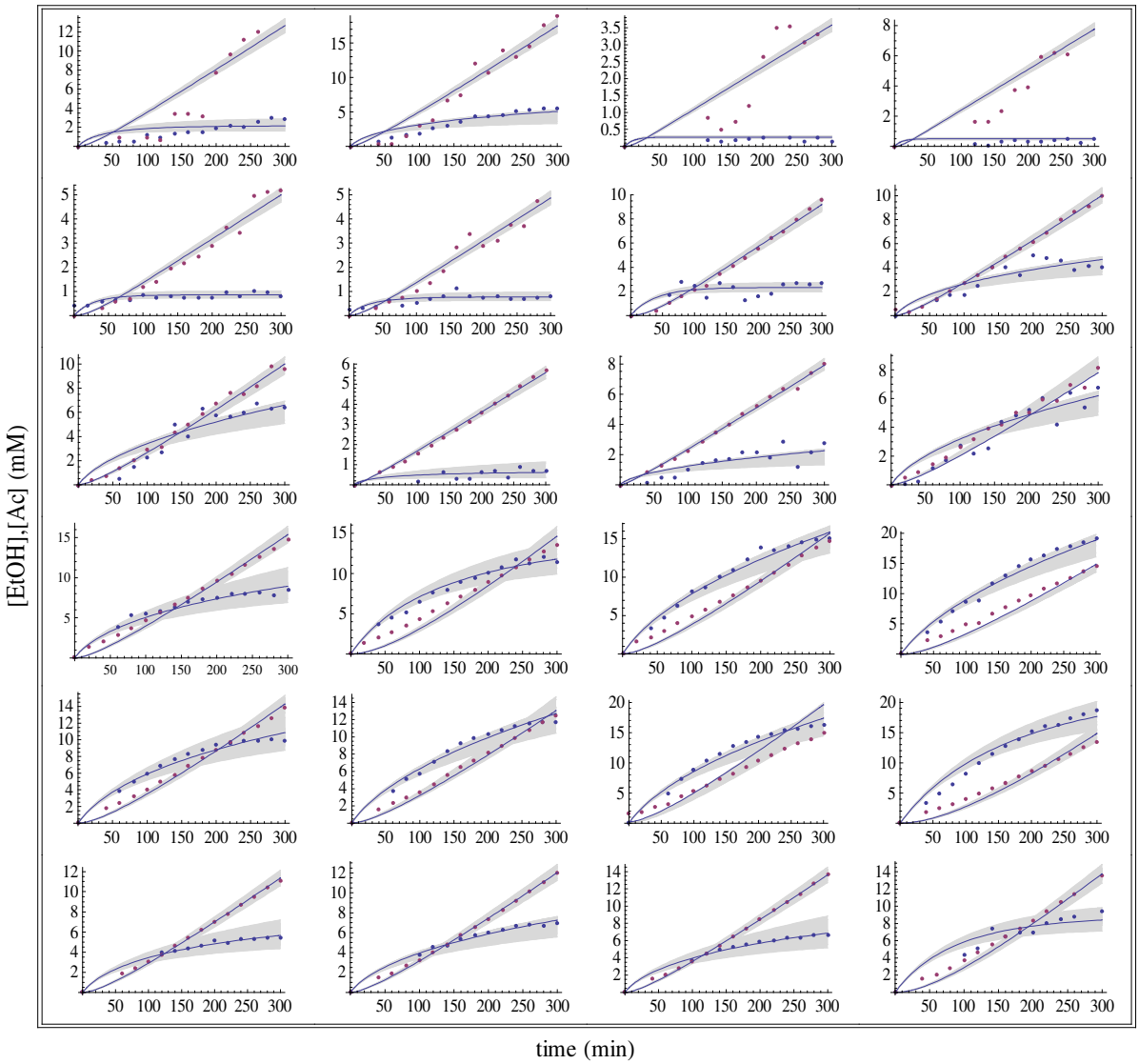

Figure 3.21 Best fits to individual mixed incubations of *S. cerevisiae* and *G. oxydans*. The model equations were fitted to each individual mixed incubation, using k_1, k_2, and K_{EtOH} as fitting parameters.

For the biomass concentrations the experimentally determined values were used. The drawn line shows the model simulation with the best fit for the parameter values; the shaded area indicate the region of acetate and ethanol concentrations that can be obtained when a 5% error value is allowed on the parameter values. Experimentally determined acetate and ethanol concentrations are indicated with purple symbols and blue symbols respectively.

We used two methods to fit the model to the experimental data set, for both methods we wrote an objective function (sum of the squared differences between experimental data points and model simulation) that we tried to minimize with a constraint variation of k_1, k_2 and K_x. For the first method we used time integration for the model simulation and the fitting algorithm was based on a steepest decent method (see Chapter 2 for details). This method gave essentially the same results but was much slower than the second method for which we used a symbolic solution to the ODEs of the model. This solution (see Chapter 2 for details), obtained via the Mathematica DSolve function, was rather complex but worked very fast in the fitting algorithms. For method 2 we used the NMinimize function of Mathematica as fitting algorithm.

Figure 3.21 shows the best fit of the simple model to each individual experiment. Most of the experiments could be fitted accurately to the model but the variance between the parameters for the best fit to each of the individual experiments was considerable. For four experiments the fitting procedure would always result in the upper boundary for the K_x value, indicating that those data sets had insufficient information for an accurate estimation of that parameter. We excluded these four experiments for our parameter estimation. Subsequently we fitted all experimental data together; this was to test whether a single parameter set could describe the complete data set. The best fit to the complete experimental data set with a single parameter set was obtained with the following parameter values: $k_1 = 5.55 \times 10^{-9}$ µmol EtOH/min/cell, $k_2 = 4.82 \times 10^{-9}$ µmol EtOH/min/cell, K_x = 13.4096 mM. For most of the mixed culture experiments the acetate production could be described fairly well using a single parameter set for all simulations but a significant error was observed for the ethanol production, specifically at low (<1 mM) and high (> 10 mM) ethanol concentrations, significant over-and under-estimation of the experimental data was apparent, respectively (Figure 3.22).

For the fitting procedure we used the symbolic solution to the model ODEs obtained with the Mathematica function DSolve (Chapter 2). The objective function (sum of squared differences) was minimized for all experimental data of the mixed incubations with k_1, k_2 and K_x as fitting parameters.

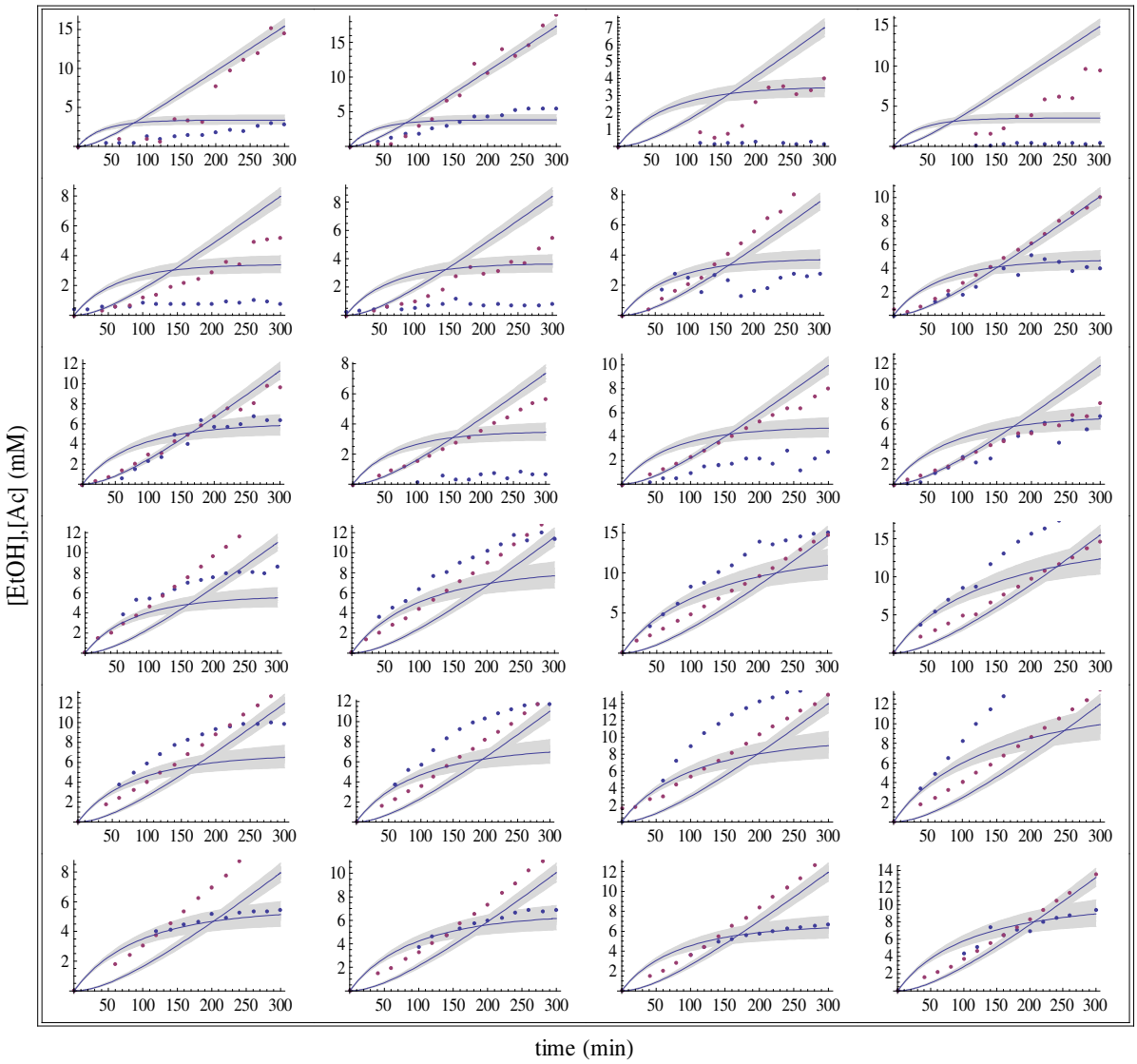

Figure 3.22 Best fits to the total set of mixed incubations of *S. cerevisiae* and *G. oxydans*: The model equations were fitted to all mixed incubations simultaneously, using k_1, k_2, and K_{EtOH} as fitting parameters.

For the biomass concentrations the experimentally determined values were used. The drawn line shows the model simulation for the parameter value set with the best fit to all mixed incubation experiments; the shaded areas indicate the region of acetate and ethanol concentrations that can be obtained when a 5% error value is allowed on the parameter values. Experimentally determined acetate and ethanol concentrations are indicated with purple symbols and blue symbols respectively.

In summary, we have determined kinetic parameters for the kinetic model describing the interaction between the two organisms using a number of different methods. First, we estimated from the pure cultures the specific activities and dependencies for ethanol (and all other systems variables). The measurement of the kinetic constant from the pure cultures is the most direct and would be preferred above the indirect estimations of kinetic constant from the mixed culture experiments. However, the kinetic constants as measured for the pure cultures could not be used directly for the description of the mixed cultures, as was clear from the absence of a steady state when the parameters were used in a kinetic model. For the second and third method to estimate the kinetic constants we used the mixed culture experiments. The second method used the steady state estimations obtained in the mixed incubations and the third method involved a fit on the time course

towards the steady state. We here summarize the different kinetic constants as obtained with the three methods in Table 3.5:

Table 3.5 Summary of parameters calculated from all methods

Method of determination	k_1 (μmol EtOH/cell/min)	k_2 (μmol EtOH/cell/min)	K_x (mM)
Pure culture experiments	1.162×10^{-8}	9.48×10^{-10}	1.392
Steady-state ethanol concentrations	4.54×10^{-9}	3.03×10^{-9}	10
Time-course from each experiment (mean)	5.36×10^{-9}	4.13×10^{-9}	4.44
Time course data all experiments best fit	5.55×10^{-9}	4.82×10^{-9}	13.4096

3.6 Ecological Control Analysis

To quantify the roles that both organisms play in determining the steady state ethanol concentration and acetate production rate, we applied ecological control analysis (ECA) on the system. We used two methods, the first by a direct analysis of the steady state experimental data, the second by analysis of the kinetic model that was built for the system.

In Figure 3.16 we plotted the steady state ethanol concentration against the ratio of *S.c./G.o*. For the ethanol concentration to be constant (steady state) its production must equal its consumption, which translates to the mixed incubation to the activity of *S. cerevisiae*. (ethanol production), which must equal that of *G. oxydans* (ethanol consumption). Under oxygen saturated conditions, the ratio of *S. cerevisiae* over *G. oxydans* was more important than their individual absolute concentrations in determining the steady state ethanol concentration. Therefore, we made the plot in Figure 3.16 against the ratio of the two organisms. The concentration summation theorem states that the sum of the concentration control coefficients for the two organisms should sum up to zero, i.e. they have equal concentration control coefficients, but of opposing signs. This means that there should be a unique, functional relation between the ratio of the organisms and the steady state ethanol concentration, i.e. doubling the absolute number of both organisms will not affect the steady state ethanol concentration, and it is only the ratio that counts.

The equation for the functional relation between the steady state ethanol concentration and the ratio of *S. cerevisiae* over *G. oxydans* is dependent on the sensitivities of the two organisms for ethanol. For the pure cultures we observed that at high glucose concentrations yeast was insensitive to ethanol in the concentration ranges observed during the mixed incubations. Therefore, the equation describing the activity of *S. cerevisiae* is very simple and directly proportional to the biomass concentration (v_{Sc}=$k1$ × S.c.biomass). For *G. oxydans* we observed a dependency for the ethanol concentration at low concentrations of this substrate. Two simple relations describing this dependency could be a linear, Equation 3.19,

$$v_2 = k_2 \bullet x(t) \bullet s_2 \quad (3.19)$$

(v_2 = ethanol consumption rate of *G. oxydans*, k_2 = specific ethanol consumption rate of *G. oxydans*, x(t) = ethanol concentration, s_2 = cell density of *G. oxydans* in cells/ml)

or a hyperbolic one as described in Section 3.4.2 and by Equation 3.3, where the second option is closer in agreement with our experimental observation for the pure culture (Section 3.2.2).

When solving for steady state, the differential equation describing the rate of ethanol production/consumption assuming the linear relation for ethanol consumption by *G. oxydans*, Equation 3.19, is given by Equation 3.20:

$$\frac{dx}{dt} = k_1 \bullet s_1 - k_2 \bullet x(t) \bullet s_2 \quad (3.20)$$

(k_1 = specific ethanol production rate of *S. cerevisiae*, s_1 = cell density of *S. cerevisiae* in cells/ml, k_2 = specific ethanol consumption rate of *G. oxydans*, x(t) = ethanol concentration, s_2 = cell density of *G. oxydans* in cells/ml)

And since the definition of a steady state still holds, where the concentration of ethanol is constant and its net rate zero, as described by Equation 3.15, we could solve for [EtOH]stst as given by Equation 3.21:

$$x(t)_{\text{stst}} = \frac{k_1}{k_2} \bullet \frac{s_1}{s_2} \quad (3.21)$$

(k_1 = specific ethanol production rate of *S. cerevisiae*, s_1 = cell density of *S. cerevisiae* in cells/ml, k_2 = specific ethanol consumption rate of *G. oxydans*, x(t) = ethanol concentration, s_2 = cell density of *G. oxydans* in cells/ml)

And for the hyperbolic dependency of *G. oxydans* for ethanol we refer to Equations 3.14 to 3.16 and Section 3.4.2 as a discussion on solving for the steady state ethanol concentration. If we examine the relation between the steady state ethanol concentration and the ratio of *S. cerevisiae* over *G. oxydans* it is evident that the proportional relation would give a bad fit. Although the relation

between the ratio and the steady state ethanol concentration is fairly linear in the range for which we have experimental data points, the line would clearly not go through the axis origin. The equation derived for the hyperbolic saturation of *G. oxydans* for ethanol fits the data points well and runs through the axis origin. The ethanol concentration control coefficients for *S. cerevisiae* and *G. oxydans* are defined as Equations 3.22 and 3.23, respectively:

$$C_1^x = \frac{dx}{d\,s_1} \bullet \frac{s_1}{x(t)} \quad (3.22)$$

(s_1 = cell density of *S. cerevisiae* in cells/ml, x(t) = ethanol concentration)

$$C_2^x = \frac{dx}{d\,s_2} \bullet \frac{s_2}{x(t)} \quad (3.23)$$

(x(t) = ethanol concentration, s_2 = cell density of *G. oxydans* in cells/ml)

From the concentration summation theorem it follows that $c_1^x = -c_2^x$. Since we can describe the steady state ethanol concentration for the system as a function of the ratio of *S. cerevisiae* / *G. oxydans* (and not as a function of either of the two organisms), we can express the control coefficients of the individual species as a function of the (*S. cerevisiae* / *G. oxydans*) ratio:

$$C_{ratio}^x = \frac{dx}{d(ratio)} \bullet \frac{(ratio)}{x(t)} = C_{1.}^x = -C_{2.}^x \quad (3.24)$$

(*ratio* = cell density of *S. cerevisiae* in cells/ml divided by cell density of *G. oxydans* in cells/ml, x(t) = ethanol concentraion)

Thus, the ethanol concentration control coefficients can be calculated from the normalized derivative from Figure 3.16. Since we have the equation for the fitted line (eq. 3.16) we can also get an analytical expression for these control coefficients:

$$\frac{dx(t)_{ststst}}{d\,s_1} \bullet \frac{s_1}{x(t)_{ststst}} = \frac{1}{1 - \frac{k_1}{k_2} \bullet \frac{s_1}{s_2}} \quad (3.25)$$

$$\frac{dx(t)_{ststst}}{d\,s_2} \bullet \frac{s_2}{x(t)_{ststst}} = \frac{-1}{1 - \frac{k_1}{k_2} \bullet \frac{s_1}{s_2}} \quad (3.26)$$

$$\frac{dx(t)_{ststst}}{d(ratio)} \bullet \frac{(ratio)}{x(t)_{ststst}} = \frac{1}{1 - \frac{k_1}{k_2} \bullet (ratio)} \quad (3.27)$$

(k_1 = specific ethanol production rate of *S. cerevisiae*, s_1 = cell density of *S. cerevisiae* in cells/ml, k_2 = specific ethanol consumption rate of *G. oxydans*, x(t) = ethanol concentration, s_2 = cell density of *G. oxydans* in cells/ml, *ratio* = cell density of *S. cerevisiae* in cells/ml divided by cell density of *G. oxydans* in cells/ml)

In Figure 3.23 we plotted the ethanol concentration control coefficient for the *S. cerevisiae* / *G. oxydans* ratio as a function of the ratio. As shown in Equation 3.24 this concentration control is equal to that for *S. cerevisiae* and minus that for *G. oxydans*. At low ratios the concentration control coefficient is 1, i.e. a 1% increase in the concentration of *S. cerevisiae* would lead to a 1% increase in the steady state ethanol concentration (and a 1% increase in *G. oxydans* in a 1% decrease). At high ratios the concentration control increases dramatically, reaching infinity at a ratio of 0.66 (i.e. k_1/k_2). In the ratios that were experimentally obtained in our mixed incubations (between 0.175 and 0.462), the concentration control coefficient varied between 1.35 and 3.24.

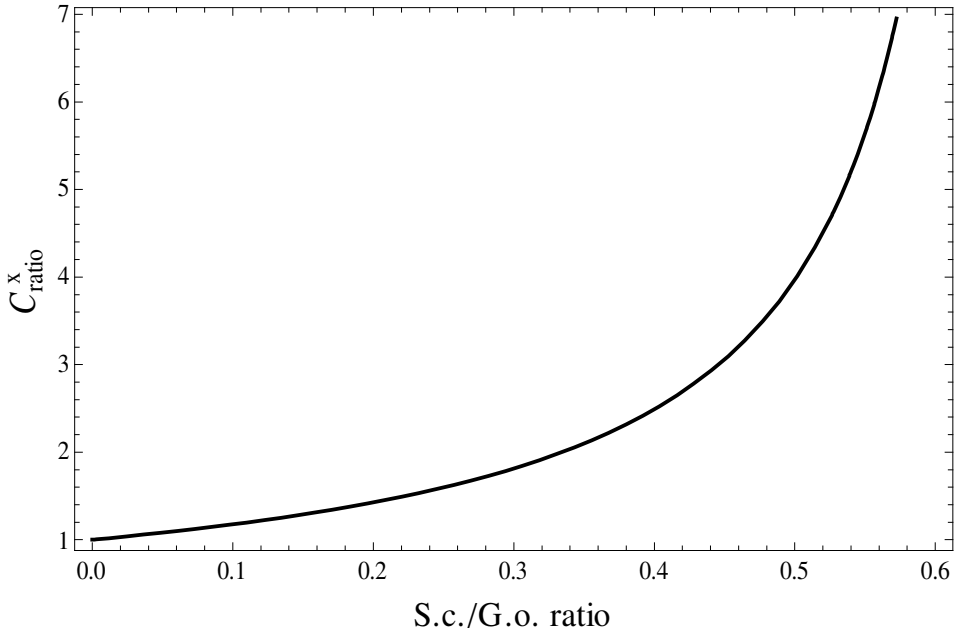

Figure 3.23: Ethanol concentration coefficient for the *S. cerevisiae* / *G .oxydans* ratio as a function of the ratio. The control coefficient was calculated from eq. 3.12, using a k1/k2 ratio of 1.496, as obtained from a fit of Equation. 3.11 to the steady state ethanol concentrations at various *S. cerevisiae* / *G .oxydans* ratios, (Figure 3.16).

The flux control coefficients of *S. cerevisiae* and *G. oxydans* are defined as Equations 3.28 and 3.29, respectively:

$$C_1^J = \frac{dJ}{d\,s_1} \bullet \frac{s_1}{J} \quad (3.28)$$

$$C_2^J = \frac{dJ}{d\,s_2} \bullet \frac{s_2}{J} \quad (3.29)$$

(s_1 = cell density of *S. cerevisiae* in cells/ml, s_2 = cell density of *G. oxydans* in cells/ml, J = acetate flux through the ecosystem)

The flux control coefficients can be estimated from the steady state acetate production rate as a function of the *S. cerevisiae* and *G. oxydans* concentrations. As can be seen in Figure3.18 (a) and (b), there is a strong correlation with the *S. cerevisiae* concentrations and a very weak correlation

with the *G. oxydans* concentration. The near proportionality of the acetate flux with the *S. cerevisiae* concentration indicates a full flux control by this organism, from the fitted line to the data points a flux control coefficient of 1.0 can be calculated by differentiation of the equation with respect to *S. cerevisiae* and normalizing for a reference state (i.e. the flux control coefficient varies between 1.03 to 1.06 dependent on the *S. cerevisiae* concentration chosen as reference state). Similarly one could calculate a flux control coefficient from the correlation of the acetate flux with *G. oxydans* of 0.4 to 0.6, but this would put too much value to the very weak correlation. Again, as can be seen from Figure 3.18, all data points fall within the 95% confidence interval in the correlation with *S. cerevisiae*, the three experimental data points with higher *G. oxydans* concentrations fall within the same confidence interval as the experiments with low *G. oxydans* concentrations. In two of the experiments with high *G. oxydans* concentrations and high flux, also the *S. cerevisiae* concentration was high, which would have contributed to the higher flux observed in these experiments.

The second method we have used to estimate the control coefficients for *S. cerevisiae* and *G. oxydans* is via ECA analysis of the kinetic models constructed for the organisms. The summation and connectivity theorems link the control coefficients to the elasticity coefficients and make it possible to express the control coefficients in terms of elasticity coefficients. The elasticity coefficients can be calculated from the rate equations used in the models and can then be used to calculate the control coefficients. For our system we only need the two elasticity coefficients of the organisms for ethanol. As we have shown for the pure cultures, yeast is insensitive for ethanol at the low concentrations that were obtained in the mixed cultures, so its elasticity coefficient is zero. *G. oxydans* shows a hyperbolic saturation curve for ethanol, which we described with a Michaelis Menten equation.

For a given steady state the elasticity coefficient and from this the control coefficients can be calculated. Therefore, by using the parameters as calculated through the methods described in Section 3.5 and summarized in Table 3.5, we could calculate the steady-state ethanol concentrations (from Equation 3.10 and Section 3.4.2) for each parameter set over specified reference ranges for the *S. cerevisiae* / *G. oxydans* ratio. By feeding each parameter set into the simplest model for the ecosystem we could generate elasticity coefficients of *G. oxydans* for ethanol over these reference ratios (elasticity coefficient of *S. cerevisiae* for ethanol equals zero) and from these the ethanol concentration control coefficients could be calculated. These concentration control coefficients

were then plotted against the *S. cerevisiae* / *G. oxydans* ratio and could be compared to the values calculated directly from the experimental data.

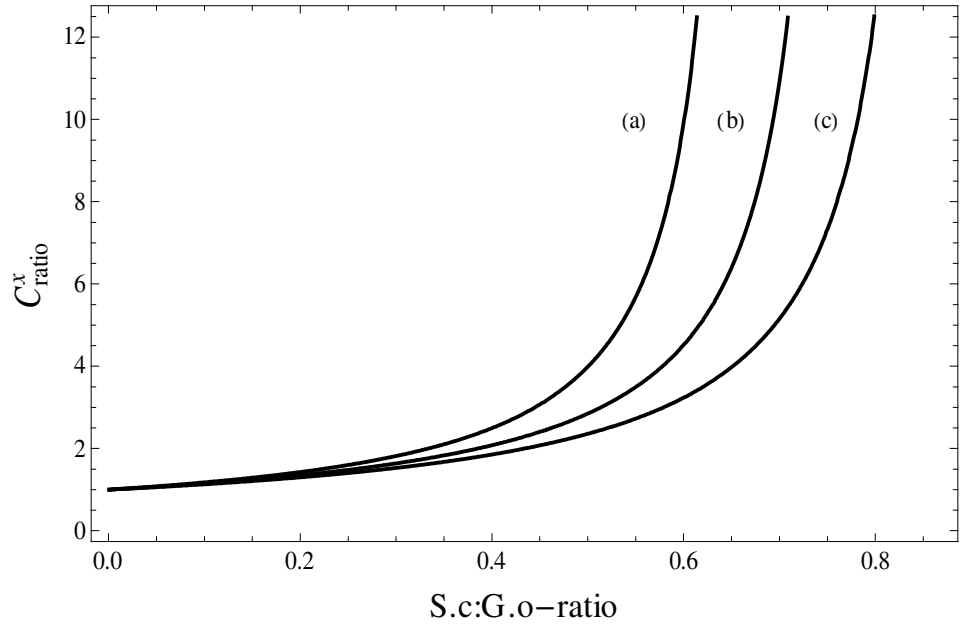

Figure 3.24: Ethanol concentration coefficient for the *S. cerevisiae* / *G. oxydans* ratio as a function of the ratio. The control coefficient was calculated with the simplest model of the ecosystem with parameters calculated from (a) the experimental steady-state ethanol concentrations (k_1 = 4.54 × 10-9, k_2 = 3.03 × 10-9, K_x = 10); (b) the average of parameters calculated from the time-course ethanol concentrations, separately (k_1= 5.36 × 10-9, k_2= 4.13 × 10-9, K_x = 4.44) and (c) the parameters calculated from all time-course ethanol concentrations combined (k_1= 5.55 × 10-9, k_2= 4.82 × 10-9, K_x = 13.4096)

Figure 3.24 (a) shows the relation between the ethanol concentration control coefficients of the *S. cerevisiae* / *G. oxydans* –ratio and the *S. cerevisiae* / *G. oxydans* –ratio for the simplest model with the parameters calculated from the experimental steady-state ethanol concentrations ($k_1 = 4.54 \times 10^{-9}$, $k_2 = 3.03 \times 10^{-9}$, $K_x = 10$). In the experimental range of *S. cerevisiae* / *G. oxydans* ratios (0.175 to 0.462) the concentration control coefficients varied from 1.35 and 3.24. At low ratios the value corresponded to 1 and reached for infinity at a value of 0.667. These values corresponded very well with the experimentally determined values given earlier in this section.

In Figure 3.24(b) we show the ethanol concentration control of the *S. cerevisiae* / *G. oxydans* ratio against the ratio for the model based on the average of parameters calculated from the time-course ethanol concentrations of each experiment separately (k_1= 5.36 × 10^{-9}, k_2 = 4.13 × 10^{-9}, K_x = 4.44). Infinity was reached at a ratio of 0.77 and the concentration control coefficients increased from 1.29 to 2.5 over the experimental *S. cerevisiae* / *G. oxydans* ratios. These are also very similar to the experimentally determined values even though a little lower, which correlates to a slightly lower

impact on the ethanol concentration by variation in organism concentrations than is experimentally observed. The concentration control coefficient for ethanol by the *S. cerevisiae* / *G. oxydans* ratio against the ratio, as calculated from the model set up with parameters calculated from all the time-course ethanol data combined (k_1 = 5.55 × 10^{-9}, k_2= 4.82 × 10^{-9}, K_x = 13.4096), is graphically presented in Figure 3.24(c). The model predicted control coefficients were slightly lower over the experimental *S. cerevisiae* / *G. oxydans* ratios, i.e. 1.25 to 2.136, and reached infinity at a much higher ratio values as well, 0.868. This is in the same order of magnitude as the experimental calculations.

For a valid assessment of the ethanol concentration coefficients calculated by the various models, we decided to compare the control coefficients at a specific *S. cerevisiae* / *G. oxydans* ratio. The most suitable ratio to the author is the middle of the experimental range of *S. cerevisiae* / *G. oxydans* ratios, i.e. 0.319. At this ratio the model set up with parameters from experimental steady-state ethanol concentrations calculated the ethanol concentration control of the *S. cerevisiae* / *G. oxydans* ratio as 1.9. The model based on the average of the same set of parameters calculated the control of the ratio over the ethanol concentration as 1.7. Finally, the model fed with the parameters calculated from time-course data of all experiments combined delivered an ethanol concentration control coefficient at this ratio of 1.58.

Chapter 4

4. Discussion

4.1 Introduction

In this Chapter we discuss the premise for our research and the results from our experimental and mathematical analyses in detail, relaying our understanding of the results we observed. We discuss the results within the context they were presented in Chapter 3 and elaborate further on the discussions emphasized in that chapter.

The current research project set out to test the feasibility of experimental control analysis for studying an ecosystem. A theoretical framework for such an analysis has been developed several years ago and was reviewed in the introduction (*4, 5*). Although MCA is mostly applied to metabolic systems, (hence the name Metabolic Control Analysis), in a more general context it can be applied to any system consisting of variables that are connected via processes, to quantify the importance of the individual processes for the steady state behavior of the variables. Thus, whereas control analysis has been applied mostly to metabolic pathways for the quantification of the control of pathway enzymes on the steady state flux and metabolite concentrations, one could envision that it could also be used for the quantification of the control of biological species on the nutrient flow through an ecosystem or on the densities of those species. Here one should be careful not to oversimplify ecosystems and not stress the comparison with metabolic systems too much; clearly in metabolic systems enzymes do not consume one another (as biological species in an ecosystem might), and enzyme concentrations are often considered as constant during the time course of the experiment (whereas species in an ecosystem could multiply or die). These (and other) differences between classical MCA and Ecological Control Analysis have been treated in the studies of Westerhoff and Getz, which showed that a hierarchical analysis is more appropriate for systems with variable biomass concentrations and also indicated that the stoichiometry of a reaction, which is constant for chemical reactions (as in metabolic systems), might be less constant for ecosystems. Lastly and important for classic control analysis (as opposed to dynamic control analysis), is the existence of a steady state in the system, a condition not necessarily fulfilled in ecosystems.

The question of whether a steady-state approach to ecosystems is a valid one has been asked before by Giersch and he was not positive about the application of MCA to ecological problems (*1*). He

had developed a sensitivity analysis, similar to control analysis including summation theorems, for ecosystems (*83*). When he applied his theory to theoretical ecosystems for herbivore-plant and predator-prey situations he could derive meaningful control structures within these ecosystems (*84*). However, he observed a large dependency of the control structure on the precise determination of the steady state and thought that MCA would not be useful for the analysis of ecosystems. Clearly the issue whether steady states are important or even exist in ecosystems in the same way as they do in enzymatic pathways (*4-6*) deserves some more attention. From a closer look into the available literature one would be inclined to conclude that steady states (also termed ecological equilibria) do indeed exist in a wide range of ecosystems from the gastro-intestinal tract (*149*) to biofilms (*150*) to oyster reefs (*145, 151*).

Analyses of such steady states have found applications ranging from determining the impact of fishing on sensitive marine ecosystems (*152*) to investigations into the evolutionary drive in ecosystems (*153*). However, none of these employed control analysis to try and quantify the importance of the role players in the ecosystems, although Schreiber *et al*. have performed (at a modeling level) a supply-demand analysis of predator-prey interactions and species-invasion of ecosystems (*154*). Some of these systems might well be suited to be studied within the framework of trophic control analysis (TCA) as suggested by Getz *et al*. (*5*). TCA can also be applied to systems where seasonal fluctuations occur by analyzing the effects of role players in such ecosystems on long-term average values. In other words the control that each constituent exerts on long-term average values can be calculated with the use of TCA even if a real steady state never occurs. Conradie *et al.* (*57*) used a different approach to analyze dynamic systems - their approach can be used to quantify the control of individual processes in oscillatory ecological systems, like seasonal fluctuations. Their approach is applicable to oscillatory systems reaching stable oscillations (limit cycles), but also to signal transduction with a single activation peak, and quantifies individual processes as they affect system variables through a well defined event such as a period in a limit cycle or a transduction peak for a signal transduction pathway.

Although Westerhoff and Getz developed their ECA almost 10 years ago, there is still no experimental application of their theory to an ecosystem. Whereas Roling *et al. (6)*, have tried to gather experimental data from the literature and use the data-set for ECA, the strength of the approach was hampered due to the fact that these experiments were never intended to be used for ECA, and were not necessarily designed for such an analysis. Instead we decided to choose a very simple system and make specific perturbations to the system with the intention to use the data for

control analysis. As such this would be the first attempt at an experimental approach for ECA to an ecosystem. We specifically chose for a simple system, to test the feasibility of the approach; if it could not be applied to a simple system, it would be unlikely to be successful for a more complicated system.

We tried to construct an ecosystem as close as possible to a metabolic system, since this would improve the chances of a successful application of MCA. So we chose a system consisting of two organisms that would interact via a single intermediate. Furthermore we chose the conditions such that the organisms would not grow, making it possible to treat biomass as a constant. Westerhoff *et al.* have shown that for the analysis of a similar ecosystem as the simple processing chain in the current investigation, the use of a hierarchical control analysis (HCA) becomes vital when the organisms were incubated under growing conditions (*4*). By reducing our system to non-growing conditions, we simplified our ecosystem to a single level processing chain analogous to a metabolic pathway improving the chance that the system can be analyzed with MCA without having to use the more complicated HCA.

4.2 The System

Even though we have constructed a to some extent artificial ecosystem by selecting two microorganisms and incubating them under non-growing conditions, the system itself is related to a naturally occurring process, i.e. the acidification of wine by acetic acid bacteria (*12*). We simplified the wine acidification system to its very basic nature to assess the feasibility of applying control analysis to an ecosystem. Thus we selected *Saccharomyces cerevisiae* for the conversion of glucose to ethanol and *Gluconobacter oxydans* for the subsequent conversion of ethanol to acetate. This system would have been the simplest ecosystem attainable, but it soon became evident that we had over-simplified the system. The first indication that the system was more complicated than we originally envisioned was given by the incomplete carbon recovery, i.e. we observed that the glucose consumed was not completely recovered in acetate (Sections 3.2.2 and 3.3.1). After careful analysis of the experimental data we could point to a number of oversimplifications we had made to the system, which turned out not to be a simple linear conversion pathway but a branched one.

It quickly became clear that *G. oxydans* does not only convert ethanol to acetate but also oxidizes glucose to gluconate. This is of course well known, the name of the organism is derived from this

process (see also Section 1.1.1). Although the glucose oxidation will lead to incomplete conversion of glucose to acetate, we still chose to use *G. oxydans* for our studies since it does not have a complete oxidative metabolic pathway, (it does not convert ethanol to CO_2), like most of the other acetic acid bacteria.

Another complication, which we had not anticipated is that *G. oxydans* did not have a complete conversion of ethanol to acetate (Figure 3.6). Under well aerated conditions an almost complete conversion of ethanol via acetaldehyde to acetate is expected (*32*). However, it has been reported (*146*) that under special conditions up to 65% of the ethanol consumed by the organism accumulates as the intermediate acetaldehyde, and only 35% is converted to acetic acid. These particular conditions included pre-growth of the *G. oxydans* on a glycerol/ yeast extract medium for 24 to 48 h and thus cannot directly explain our incomplete conversion of ethanol to acetate. In our system we only retrieved 66% of the ethanol consumed by *G. oxydans* as acetate. Since *G. oxydans* is not capable of direct oxidation of ethanol to carbon dioxide, one could speculate that acetaldehyde might have accumulated during the conversion assay. However, no acetaldehyde was detected in HPLC analyses of samples taken during the incubation assay. Acetaldehyde is very volatile and might have evaporated from the incubations despite the cold trap that was applied and which worked well to prevent evaporation of ethanol and acetate.

Finally we observed that under aerobic conditions (necessary for the obligately aerobic *G. oxydans*), *S. cerevisiae* did not convert all the glucose it consumes to ethanol but had a purely oxidative metabolism as well. *S. cerevisiae* is a Crabtree positive yeast (*155*) and even under aerobic conditions it converts most of the glucose it consumes to ethanol, as long as the glucose concentration remains high. Yeast was pre-grown under anaerobic conditions to try and make the oxidative contribution in its metabolism as small as possible. Despite these precautions we still observed a non-complete conversion of glucose to ethanol during the (aerobic) incubation of yeast in the conversion assay. We confirmed that this incomplete conversion was due to the aerobic conditions by performing an anaerobic control incubation. We subsequently also tested whether yeast underwent adaptations during the conversion assay by measuring the oxygen uptake capacity of yeast before and after the conversion assay (Section 3.3.1 and Figure 3.8). An increase in oxygen consumption capacity was observed (before incubation the oxygen consumption rate was virtually zero), indicating that the yeast did adapt itself to a more oxidative metabolism during the incubation, although the vast majority of the glucose was converted to ethanol.

Under given constraints, (gluconate production in *G. oxydans*; incomplete ethanol to acetate production in *G. oxydans*; oxidative metabolism in yeast), we could recover virtually all carbon entering the system, indicating that we had included a fairly complete set of reactions of the system.

4.3 Steady state

Central to classic metabolic control analysis (MCA) is the requirement that the system under investigation should reach a steady state, i.e. a state where intermediary metabolite concentrations remain constant with time (*85, 86, 97, 102, 111, 156, 157*). Although MCA has been extended to deal with dynamic systems as well, for instance to study time invariant behaviour in oscillatory systems (*50*) and even time dependent behaviour (*57*), our aim here was to apply a classic MCA approach to an ecosystem.

To reach a true steady state, a system must be incubated in a constant environment, typically this would be an open system with a continuous supply of substrate and removal of products, such that these external variables are essentially clamped. Although continuous cultivation techniques exist, for instance a chemostat is a well-known example, these would necessitate working with growing organisms and would make the study much more complicated. Another method that is often used for MCA analyses, is to work under quasi steady state conditions, where substrate and products change with time but the intermediates of the system relax (at least temporarily) to a steady state, e.g. (*158-160*) . In these studies a high substrate concentration is used such that it remains saturating during the experiment, and the assay is finished before products accumulate to inhibitory levels. For our system we needed to check: 1) that the ethanol concentration reaches a constant level and 2) that the system is insensitive towards changes in concentrations of substrates and products within the ranges reached in the incubations.

In several of the mixed incubations a constant ethanol concentration was reached within the experimental time window of 5 hours and in many others a relaxation towards such a steady state was observed, in these latter cases we estimated the steady state ethanol concentration with a second order polynomial fit. In many other cases, some of which are shown in Chapter 3, no steady state was reached. We did not use a formal method to decide whether (or when) a steady state was reached, this was mostly an arguably arbitrary decision on the basis of the (projected) time course of ethanol concentrations. Due to experimental error in the ethanol determination and scatter in the

data it was not trivial to define a good steady state criterion that could be used on the experimental data set. One could argue that a hyperbolic increase in ethanol concentrations is not a sufficient condition to determine whether a steady state exists for the system and cannot be used to estimate such a steady state. However, it should be realized that the insensitivity of yeast for ethanol under the experimental conditions that we applied, would lead to a constant influx rate of ethanol and the existence of a steady state would be determined by the maximal activity of *G. oxydans*. If the ethanol production rate of yeast exceeded the maximal activity of *G. oxydans* then ethanol will increase linearly with time and no steady state would exist.

We checked the sensitivity of *S. cerevisiae* and *G. oxydans* for changes in the concentrations of all variables in the system. Remarkably both organisms were insensitive in terms of metabolic activity for changes within the range of concentrations reached during the mixed culture incubations for any of the variables, with the sole exception that *G. oxydans* was sensitive for ethanol at low concentrations (Figure 3.4).

Having tested that a steady state was reached in the mixed culture experiments we set out to determine the sensitivity of this steady state for changes in the concentration of both organisms.

4.4 Sensitivity of the steady state for perturbations to the system

For MCA a steady state is a necessary but not sufficient condition; one also must be able to make perturbations to the system and quantify the sensitivity of the original steady state towards these perturbations. For metabolic systems one would make small changes in enzyme activities around the reference state. Typically this would involve inhibitor titrations or genetic manipulations of enzyme expression levels leading to small changes in enzyme activity around the wild type activity. For good examples of such studies see the work of the Jensen-group on H^+-ATPases in combination with the work by Snoep *et al*. on gyrases and topisomerases (*158-160*). The reference state is of great importance in such studies, typically one would be interested in the control coefficient of an enzyme in the wild type strain, and therefore one must make perturbations around the wild type activity. In the same set of experiments by the Jensen group it is also evident that the values of the control coefficients can be very dependent on the expression level of the enzyme. In a number of studies it has been observed that enzymes quickly loose their control when expressed at higher levels than the wild type level (*158-160*).

For our experimental system it was relatively simple to make changes to the activities of the individual processes, this could be achieved by varying the biomass concentration of the two organisms. Since we were not really analyzing a reference state, we decided to make mixed culture incubations over a wide range of biomass concentrations. Since it was relatively hard to obtain sufficient biomass of *G. oxydans* (due to poor growth of the organism), we mostly varied the concentration of *S. cerevisiae*.

Upon variation of the *S. cerevisiae/G. oxydans* ratio, marked effects were observed on the steady state. Firstly, there were rather strict limitations to the magnitude of the ratio at which a steady state was reached; above a ratio of 0.6 no steady state was reached and the ethanol concentration would increase linearly with time. Importantly, whereas we observed that the steady state ethanol concentration was dependent on the ratio of the two organisms (Figure 3.16), the steady state flux (i.e. acetate production rate) was solely dependent on the yeast concentration (Figure 3.18).

From the proportional relation between the yeast concentration and the acetate production rate it was derived that yeast sets the pace for the system, the organism is the rate-limiting step for the system. This can be understood from the insensitivity of yeast for ethanol at the concentrations observed in the incubations; at saturating glucose concentrations and without product inhibition yeast was not affected by the system at all, it converted glucose to ethanol at a rate proportional to its concentration. For the system to reach a steady state, *G. oxydans* must attain a metabolic activity equal to yeast, i.e. it must consume ethanol at the same rate at which yeast produces it. In the system the metabolic activity of *G. oxydans* was completely determined by the ethanol concentration; at high *S. cerevisiae/G. oxydans* ratios, a high metabolic activity of *G. oxydans* was needed which can only be attained at a high ethanol concentration. This resulted in a saturation curve in Figure 3.19. These results also explain the steep increase in the steady state ethanol concentration at high *S. cerevisiae/G. oxydans* ratios; at high ethanol concentrations where the *G. oxydans* is relatively insensitive to ethanol due to saturation, a much larger increase in ethanol concentration is required to increase the activity of the organism than would have been necessary at low ethanol concentrations. Clearly, the maximal *S. cerevisiae/G. oxydans* ratio at which a steady state can be obtained is set by the relative specific activities of the two organisms.

Thus, yeast appears to be rate limiting and the control of the ethanol concentration is shared by the two organisms. However, to quantify the control coefficients of the two organisms from the experimental data set was not so simple. Normally one would perturb one activity and quantify its effect to determine its control coefficient, but in our set-up we usually had small perturbations in the concentration of both organisms and the data set was not large enough to estimate the contribution of each of the two organisms.

We therefore decided to construct a mathematical model for the metabolic activity of the two organisms. Control coefficients can be calculated with such a model, and in addition the rate equations in such a model would allow a direct estimation of the control coefficients from the experimental data.

4.5 Modeling the system

An important decision that must be made when building a mathematical model for a system is the level of detail that the model should have. This decision will largely be dependent on what one wants to do with the model and what information can be obtained for the system. For the current study we wanted to construct a mathematical model for an ecosystem that we could use for the analysis of our experimental data. With such an analysis we want to get a quantitative understanding of the contribution of both species to the steady state behaviour of the system in terms of the metabolic control analysis framework. This approach defines the level of detail at which we need to model the system to the species level. There was no need to work at a more detailed level, such as the enzyme activity level that is normally used in MCA studies, since we did not aim to understand the system at the enzyme level, but at the species level. Therefore, we needed to obtain a kinetic description at the species level in terms of input-output functions, treating the intracellular environment as a black box. We did not make intracellular perturbations in our experimental set-up; we described the system in terms of extracellular variables and species densities.

Since this is the first attempt at an experimental control analysis approach to study an ecosystem, we wanted to keep the system and the mathematical description as simple as possible. The system was chosen such that it is very similar to a metabolic system to improve the chances of a successful application of MCA (see previous section), and we tried to minimize the sensitivities of the

organisms to the external variables (i.e. work at saturating values of substrates and low concentrations of products).

We investigated the sensitivity of both organisms for all variables in the system: glucose, ethanol, acetate, gluconate and oxygen and observed that at the concentration ranges in the mixed culture experiments, the only non zero elasticity was that of *G. oxydans* for ethanol. Therefore we could use realtively simple rate equations for the description of the metabolic activities of both organisms. Thus, the metabolic activity of yeast could be described with a linear equation, consisting of the specific activity multiplied by the yeast biomass (Equation 3.1). For *G. oxydans* we used a Monod-type of equation to describe the metabolic activity as a function of the ethanol concentration (Equation 3.3).

For the parameterisation of these rate equations we tried to use experimental data determined for the pure cultures. Whereas the standard approach for parameterisation would have been to use mixed culture data, i.e. the complete system, we preferred to construct the model using data for the isolated components. There are several advantages to using data obtained with the pure cultures for model construction. Firstly, it creates a good separation between data sets for model construction and data sets for model validation, where we would use pure cultures for model construction and mixed cultures for model validation. Thus, if successful we would be able to *predict* the time dynamics and steady state behaviour of the mixed cultures on the basis of the characteristics of the individual species. This is importantly different from the approach where one would fit the model parameters on mixed culture data. In the latter case one would test the model for its ability to *describe* the mixed culture data. As a consequence, if one were to fit the model parameters on the mized culture data, there would 1) be no prediction of the data set (the data is used for a fit); 2) no validation of the model (there is no test on model quality only on model ability); and 3) no direct link could be made to the characteristics of the individual species.

These advantages might sound subtle but some of the consequences are far reaching. For instance when model parameters are fitted on the complete system it is very easy to smooth out unknown interactions between the organisms. This would result in obtaining apparent parameter values, which would be different from the real parameter values, and the difference would hide the unknown interaction. In such a way, a (hypothetical) direct inhibition of yeast by *G. oxydans* would be hidden in an apparent lower specific activity of yeast. In contrast, when the real specific activity

of yeast would be used, the model would (if the interaction was strong enough) give a poor prediction of the mixed culture and one would have to investigate the cause of this poor performance. Fitting parameters on the complete system will often lead to 'better' descriptions of the data set, but then the researcher should include additional data sets that are sufficiently different from the "training" data set to validate the model. Here the crux lies in the sufficiently different, which is not trivial to define.

A final advantage to constructing models on the basis of the characteristics of the isolated model components is that it makes the model much more flexible for extension. If the model components are fitted to data sets obtained with the complete system, then such parameter values tend to be context dependent (i.e. they are apparent for the system, not true physical constants for which a mechanistic interpretation exists). This in contrast to the parameter values obtained with the pure cultures, such parameter values are independent on the contents of the mixed culture experiment for which they will be used. Here a critical note must be placed; even the parameter values for the pure cultures are not completely context independent, they are for instance dependent on the growth history of the cells, but they are not dependent on the environment in which the cells will be placed. This discussion on model construction and validation is closely related to the Silicon Cell type of modelling approach as suggested for metabolic systems (*161-164*).

4.5.1 Parameterization of the model: pure culture experiments

A significant effort was invested in setting up well-controlled experimental conditions. It turned out to be very difficult to culture *G. oxydans* reproducibly, i.e. the organism had a very slow growth rate, was decidedly temperamental, and although being classified as an acetic acid bacterium, did not particularly like growing on ethanol (*9-12, 44*). Although the organism could relatively easily be pre-grown on glucose containing medium its capacity for ethanol consumption would then be low. We therefore used an ethanol-based medium, which reproducibly delivered *G. oxydans* cells with a high ethanol consumption capacity albeit at a low culture density and low specific growth rate. For the incubation of the pure cultures (and later also for the mixed cultures) we developed an aeration funnel with a good oxygen transfer rate and cold trap to contain volatile metabolites in the culture. Oxygraphs were used for the estimation of the affinity of *G. oxydans* for ethanol and oxygen.

An advantage of working at the species level is that one can use the same incubation environment for the model construction (pure culture experiments) as for the model validation (mixed culture incubations). This is in contrast with the metabolic systems where one needs to simulate the intracellular environment to characterize the isolated enzymes, and then one is always unsure whether the parameter values thus determined are valid for the intracellular environment.

We determined the specific activity for both organisms from their substrate consumption and product formation rates as a function of biomass concentration, Figures 3.2 and 3.6 for the yeast and *G. oxydans*, respectively. The proportional relationship between the metabolic activity and the biomass concentration indicated that our experimental set up was adequate for maintaining a constant environment for a sufficiently long time period to estimate the specific activities for both organism. We did observe that at high biomass concentrations of *G. oxydans* a linear relation between biomass and metabolic activity was no longer observed which we suggested to be due to oxygen limited conditions. To test this suggestion we needed an estimate for the affinity of *G. oxydans* for oxygen. The off-line estimation of metabolic activities as applied to the aerated reactors was too slow to estimate the activities under non-saturating conditions; i.e. during the time it took to measure the activity the substrate concentration had significantly changed. For this reason we used oxygraphs to estimate the metabolic activity of *G. oxydans* under non-saturating oxygen and ethanol conditions. The on-line recording of the dissolved oxygen concentrations was used to estimate the metabolic activity on a minute time scale (at low density cultivations) as opposed to the hour time scale for the reactor set-up. For the pure *G. oxydans* culture K_s values for oxygen of 0.01 mM (Figure 3.10) and for ethanol 1.4 mM (Figure 3.4) were determined in the oxygraph experiments.

To test our hypothesis that at high *G. oxydans* concentrations the available oxygen limited the metabolic activity we needed to estimate the oxygen transfer rate for the reactors. This was determined by measuring the dissolved oxygen concentration during an incubation of *G. oxydans* for which the metabolic activity had been measured. During this incubation the dissolved oxygen concentration was constant; i.e. the consumption rate of oxygen by the bacterium equalled the influx of oxygen into the reactor. From such measured influx rates at a known dissolved oxygen concentration we could estimate the oxygen transfer rate.

In a kinetic model we could subsequently predict the dissolved oxygen concentration as a function of the biomass concentration and its effect on the metabolic activity of *G. oxydans* (Figure 3.13).

This experiment can be seen as a validation of the model in terms of oxygen transfer and oxygen sensitivity of *G. oxydans*.

We tried to measure the ethanol sensitivity of *G. oxydans* in oxygraphs in the presence of glucose, which would be the relevant conditions for the mixed culture experiments. However, in the presence of glucose the oxygen consumption rate of *G. oxydans* was significantly higher than in its absence, so much so that no significant increase could be observed in the oxygen consumption rate upon addition of ethanol. Therefore it was not possible to estimate the affinity of ethanol in the presence of glucose.

4.5.2 Validation of the model: mixed culture experiments

From the specific activities one can immediately calculate the upper boundary of *S. cerevisiae/G. oxydans* ratios with which one expects a steady state to be reached, i.e. the upper boundary is limited by the maximal activity of *G. oxydans*. From the experimental data obtained with the mixed cultures it was evident that a steady state was reached at *S. cerevisiae/G. oxydans* ratios that were much higher (0.175 to 0.462) (Figure 3.16) than the upper ratio predicted on the basis of the pure culture experiments (0.081). Thus, here we observed a marked difference between the apparent specific activities of the two organisms in the mixed cultures as compared to the specific activity of the organisms in pure cultures. The respective specific activities were 1.16×10^{-8} (+/- 0.1×10^{-8} SEM) and 5.5×10^{-9} (+/-3.73×10^{-10} SEM) µmole EtOH/cell/min for yeast in the pure and mixed cultures respectively. Thus, for the best description of the mixed cultures we needed to use a roughly 2 fold lower specific activity for yeast than was measured in the pure culture. In contrast, for *G. oxydans* we observed an apparent increase in specific activity in the mixed cultures (4.0×10^{-8} (+/-1.1×10^{-9} SEM) µmol EtOH/cell/min; compared to the pure cultures (9.5×10^{-10} (+/- 1.4×10^{-10} SEM) µmol EtOH/cell/min). In addition for *G. oxydans* a lower affinity for ethanol was observed in the mixed cultures (9 mM ethanol (+/-1.4 SEM)) compared to 1.4 mM for the pure culture.

As far as we know there is no direct interaction between yeast and *G. oxydans* and it is hard to explain why different specific activities for the two organisms would be observed under mixed culture conditions compared to the pure cultures. One very speculative explanation could reside in the incomplete carbon recovery that we observed for *G. oxydans* for which we proposed acetaldehyde accumulation as a potential explanation. If such acetaldehyde were to be produced in

the mixed culture and converted by yeast to acetate, then this would lead to a higher apparent metabolic activity of *G. oxydans* (the 'extra' acetate production would be attributed to this organism). Such acetaldehyde production could potentially inhibit the ethanol production rate in yeast leading to a lower apparent specific metabolic activity for this organism. This is a rather far fetched and speculative explanation, for which we have no direct evidence; it was not possible to calculate a carbon balance in the mixed cultures; due to the necessary high glucose concentrations it is impossible to accurately measure the glucose consumption rate. However, we also observed an increase in the specific gluconate production rate, which was also 3-fold higher for the mixed cultures (1.04×10^{-9} (+/- 1.43×10^{-10} SEM) µmol gluconate/cell/min) in comparison with pure cultures (3.40×10^{-10} (+/- 2.07×10^{-11} SEM) µmol gluconate/cell/min) indicating that there was a generally higher metabolic activity of *G. oxydans* in the mixed cultures.

For the difference in apparent affinity of *G. oxydans* for ethanol in the pure and mixed cultures we have a less speculative explanation. In the pure culture we had already observed that *G. oxydans* had a high oxygen consumption rate when incubated with glucose and that it was not possible to measure a significant increase in oxygen consumption rate upon addition of ethanol to the oxygraph. This points to a competition of glucose and ethanol metabolism, most probably at the level of oxidation of reducing equivalent at the respiratory chain. Deppenheimer *et al.* (*32*) showed that the membrane-bound PQQ-dependent glucose and alcohol dehydrogenases, also shown by Matsushita *et al.* (*31, 33, 39, 165*), both form part of the ubiquinone-ubiquinol cycle towards the electron-transport chain within the periplasmic space of *G. oxydans*. Under oxygen and glucose saturated conditions it is likely that the affinity of the organism for ethanol through this direct oxidation pathway might be lowered, i.e. leading to an increase in its apparent K_{EtOH}, due to the already high activity of the respiratory chain from glucose oxidation. This is particularly relevant for the mixed cultures since ethanol was not present at saturating conditions. The cytosolic alcohol and acetaldehyde dehydrogenases are far less active under non-growing conditions which place even more emphasis on the importance of the ubiquinone-ubiquinol cycle linked to the very active membrane-bound PQQ-dependent alcohol and acetaldehyde dehydrogenases (*28, 32*). Note that this competition between glucose and ethanol would only affect the affinity of *G. oxydans* for ethanol, not its maximal ethanol consumption rate. In the pure cultures we estimated the ethanol consumption rate in the presence of glucose and high ethanol concentrations.

As indicated above, when we extended the simple model to include oxygen as a free variable, we were able to predict the non-linear relation between the acetate production rate and biomass

concentration at high densities of *G. oxydans*. This was a strong prediction on the basis of characteristics measured in the oxygraph and on the oxygen transfer rate as measured in the aeration funnels. Although this result was positive we still decided not to run mixed culture experiments under oxygen limiting conditions since this would most likely decrease the stability of the steady state, i.e. lead to a higher variation in ethanol concentrations. *S. cerevisiae* would be pushed more towards anaerobic metabolism which would deliver a higher metabolic activity towards ethanol whilst *G. oxydans* would be limited in its flexibility in metabolic activity with respect to ethanol consumption (*9*). In fact, the activity of *G. oxydans* under these conditions would become largely independent of its biomass concentration, and more dependent on the dissolved oxygen concentration, i.e. linked to the rate of oxygen supply.

We used two approaches to estimate the kinetic parameters of the kinetic model from the mixed culture data; the first focussing on steady state properties and the second taking the complete time integration into account. Both approaches yielded comparable results, and this could be seen as a confirmation of the validity of the values (Fig 3.24, Table3.5). As indicated above we would have preferred to use the kinetic parameters obtained in the pure cultures, to calculate the elasticities of our ecosystem in vitro similar to the traditional methods (*86, 111, 156*). But since we were not able to describe the mixed culture experiments with these parameter values accurately, we mainly used the parameter values fitted to the mixed culture assays for the calculation of the control coefficients in the next section.

4.6 Ecological Control Analysis

4.6.1 ECA of the model ecosystem

Due to the marked differences between the parameters as calculated from the pure culture experiments and the mixed culture experiments, we chose two strategies based on the fundamentals of metabolic control analysis combined with enzyme kinetics to derive the control structure of our model ecosystem from the mixed population experiments.

In the first strategy we calculated the control coefficients directly from the experimental data using the definition of control coefficients. This is similar to the original method of deriving control coefficients directly from experimental data as discussed by Fell in Chapter 5 of “Understanding the

Control of Metabolism" (*111*). Flux control coefficients were calculated from the acetate flux data (Section 3.4.3, Figure 3.18) and showed that all control resided with *S. cerevisiae* while the control over steady-state ethanol was shared as calculated from the steady-state ethanol data. (Figure 3.16, Section 3.6). The concentration control coefficients showed a sharp increase in magnitude at higher experimental *S. cerevisiae* / *G. oxydans* ratios (Figure 3.16 for experimental and Figure 3.24 for model descriptions)

In the second strategy, the control coefficients were calculated from elasticities, using the rate equations in the models, as described in the theory of metabolic control analysis (*86, 99, 102, 111, 156*). Determination of control coefficients from elasticities was further simplified in the model ecosystem since yeast was insensitive to ethanol and therefore its elasticity coefficient for ethanol was zero. Thus, from a control analytic perspective the system had become very simple, with only one elasticity, reflecting the sensitivity of *G. oxydans* for ethanol. (Figure 3.19) Hence, both the flux and concentration control coefficients for both organisms could be calculated from this single elasticity coefficient. Such a simple system, with a high importance for the sensitivity of *G. oxydans* for ethanol, leads to an inherent instability at high concentrations of ethanol where this elasticity would also veer towards zero. Under those conditions the concentration control coefficients would become infinitely large, making the system very sensitive for changes in biomass concentrations at high *S. cerevisiae* / *G. oxydans* ratios.

The sensitivity of the *S. cerevisiae-G. oxydans* system for perturbations in biomass concentrations was not only apparent from the model analysis but is also clearly visible in the experimental data (Figure 3.16) This sensitivity was actually one of the major difficulties within the experimental set up where slight perturbations in the concentrations of either of the organisms at high *S. cerevisiae* / *G. oxydans* ratios caused large changes in steady-state ethanol concentrations.

Even though Ehlde *et al.* (*166*) showed that experimental errors can impact negatively on the calculation of flux control coefficients directly from experimental data, which was in our experience the easier method to calculate control coefficients, we found reasonable correlations between the sets of control coefficients calculated by both methods. In addition to Ehlde *et al.*, Ainscow and Brand (*137*) emphasized that calculating control coefficients from elasticities was a more robust strategy than their calculation directly from experimental data regarding flux or steady-state concentrations. There is a danger in the latter strategy that the design of the model will influence the

control structure derived from the elasticities, but if the model describes the kinetic behavior of the ecosystem satisfactorily, as in our case, one would assume that the control structure remains intact. Most likely these issues in relation to the calculation of control coefficients directly from experimental data or from elasticity values, become more important with more complex systems. Our system was relatively simple and the model was so strongly based on the experimental data set that it was not surprising to find a good agreement between the two methods for our study.

Our ecosystem was very simple, two non-growing micro-organisms interacting via a common intermediate, and it would be good to speculate on the applicability of the ECA/TCA framework to larger, more complete networks. Although our system was simple it took a lot of effort to set up our experiments such that we could obtain reproducible results. Some of these experimental problems are not uncommon to biological studies and can mostly be related to variability in the biological material, but for the specific type of experiments necessary for ECA, i.e. small perturbations and precise determination of steady-state behaviour, we had to take extensive precautions to make this variability as small as possible.

To extend the current study to larger systems its limitation will most likely be in the experimental approach. The theoretical framework has been treated extensively by Westerhoff *et al.* (*4*), and Getz *et al.* (*5*), but the experimental approaches are not so well developed. The greatest challenges that we could see in the extension of experimental ECA to larger systems would lie in the number of variables, the number of levels in hierarchical systems, and the type of interactions between organisms in the ecosystem. The number of variables within one level would easily be extended without great difficulty as long as they can be quantified (preferably via on-line methods) and as long as a (quasi)-steady state is reached.

More challenging would be to analyse ecosystems with multiple hierarchical levels, e.g. systems with variable biomass. Not only would it be more difficult to reach a steady state in such a system, i.e. one would need a continuous flow type of set-up, but the levels would also introduce time-scales in the system, i.e. fast metabolic and slow biomass variables. In addition the biomass variables would not be ordinary variables but would be multipliers for the processes on the metabolic level. An important practical aspect to be considered for such systems with growing organisms would be the issue of perturbation of the system. Where as we could relatively easily perturb the biomass concentration in our incubations, this cannot be done in growing cultures where

biomass is a variable and not a parameter. For such systems perturbations could be made to specific growth rate of the organisms via inhibitors, but this could be more complicated.

The last type of extension of ecosystems to include more direct interactions between organisms would probably be the most challenging. For instance for analysis of trophic chains, where species might predate on one another, it would be much more difficult to build a mechanistic model bottom-up, i.e. constructed with pure cultures. Invariably such systems would have variable biomass concentrations and changes in the concentrations of a predator would not only affect the speed of predation, but also the concentrations of other catalysts. Often trophic chains will not relax to a global steady state, which would then complicate the analysis (*68, 167*).

4.6.2 Implications of ECA for other ecological studies

As mentioned in Section 4.1, there are several examples where a control analytic approach to ecosystems could be applied. Three of the more recent publications are discussed below with reference to how our control analysis could have been used to gain more information from the sometimes very detailed data sets.

A recent review on clinical gastroenterology by Neish has emphasized the interplay between the host, e.g. human, and its intestinal microbes to maintain gastrointestinal homeostasis and consequent health (*149*). Even though there is no explicit referral to steady states, terms such as "homeostasis" and "stable niches" have a similar meaning in physiological studies. The review shows a variety of mechanisms developed by both the eukaryotic host and the gut microbes to establish a stable micro-ecosystem in the gastrointestinal tract driven by their co-evolution. This co-evolution was probably initially driven by the added metabolic activities of the microbes, which led to substantial benefits to the host. But the symbiosis is carefully maintained by both the host (on a cellular level by producing microbiological modulators such as peptides or reactive oxygen species) and by the microbial inhabitants manipulating the host-responses. This homeostasis is characterized by the stability of beneficial microbial populations and the low to non-existent levels of pathogens. However, the reviewer placed emphasis on gaining an understanding of this symbiosis under healthy conditions and that it would lead to a broadening of the knowledge of disorders of the gut and the development of therapies that could be most useful. This is exactly where a control analytical approach could be useful since it is designed for situations where steady states (homeostasis) are perturbed. Reproducible size of perturbations to the homeostatic gut ecosystem

and precise measurement of identified markers for diseases would be vital in such a control analytical approach. Our approach especially could be useful when combined with non-invasive experimental techniques such as magnetic resonance of the gastro-intestinal tract *in vivo*, while *in vitro* experiments could be used to elucidate the kinetic behavior of the major beneficial populations of gut microbes. Such a study could either involve the control subject (without the metabolic, immunological or inflammatory disorders) as a reference state and then drawing a comparison with subjects who suffer from various degrees of such disorders (seen as perturbations to these homeostatic intestinal ecosystems), but this could be potentially very expensive and "levels" of disease very difficult to define. Animal models may be a better choice for a control analytical study, where manipulation of their intestinal microbiological content through the addition of pure microbiological cultures could be performed as a direct perturbation of the microbial content. On the other hand, the use of inhibitor/activator titrations to force animals into measurable degrees of a metabolic disease could be used as an approach on the host itself for an indirect perturbation of microbial populations in the gut. Microbes that form a vital part in the alleviation or manifestation of these disorders could be identified from these perturbations to the homeostatic ecosystem. The control they exert on markers for particular diseases, e.g. blood sugar levels in diabetes, can be gauged by a control analytical approach. If such useful microbial populations could be identified and their effects quantified, they would then form ideal candidates in a microbiological approach to gastrointestinal disorders.

In a second example, Dibdin and Wimpenny published a detailed work on the steady states observed in various bio-film types with special focus on experimental setups and theoretical models to describe such biofilms (*150*). They established that homogeneous steady states, i.e. submerged cultures in a chemostat, were not applicable to natural biofilms that reached heterogeneous steady states in nature and are far more difficult to maintain in experimental conditions. For this purpose they suggested a constant depth film fermentor (CDFF) where the depth/height/thickness of the biofilms were mechanically controlled. Several different types of biofilms exist from individual microbial stacks to biofilms containing pores and channels to the very dense biofilms found at very high substrate availability, e.g. dental plaque. Their study investigated steady states in several different situations from organisms commonly found in the human oral cavity, where high substrate levels are maintained, to biofilm contamination of metal working fluids, to natural riverine biofilms and finally the biofilms forming in bladder catheters. Steady states in their experimental system were defined by constant viable cell counts and protein concentration and could be maintained in their set up for prolonged periods.

A number of significant differences exist between their experimental conditions and the computer models that were built to simulate the biofilms. In the models they defined steady states as the state in which the thickness of the biofilm, bacterial density and distribution as well as biochemical activities become invariant with time. It is debatable whether this corresponded with the steady states as observed in the CDFF-experiments. All biofilms in the model set up are considered to be homogeneous even though they made a considerable effort to emphasize the heterogeneity of natural bio-films. Furthermore, their model simplification does not allow for active transport of metabolites through the film, leaving only passive diffusion as a means for distribution of nutrients through the film. The authors realize these discrepancies between their modeling and experimental set-up and they set out a set of rules for future models that addresses all of the abovementioned inadequacies.

The experimental system for studying the biofilms was designed to apply small perturbations to the steady states that would make it a good system for a control analytic study. Such a study would indicate which of the processes in the system controls the steady state properties such as the biofilm thickness, substrate gradient in the biofilm etc. If one follows their premise that naturally occurring biofilms are heterogenous it leads to interesting experiments regarding the optimization of such systems for beneficial use or as a means to diminish such biofilms in areas where they could be detrimental. The CDFF would be an ideal tool to ascertain the dynamic growth kinetics of homogeneous biofilms under standard conditions, analogous to our approach with pure culture bioconversion assays. By performing these CDFF-experiments on all the constituents of heterogeneous biofilms, a set of model parameters could be derived which could then be used to predict a heterogeneous biofilm on the basis of homogeneous biofilm parameters. Thus a simulated heterogeneous biofilm could be created on which several perturbations could be performed in silico. As is the case in our data, interactions between biofilm constituents, which might not be as intuitively realized, might be brought to the fore, e.g. a higher activity of *G. oxydans* in mixed populations relative to pure culture assays. By taking this investigation further, if passive diffusion is assumed as the only means of nutrient transport through the biofilm one can measure the control it exerts on biofilm growth and thickness by using a simulation based on the data and formulas supplied by Dibdin and Wimpenny. One would assume that in a biofilm where no channels or pores are present, the growth/survival of the layers would become more and more dependent on the supply of nutrients the further the layer are distanced from the surface/source, but this can be quantified with a control analytical approach. Experimentally one could use the CDFF as a means to vary the thickness of homogeneous biofilms under the similar nutrient conditions and measure the

vitality/growth rate of the layers of the biofilm towards steady state. This would allow for a steady-state analysis on how the distance from a food source determines the vitality of an organism in a biofilm, i.e. the control exerted by passive diffusion on cellular metabolism in biofilms. In heterogenous biofilms it might be possible to ascertain which organisms would survive at certain depths in a biofilm based on the experimental results obtained from homogeneous CDFF experiments.

In a further interesting example, human fishing activity was studied by Manickchand-Heileman, treating it as a special form of predation. As such it might be possible to apply TCA or ECA to get a quantitative assessment of the impact of fishing on a sensitive marine ecosystem (*152*). In their study they used detailed ecological models and software to calculate the effects in three scenarios of fishing on several layers of the ecosystem of the Gulf of Paria from detritus up to the higher predators, i.e. sharks. The scenarios were seen as different levels of perturbation to the ecosystem by fishing. The impact of each level's biomass on the biomass at all other levels was used as a means to calculate where the control on the ecosystem lay by using the Leontief matrix routine. Their analysis indicated that most of the control / trophic impact was lodged in the lower levels of the ecosystem and especially the detritus, a common feature of continental shelves. However, this impact is measured as the number of the positive impacts it has on the biomass of other participants in the ecosystem. As a means of determining the impact fishing has on the ecosystem, it is not clear whether their analysis gives a satisfactory answer towards a quantifiable estimate of this impact. Although there are similarities between the analysis used in this study and the ECA approach we have used in our study, they are different approaches. It is not simple to estimate whether either TCA or ECA would deliver a different answer for this detailed set of data with regards to trophic impact. The analogy between the different approaches is interesting and it would be worthwhile to try and apply ECA to the system.

4.7 Concluding remarks

We set out to test the feasibility of applying control analysis in ecosystems by applying the procedures and techniques of biochemistry on the simplest ecosystem we could devise. This was not such a trivial exercise mainly due to metabolic complexity of the organisms leading to a branched pathway and not the linear processing chain we envisioned at the onset of our research. Nonetheless, the procedures for calculating kinetic parameters with techniques from biochemistry

were transferred to our ecosystem. Pure culture experiments delivered kinetic parameters that could be used to describe these cultures, within the constraints of constant external conditions, as was seen with the lack of linearity in the metabolic activity of *G. oxydans* at higher cell densities. New methods were developed to determine the ethanol and oxygen sensitivity of *G. oxydans* and these oxygen related parameters for *G. oxydans* were validated in a more detailed model, predicting the lack of linearity between metabolic activity and biomass concentrations in pure culture assays of *G. oxydans*. This was a strong validation, in terms of the kinetic equations used in the model set up for *G. oxydans* – we could predict where the metabolic activity of *G. oxydans* would no longer be proportional with biomass concentration on the basis of reactor and organism characteristics.

As far as ecological control analysis is concerned, we could calculate the control coefficients directly from the experimental data using the classical definitions of control analysis since our ecosystem reached steady states. Furthermore, these control coefficients could be calculated by the models, with their parameter sets from the mixed populations, from elasticity coefficients using the fundamentals of control analysis (*1-3*). The sets of experimental control coefficients and model control coefficients compared well and showed that yeast had all the control over the acetate flux while the control over the ethanol concentration was shared between the two organisms which is congruent with the theory of MCA. Furthermore, the high sensitivity of the steady-state ethanol concentration for the ratio between *S. cerevisiae* and *G. oxydans* could elegantly be described via the expression of the control coefficients in terms of the elasticities and could ultimately be related to the affinity of *G. oxydans* for ethanol. We feel that this good correlation between the model values and those experimentally determined are a validation of the model's ability to calculate the control structure of the simple ecosystem and predict its metabolic behavior. We have shown a great influence of the ratio of *S. cerevisiae/G. oxydans* on the steady-state ethanol concentrations reached in mixed population experiments. This was especially pertinent at higher ratios where steady state ethanol concentrations would be very unpredictable or no steady states would be reached. This was confirmed in all the model calculations, at high *S. cerevisiae/G. oxydans* ratios theconcentration control coefficient of the ratio increased sharply. This indicated that at those ratios, small changes in either organism's biomass would lead to large effects on the ethanol concentration as we have observed in our experimental results.

We have therefore, accomplished our aim through the description of a simple experimental ecosystem analogous to that of an enzymic pathway. The framework of ECA was applied to such an ecosystem using methods similar to MCA for biochemical systems. The strength of our approach

lies in designing the experiments with a control analysis approach in mind, but this does not exclude its application to systems where such design is impossible or to naturally occurring ecosystems. We have shown that even for a simple processing chain this experimental approach is non-trivial and specifically from an experimental standpoint very challenging, but ultimately rewarding due to the extra information thus obtained.

Finally, we illustrated at the hands of some recent research examples that our approach to ECA could add value to such ecological studies in the determination of major role players in ecosystems and calculate the magnitude of their impacts on sensitive ecosystems (*149, 150, 152*)

References

1. Giersch, C. (1995) Flux control in ecosystems, *Trends in Ecology & Evolution 10*, 245.
2. Schulze, E.-D. (1995) Reply from E-D. Schulze, *Trends in Ecology & Evolution 10*, 245-246.
3. Jorgensen, S. E. (1988) *Fundamentals of Ecological Modelling*, Vol. 9, 2nd ed., Elsevier, Amsterdam, New York (for USA and Canada).
4. Westerhoff, H. V., Getz, W. M., Bruggeman, F., Hofmeyr, J.-H. S., Rohwer, J. M., and Snoep, J. L. (2002) ECA: Control in Ecosystems, *Molecular Biology Reports 29*, 113-117.
5. Getz, W. M., Westerhoff, H. V., Hofmeyr, J.-H. S., and Snoep, J. L. (2003) Control analysis of trophic chains, *Ecological Modelling 168*, 153-171.
6. Roling, W. F. M., van Breukelen, B. M., Bruggeman, F. J., and Westerhoff, H. V. (2007) Ecological control analysis: being(s) in control of mass flux and metabolite concentrations in anaerobic degradation processes, *Environmental Microbiology 9*, 500-511.
7. Hofmeyr, J.-H. S., and Westerhoff, H. V. (2001) Building the Cellular Puzzle: Control in Multi-level Reaction Networks, *Journal of Theoretical Biology 208*, 261-285.
8. ter Kuile, B. H., and Westerhoff, H. V. (2001) Transcriptome meets metabolome: hierarchical and metabolic regulation of the glycolytic pathway, *FEBS Letters 500*, 169-171.
9. Schlegel, H. G., and Schmidt, K. (1988) *General Microbiology*, 6th ed., Cambridge University Press, Cambridge.
10. Prieto, C., Jara, C., Mas, A., and Romero, J. (2007) Application of molecular methods for analysing the distribution and diversity of acetic acid bacteria in Chilean vineyards, *International Journal of Food Microbiology 115*, 348-355.
11. Ribereau-Gayon, P., Dubourdieu, D., Doneche, B., and Lonvaud, A. (2000) Chapter 7: Acetic Acid Bacteria, in *Handbook of Enology*, John Wiley & Sons Ltd.
12. Joyeux, A., Lafon-Lafourcade, S., and Ribereau-Gayon, P. (1984) Evolution of Acetic Acid bacteria During Fermentation and Storage of Wine, *Applied and Environmental Microbiology 48*, 153-156.
13. Drysdale, G. S., and Fleet, G. H. (1988) Acetic Acid Bacteria in Winemaking: A Review, *American Journal of Enology and Viticulture 39*, 143-154.
14. Cancalon, P. F., and Parish, M. E. (1995) Changes in the chemical composition of orange juice during growth of Saccharomyces cerevisiae and Gluconobacter oxydans, *Food Microbiology 12*, 117-124.
15. Batty, A. S., and Schaffner, D. W. (2001) Modelling bacterial spoilage in cold-filled ready to drink beverages by Acinetobacter calcoaceticus and Gluconobacter oxydans, *Journal of Applied Microbiology 91*, 237-247.
16. Brand, M. D. (1998) Top-down elasticity analysis and its application to energy metabolism in isolated mitochondria and intact cells., *Mol. Cell Biochem. 184*, 13-20.
17. Brand, M. D. (1996) Top Down Metabolic Control Analysis, *Journal of Theoretical Biology 182*, 351-360.
18. Hofmeyr, J. H. S., and Cornish-Bowden, A. (2000) Regulating the cellular economy of supply and demand, *FEBS Letters 476*, 47-51.
19. Gupta, A., Singh, V. K., Qazi, G. N., and Kumar, A. (2001) *Gluconobacter oxydans*: Its Biotechnological Applications., *J. Mol. Microbiol. Biotechnol. 3*, 445-456.
20. Asai, T. (1968) *Acetic Acid bacteria: Classification and Biochemical Activities*, 1st ed., University of Tokyo Press, Tokyo.
21. Swings, J. (1992) Chapter 111: The Genera *Acetobacter* and *Gluconobacter*, in *The Procaryotes* (Balows, A., Trupper, H. G., Dworkin, M., Harder, W., and Schleifer, K. H., Eds.), pp 2268-2286, Springer Verlag, New York.
22. Prust, C., Hoffmeister, M., Liesegang, H., Wiezer, A., Fricke, W. F., Ehrenreich, A., Gottschalk, G., and Deppenmeier, U. (2005) Complete genome sequence of the acetic acid bacterium Gluconobacter oxydans, *Nature Biotechnology 23*, 195-200.

23. Harvey, B. M. L. (2005) Energy well spent on a prokaryotic genome, *Nature Biotechnology 23*, 186-187.
24. Akiko Fujiwara, Tatsuo Hoshino, and Masako Shinjoh. (1995) Co-enzyme-independent L-sorbosone dehydrogenase of Gluconobacter oxydans: Isolation, characterization, and cloning and autologus expression of the gene in *Biotechnology Advances*, pp 266-124.
25. Akiko Fujiwara, Tatsuo Hoshino, and Masako Shinjoh. (1995) Co-enzyme-independent L-sorbosone dehydrogenase of Gluconobacter oxydans: Isolation, characterization, and cloning and autologus expression of in *Biotechnology Advances*, pp 283-124.
26. Akira, A., and Kanagawa, H. T. (1996) Alcohol/aldehyde dehydrogenase from gluconobacter oxydans DSM 4025 FERM BP-3812 in *Biotechnology Advances*, pp 507-508.
27. Claret , C., Salmon, J. M., Romieu, C., and Bories, A. (1994) Physiology of Gluconobacter oxydans during dihydroxyacetone production from glycerol, *Appl Microbiol Biotechnol. 41*, 359-365.
28. Macauly, S., McNeil, B., and Harvey, L. M. (2001) The Genus *Gluconobacter* and Its Applications in Biotechnology, *Critical reviews in Biotechnology 21*, 1-25.
29. Sievers, M., and Swings, J. (2005) Family II. Acetobacteraceae, in *Bergey's Manual of Systematic Bacteriology* (Brenner, D. J., Krieg, N. R., and Staley, J. T., Eds.) Second Edition ed., pp 41-95, Springer.
30. Adachi, O., Moonmangmee, D., Shinagawa, E., Toyama, H., Yamada, M., and Matsushita, K. (2003) New quinoproteins in oxidative fermentation, *Biochimica et Biophysica Acta (BBA) - Proteins & Proteomics - 3rd International Symposium on Vitamin B6, PQQ, Carbonyl Catalysis and Quinoproteins 1647*, 10-17.
31. Matsushita, K., Yakushi, T., Takaki, Y., Toyama, H., and Adachi, O. (1995) Generation mechanism and purification of an inactive form convertible in vivo to the active form of quinoprotein alcohol dehydrogenase in Gluconobacter suboxydans, *J Bacteriol 177*, 6552-6559.
32. Deppenmeier, U., Hoffmeister, M., and Prust, C. (2002) Biochemistry and biotechnological applications of Gluconobacter strains, *Applied Microbiology and Biotechnology 60*, 233-242.
33. Matsushita, K., Yakushi, T., Toyama, H., Shinagawa, E., and Adachi, O. (1996) Function of multiple heme c moieties in intramolecular electron transport and ubiquinone reduction in the quinohemoprotein alcohol dehydrogenase-cytochrome c complex of Gluconobacter suboxydans, *J Biol Chem 271*, 4850-4857.
34. Armstrong, F. B. (1989) Anaerobic Synthesis of ATP (Glycolysis) and Pentose Phosphate pathway, in *Biochemistry* 3rd edn ed., pp 257 - 285, Oxford University Press, New York.
35. Merfort, M., Herrmann, U., Bringer-Meyer, S., and Sahm, H. (2006) High-yield 5-keto-D-gluconic acid formation is mediated by soluble and membrane-bound gluconate-5-dehydrogenases of Gluconobacter oxydans, *Appl Microbiol Biotechnol. (Aplied Microbial and Cell Physiology) 73*, 443-451.
36. Basseguy, R., Delecouls-Servat, K., and Bergel, A. (2004) Glucose oxidase catalysed oxidation of glucose in a dialysis membrane electrochemical reactor (D-MER), *Bioprocess Biosyst Eng 26*, 165-168.
37. Buse, R., Onken, U., Qazi, G. N., Sharma, N., Parshad, R., and Verma, V. (1992) Influence of dilution rate and dissolved oxygen concentration on continuous keto acid production by Gluconobacter oxydans subsp. melanogenum, *Enzyme and Microbial Technology 14*, 1001-1006.
38. Silberbach, M., Maier, B., Zimmermann, M., and Buchs, J. (2003) Glucose oxidation by Gluconobacter oxydans: characterization in shaking-flasks, scale-up and optimization of the pH profile, *Appl Microbiol Biotechnol. 62*, 92-98.
39. Matsushita, K., Yakushi, T., Toyama, H., Adachi, O., Miyoshi, H., Tagami, E., and Sakamoto, K. (1999) The quinohemoprotein alcohol dehydrogenase of Gluconobacter

suboxydans has ubiquinol oxidation activity at a site different from the ubiquinone reduction site, *Biochimica et Biophysica Acta (BBA) - Bioenergetics 1409*, 154-164.
40. Raska, J., Skopal, F., Komers, K., and Machek, J. (2007) Kinetics of glycerol biotransformation to dihidroxyacetone by immobilized Gluconobacter oxydans and effect of reaction conditions., *Collection of Czechoslovak Chemical Communications. 72*, 1269-1283.
41. Ohrem, L. H., and Vöss, H. (1996) Process model of the oxidation of glycerol with Gluconobacter oxydans, *Process Biochemistry 31*, 295-301.
42. Navratil, M., Tkac, J., Svitel, J., Danielsson, B., and Sturdik, E. (2001) Monitoring of the bioconversion of glycerol to dihydroxyacetone with immobilized Gluconobacter oxydans cell using thermometric flow injection analysis, *Process Biochemistry 36*, 1045-1052.
43. Hekmat, D., Bauer, R., and Fricke, J. (2003) Optimization of the microbial synthesis of dihydroxyacetone from glycerol with Gluconobacter oxydans, *Bioprocess Biosyst Eng 26*, 109-116.
44. Drysdale, G. S., and Fleet, G. H. (1989) The effect of acetic acid bacteria upon the growth and metabolism of yeasts during the fermentation of grape juice., *Journal of Applied Bacteriology 67*, 471 - 481.
45. Elfari, M., Ha, S.-W., Bremus, C., Merfort, M., Khodaverdi, V., Herrmann, U., Sahm, H., and Görisch, H. (2005) A Gluconobacter oxydans mutant converting glucose almost quantitatively to 5-keto-D-gluconic acid, *Appl Microbiol Biotechnol. 66*, 668-674.
46. Gao, K., and Wei, D. (2006) Asymmetric oxidation by Gluconobacter oxydans, *Appl Microbiol Biotechnol. 70*, 135-139.
47. Moat, A. G. (1979) *Microbial Physiology*, First edn ed., John Wiley & Sons, New York.
48. Schaaff, I., Heinisch, J., and Zimmerman, F. K. (1989) Overproduction of Glycolytic Enzymes in Yeast, *Yeast 5*, 285 - 290.
49. Hauf, J., Zimmermann, F. K., and Müller, S. (2000) Simultaneous genomic overexpression of seven glycolytic enzymes in the yeast Saccharomyces cerevisiae, *Enzyme and Microbial Technology 26*, 688-698.
50. Reijenga, K. A., Snoep, J. L., Diderich, J. A., van Verseveld, H. W., Westerhoff, H. V., and Teusink, B. (2001) Control of Glycolytic Dynamics by Hexose Transport in Saccharomyces cerevisiae, *Biophysical Journal 80*, 626-634.
51. Snoep, J. L., Mrwebi, M., Schuurmans, J. M., Rohwer, J. M., and Teixeira de Mattos, M. J. (2009) Control of specific growth rate in Saccharomyces cerevisiae, *Microbiology 155*, 1699-1707.
52. Cascante, M., Curto, R., and Sorribas, A. (1995) Comparative characterization of the fermentation pathway of Saccharomyces cerevisiae using biochemical systems theory and metabolic control analysis: Steady-state analysis, *Mathematical Biosciences 130*, 51-69.
53. Curto, R., Sorribas, A., and Cascante, M. (1995) Comparative characterization of the fermentation pathway of Saccharomyces cerevisiae using biochemical systems theory and metabolic control analysis: Model definition and nomenclature, *Mathematical Biosciences 130*, 25-50.
54. Sorribas, A., Curto, R., and Cascante, M. (1995) Comparative characterization of the fermentation pathway of Saccharomyces cerevisiae using biochemical systems theory and metabolic control analysis: Model validation and dynamic behavior, *Mathematical Biosciences 130*, 71-84.
55. Brand, M. D., and Curtis, R. K. (2002) Simplifying metabolic complexity., *Biochem Soc.Trans. 30*, 25-30.
56. Schuster, S., Kholodenko, B. N., and Westerhoff, H. V. (2000) Cellular information transfer regarded from a stoichiometry and control analysis perspective, *Biosystems 55*, 73-81.
57. Conradie, R., Westerhoff, H. V., Rohwer, J. M., Hofmeyr, J.-H. S., and Snoep, J. L. (2006) Summation theorems for flux and concentration control coefficients of dynamic systems, *IEE Proceedings - Systems Biology 153*, 314 - 317.

58. Rizzi, M., Baltes, M., Theobald, U., and Reuss, M. (1997) In Vivo Analysis of Metabolic Dynamics in Saccharomyces cerevisiae: II. Mathematical Model, *Biotechnol Bioeng. 55*, 592-608.
59. Rizzi, M., Theobald, U., Querfurth, E., Rohrhirsch, T., Bakes, M., and Reuss, M. (1996) In Vivo Investigations of Glucose Transport in Saccharomyces cerevisiae, *Biotechnol Bioeng. 49*, 316-327.
60. Theobald, U., Mailinger, W., Baltes, M., Rizzi, M., and Reuss, M. (1997) In Vivo Analysis of Metabolic Dynamics in Saccharomyces cerevisiae: I. Experimental Observations, *Biotechnol Bioeng. 55*, 305-312.
61. Teusink, B., Passarge, J., Reijenga, C. A., Esgalhado, E., van der Weijden, C. C., Schepper, M., Walsh, M. C., Bakker, B. M., van Dam, K., Westerhoff, H. V., and Snoep, J. L. (2000) Can yeast glycolysis be understood in terms of in vitro kinetics of the constituent enzymes? Testing biochemistry, *Eur. J. Biochem. 267*, 5313-5329.
62. Kurz, T., Mieleitner, J., Becker, T., and Delgado, A. (2002) A Model Based Simulation of Brewing Yeast Propagation, *Journal of the Institute of Brewing 108*, 248-255.
63. Verma, M., Bhat, P. J., Bhartiya, S., and Venkatesh, K. V. (2004) A steady-state modeling approach to validate an in vivo mechanism of the GAL regulatory network in Saccharomyces cerevisiae, *Eur J Biochem 271*, 4064-4074.
64. Hanegraaf, P. P. F., Stouthamer, A. H., and Kooijman, S. A. L. M. (2000) A mathematical model for yeast respiro-fermentative physiology, *Yeast 16*, 423 - 437.
65. Giuseppin, M. L. F., and van Riel, N. A. W. (2000) Metabolic Modeling of Saccharomyces cerevisiae Using the Optimal Control of Homeostasis: A Cybernetic Model Definition, *Metabolic Engineering 2*, 14-33.
66. van Riel, N. A. W. (2000) A cybernetic modelling approach for cell biology: Case study of the Central Nitrogen Metabolism in Saccharomyces cerevisiae, in *Moleculaire Celbiologie*, p 208, Universiteit Utrecht, Utrecht.
67. Mayrand, D., and Grenier, D. (1998) Bacterial interactions in periodontal diseases, *Bulletin de l'Institut Pasteur 96*, 125-133.
68. Odum, E. P. (1971) *Basic Ecology*, 3rd ed., Saunders College Publishing, New York.
69. Bakker, B. M., Westerhoff, H. V., Opperdoes, F. R., and Michels, P. A. M. (2000) Metabolic control analysis of glycolysis in trypanosomes as an approach to improve selectivity and effectiveness of drugs, *Molecular and Biochemical Parasitology 106*, 1-10.
70. Forst, C. V. (2006) Host-pathogen systems biology, *Drug Discovery Today 11*, 220-227.
71. Fraunholz, M. J. (2005) Systems biology in malaria research, *Trends in Parasitology 21*, 393-395.
72. Braun, J. (2002) Unsettling facts of life: Bacterial commensalism, epithelial adherence, and inflammatory bowel disease, *Gastroenterology 122*, 228-230.
73. Marazioti, C., Kornaros, M., and Lyberatos, G. (2003) Kinetic modeling of a mixed culture of Pseudomonas Denitrificans and Bacillus subtilis under aerobic and anoxic operating conditions, *Water Research 37*, 1239-1251.
74. Pommier, S., Strehaiano, P., and Delia, M. L. (2005) Modelling the growth dynamics of interacting mixed cultures: a case of amensalism, *International Journal of Food Microbiology (The Fourth International Conference on Predictive Modelling in Foods) 100*, 131-139.
75. Aziza, M., and Amrane, A. (2006) Commensalism during submerged mixed culture of Geotrichum candidum and Penicillium camembertii on glutamate and lactate, *Process Biochemistry 41*, 2452-2457.
76. Cordes, E. E., Arthur, M. A., Shea, K., Arvidson, R. S., and Fisher, C. R. (2005) Modeling the mutualistic interactions between tubeworms and microbial consortia, *PLoS Biol 3*, e77.
77. Kikuchi, Y., and Graf, J. (2007) Spatial and temporal population dynamics of a naturally occurring two-species microbial community inside the digestive tract of the medicinal leech., *Appl Environ Microbiol 73*, 1984 - 1991.

78. Manjarrez, E. S., Albasi, C., and Riba, J. P. (2000) A two-reservoir, hollow-fiber bioreactor for the study of mixed-population dynamics: design aspects and validation of the approach., *Biotechnol Bioeng. 69*, 401-408.
79. Heard, S. B. (1995) Short-term dynamics of processing chain systems, *Ecological Modelling 80*, 57-68.
80. Pirt, S. J. (1975) *Principles of Microbe and Cell Cultivation*, First ed., Blackwell Scientific Publications, Oxford, London, Edinburgh, Melbourne.
81. McMahon, K. D., Martin, H. G., and Hugenholtz, P. (2007) Integrating ecology into biotechnology, *Current Opinion in Biotechnology (Energy biotechnology / Environmental biotechnology) 18*, 287-292.
82. May, R. M., (Ed.) (1981) *Theoretical Ecology: Principles and Applications*, Second edition ed., Blackwell Scientific Publications, Oxford, London, Edinburgh, Boston, Melbourne.
83. Giersch, C. (1991) Sensitivity analysis of ecosystems: an analytical treatment, *Ecological Modelling 53*, 131-146.
84. Wennekers, T., and Giersch, C. (1991) Sensitivity analysis of a simple model food chain, *Ecological Modelling 54*, 265-276.
85. Allison, S. M., Small, J. R., Kacser, H., and Prosser, J. I. (1993) Control Analysis of microbial interactions in continuous culture: a simulation study, *Journal of General Microbiology 139*, 2309 - 2317.
86. Kacser, H., and Burns, J. A. (1995) The Control of Flux: 21 years on, Reprint of Symp. Soc. Exp. Biol. 27: 65- 104 (1973) *Biochem. Soc. Trans. 23*, 341 - 366.
87. Heinrich, R., and Rapoport, T. A. (1974) A Linear Steady-State Treatment of Enzymatic Chains: General Properties, Control and Effector Strength, *European Journal of Biochemistry 42*, 89-95.
88. Heinrich, R., and Rapoport, T. A. (1974) A Linear Steady-State Treatment of Enzymatic Chains:Critique of the Crossover Theorem and a General Procedure to Identify Interaction Sites with an Effector, *European Journal of Biochemistry 42*, 97-105.
89. Bayram, M., and Yildirim, N. (2005) Metabolic control analysis of trio enzymes system, *Applied Mathematics and Computation 170*, 948-957.
90. Brown, G. C., Westerhoff, H. V., and Kholodenko, B. N. (1996) Molecular Control Analysis: Control within Proteins and Molecular Processes, *Journal of Theoretical Biology 182*, 389-396.
91. Cascante, M., Ortega, F., and Marti, E. (2000) New insights into our understanding of the regulation and organization of cell factories, *Trends in Biotechnology 18*, 181-182.
92. Cornish-Bowden, A., Cardenas, M. L., Letelier, J.-C., Soto-Andrade, J., and Abarzua, F. G. (2004) Understanding the parts in terms of the whole, *Biology of the Cell 96*, 713-717.
93. Cornish-Bowden, A., and Hofmeyr, J.-H. S. (2005) Enzymes in context, *The Biochemist*, 11-14.
94. Cornish-Bowden, A., Hofmeyr, J.-H. S., and Cardenas, M. L. (1995) Strategies for Manipulating Metabolic Fluxes in Biotechnology, *Bioorganic Chemistry 23*, 439-449.
95. de la Fuente, A., Snoep, J. L., Westerhoff, H. V., and Mendes, P. (2002) Metabolic control in integrated biochemical systems., *Eur J Biochem 269*, 4399-4408.
96. Delgado, J., and Liao, J. C. (1992) Determination of Flux Control Coefficients from transient metabolite concentrations, *Biochem. J 282*, 919-927.
97. Fell, D. A. (1992) Metabolic Control Analysis:a survey of its theoretical and experimental development, *Biochem J 286*, 313-330.
98. Fell, D. A. (1998) Increasing the Flux in Metabolic Pathways: A Metabolic Control Analysis Perspective, *Biotechnol Bioeng. 58*, 121-124.
99. Fell, D. A. (2005) Enzymes, metabolites and Fluxes, *Journal of Experimental Botany (Making Sense of the Metabolome Special Issue) 56*, 267-272.
100. Hatzimanikatis, V., and Bailey, J. E. (1996) MCA Has More to Say, *Journal of Theoretical Biology 182*, 233-242.

101. Hofmeyr, J. H., and Cornish-Bowden, A. (1991) Quantitative assessment of regulation in metabolic systems., *Eur J Biochem 200*, 223-236.
102. Hofmeyr, J.-H. S. (2001) Metabolic control analysis in a nutshell, in *Proceedings of the 2nd International Conference on Systems Biology* (Yi, T.-M., Hucka, M., Morohashi, M., and Kitano, H., Eds.), pp 291–300, Omnipress, Madison, WI.
103. Kholodenko, B. N., Sauro, H. M., and Westerhoff, H. V. (1994) Control by enzymes, coenzymes and conserved moieties, *Eur. J. Biochem. 225*, 179-186.
104. Moreno-Sanchez, R., Bravo, C., and Westerhoff, H. V. (1999) Determining and understanding the control of flux, *Eur. J. Biochem. 264*, 427-433.
105. Nielsen, J. (1997) Metabolic control analysis of biochemical pathways based on a thermokinetic description of reaction rates, *Biochem J 321*, 133-138.
106. Reder, C. (1988) Metabolic control theory: a structural approach., *J. Theor. Biol 135*, 175-201.
107. Stephanopoulos, G. (1999) Metabolic Fluxes and Metabolic Engineering, *Metabolic Engineering 1*, 1-11.
108. Stephanopoulos, G. N., Aristidou, A. A., and Nielsen, J. (1998) Metabolic Control Analysis Metabolic Engineering, pp 461-533, Academic Press, San Diego.
109. Wang, L., Birol, I., and Hatzimanikatis, V. (2004) Metabolic control analysis under uncertainty: framework development and case studies., *Biophys J. 87*, 3750-3763.
110. Wildermuth, M. (2000) Metabolic control analysis: biological applications and insights., *Genome Biol 1*.
111. Fell, D. A. (1997) *Understanding the Control of Metabolism*, First edn Reprint ed., Portland Press Ltd, London.
112. Delgado, J., and Liao, J. C. (1992) Metabolic control analysis using transient metabolite concentrations. Determination of metabolite concentration control coefficients., *Biochem J 285*, 965-972.
113. Ehlde, M., and Zacchi, G. (1997) A general formalism for Metabolic Control Analysis, *Chemical Engineering Science - Mathematical modelling of chemical and biochemical processes 52*, 2599-2606.
114. Torres, N. V. (1996) Metabolic Control Analysis of Inhibitory feedback Interaction: Application to Biotechnological Processes, *Journal of Theoretical Biology 182*, 405-410.
115. Giersch, C. (1997) Co-response Coefficients, Monovalent Units, and Combinatorial Rules: Unification of Concepts in Metabolic Control Analysis, *Journal of Theoretical Biology 189*, 1-9.
116. Thomas, S., and Fell, D. A. (1996) Design of Metabolic Control for Large Flux Changes, *Journal of Theoretical Biology 182*, 285-298.
117. Kholodenko, B. N., and Westerhoff, H. V. (1995) How to reveal various aspects of regulation in group-transfer pathways, *Biochimica et Biophysica Acta (BBA) - Bioenergetics 1229*, 275-289.
118. Kholodenko, B. N., and Westerhoff, H. V. (1995) Control theory of group transfer pathways, *Biochimica et Biophysica Acta (BBA) - Bioenergetics 1229*, 256-274.
119. Kholodenko, B. N., Molenaar, D., Schuster, S., Heinrich, R., and Westerhoff, H. V. (1995) Defining control coefficients in non-ideal metabolic pathways, *Biophysical Chemistry 56*, 215-226.
120. Rohwer, J. M., Schuster, S., and Westerhoff, H. V. (1996) How to Recognize Monofunctional Units in a Metabolic System, *Journal of Theoretical Biology 179*, 213-228.
121. Kholodenko, B. N., Schuster, S., Garcia, J., Westerhoff, H. V., and Cascante, M. (1998) Control analysis of metabolic systems involving quasi-equilibrium reactions, *Biochimica et Biophysica Acta (BBA) - General Subjects 1379*, 337-352.
122. Peletier, M. A., Westerhoff, H. V., and Kholodenko, B. N. (2003) Control of spatially heterogeneous and time-varying cellular reaction networks: a new summation law, *Journal of Theoretical Biology 225*, 477-487.

123. de Atauri, P., Curto, R., Puigjaner, J., Cornish-Bowden, A., and Cascante, M. (1999) Advantages and disadvantages of aggregating fluxes into synthetic and degradative fluxes when modelling metabolic pathways, *European Journal of Biochemistry 265*, 671-679.
124. Kholodenko, B. N., Schuster, S., Rohwer, J. M., Cascante, M., and Westerhoff, H. V. (1995) Composite control of cell function: metabolic pathways behaving as single control units, *FEBS Letters 368*, 1-4.
125. Cascante, M., Canela, E. I., and Franco, R. (1990) Control analysis of systems having two steps catalyzed by the same protein molecule in unbranched chains, *Eur. J. Biochem. 192*, 369-371.
126. Hofmeyr, J.-H. S., and Cornish-Bowden, A. (1996) Co-response Analysis: A New Experimental Strategy for Metabolic Control Analysis, *J. Theor. Biol 182*, 371-380.
127. Bayram, M., and Celik, E. (2003) Application of computer algebra-techniques to metabolic control analysis, *Computational Biology and Chemistry 27*, 141-146.
128. Franco-Lara, E., and Weuster-Botz, D. (2007) Application of fuzzy-logic models for metabolic control analysis, *Journal of Theoretical Biology 245*, 391-399.
129. Heijnen, J. J., van Gulik, W. M., Shimizu, H., and Stephanopoulos, G. (2004) Metabolic flux control analysis of branch points: an improved approach to obtain flux control coefficients from large perturbation data, *Metabolic Engineering 6*, 391-400.
130. Nikolaev, E. V., Atlas, J. C., and Shuler, M. L. (2007) Sensitivity and control analysis of periodically forced reaction networks using the Green's function method, *Journal of Theoretical Biology 247*, 442-461.
131. Kholodenko, B. N., Rohwer, J. M., Cascante, M., and Westerhoff, H. V. (1998) Subtleties in control by metabolic channelling and enzyme organization., *Mol. Cell Biochem. 184*, 311-320.
132. Ao, P. (2005) Metabolic network modelling: Including stochastic effects, *Computers & Chemical Engineering - Selected Papers Presented at the Symposium on Modeling of Complex Processes 29*, 2297-2303.
133. Hofmeyr, J. H. S. (1989) Control-pattern analysis of metabolic pathways: Flux and concentration control in linear pathways, *Eur J Biochem 186*, 343-354.
134. Acerenza, L., and Ortega, F. (2006) Metabolic control analysis for large changes: extension to variable elasticity coefficients, *IEE Proc.-Syst. Biol., 153*, 323-326.
135. Visser, D., and Heijnen, J. J. (2003) Dynamic simulation and metabolic re-design of a branched pathway using linlog kinetics, *Metabolic Engineering 5*, 164-176.
136. Elsner, L., and Giersch, C. (1998) Metabolic Control Analysis: Separable Matrices and Interdependence of Control Coefficients, *Journal of Theoretical Biology 193*, 649-661.
137. Ainscow, E. K., and Brand, M. D. (1998) Errors Associated with Metabolic Control Analysis. Application of Monte-Carlo Simulation of Experimental Data, *Journal of Theoretical Biology 194*, 223-233.
138. Schuster, S. (1996) Control Analysis in Terms of Generalized Variables Characterizing Metabolic Systems, *J. Theor. Biol 182*, 259-268.
139. Visser, D., and Heijnen, J. J. (2002) The Mathematics of Metabolic Control Analysis Revisited, *Metabolic Engineering 4*, 114-123.
140. van Dam, K., van der Vlag, J., Kholodenko, B. N., and Westerhoff, H. V. (1993) The sum of the control coefficients of all enzymes on the flux through a group-transfer pathway can be as high as two, *Eur J Biochem 212*, 791-799.
141. Giersch, C. (1995) Determining elasticities from multiple measurements of flux rates and metabolite concentrations, *Eur J Biochem 227*, 194-201.
142. Westerhoff, H. V., and Kell, D. B. (1987) Matrix method for the determining the steps most rate-limiting to metabolic fluxes in biotechnological processes, *Biotechnol Bioeng. 30*, 101-107.
143. Schulze, E.-D. (1995) Flux control at the ecosystem level, *Trends in Ecology & Evolution 10*, 40-43.

144. Thomas, S., Moniz-Barreto, J. P., Fell, D. A., Woods, J. H., and Poolman, M. G. (1995) Flux control in ecosystems, *Trends in Ecology & Evolution 10*, 245.
145. Tollner, E. W., Kazanci, C., Schramski, J. R., and Patten, B. C. (2009) Control system approaches to ecological systems analysis: Invariants and frequency response, *Ecological Modelling 220*, 3233-3240.
146. Villa, R., Romano, A., Gandolfi, R., Sinisterra Gago, J. V., and Molinari, F. (2002) Chemoselective oxidation of primary alcohols to aldehydes with Gluconobacter oxydans, *Tetrahedron Letters 43*, 6059-6061.
147. Albin, A., Bader, J., Mast-Gerlach, E., and Stahl, U. (2007) Improving fermentation and biomass formation of Gluconobacter oxydans, *Journal of Biotechnology , ECB13, 13th European Congress on Biotechnology 131*, S160-S161.
148. Adlercreutz , P., Hoist, O., and Mattiasson, B. (1985) Characterization of Gluconobacter oxydans immobilized in calcium alginate, *Appl Microbiol Biotechnol. 22*, 1-7.
149. Neish, A. S. (2009) Microbes in Gastrointestinal Health and Disease, *Gastroenterology 136*, 65-80.
150. Dibdin, G., Wimpenny, J., and Ron, J. D. (1999) [23] Steady-state biofilm: Practical and theoretical models, in *Methods in Enzymology*, pp 296-322, Academic Press.
151. Whipple, S. J. (1999) Analysis of ecosystem structure and function: extended path and flow analysis of a steady-state oyster reef model, *Ecological Modelling 114*, 251-274.
152. Manickchand-Heileman, S., Mendoza-Hill, J., Kong, A. L., and Arocha, F. (2004) A trophic model for exploring possible ecosystem impacts of fishing in the Gulf of Paria, between Venezuela and Trinidad, *Ecological Modelling 172*, 307-322.
153. Michaelian, K. (2005) Thermodynamic stability of ecosystems, *Journal of Theoretical Biology 237*, 323-335.
154. Schreiber, S. J., and Gutierrez, A. P. (1998) A supply/demand perspective of species invasions and coexistence: applications to biological control, *Ecological Modelling 106*, 27-45.
155. Postma, E., Verduyn, C., Scheffers, W. A., and Van Dijken, J. P. (1989) Enzymic analysis of the crabtree effect in glucose-limited chemostat cultures of Saccharomyces cerevisiae, *Appl Environ Microbiol 55*, 468-477.
156. Cornish-Bowden, A. (2001) *Fundamentals of Enzyme kinetics*, Revised edition ed., Portland Press Ltd, London.
157. Hofmeyr, J.-H. S. (1986) Steady-state modelling of metabolic pathways: A guide for the prospective simulator, *CABIOS 2*, 5-11.
158. Jensen, P. R., Michelsen, O., and Westerhoff, H. V. (1995) Experimental determination of control by the H+-ATPase in Escherichia coli, *J Bioenergetics Biomembranes 27*, 543-554.
159. Jensen, P. R., Van Der Weijden, C. C., Bogø Jensen, L., Westerhoff, H. V., and Snoep, J. L. (1999) Extensive regulation compromises the extent to which DNA gyrase controls DNA supercoiling and growth rate of Escherichia coli, *European Journal of Biochemistry 266*, 865-877.
160. Snoep, J. L., Van Der Weijden, C. C., Andersen, H. W., Westerhoff, H. V., and Jensen, P. R. (2002) DNA supercoiling in Escherichia coli is under tight and subtle homeostatic control, involving gene-expression and metabolic regulation of both topoisomerase I and DNA gyrase, *European Journal of Biochemistry 269*, 1662-1669.
161. Snoep, J. L., Bruggeman, F., Olivier, B. G., and Westerhoff, H. V. (2006) Towards building the silicon cell: A modular approach, *Biosystems, 5th International Conference on Systems Biology - ICSB 2004 83*, 207-216.
162. Snoep, J. L. (2005) The Silicon Cell initiative: working towards a detailed kinetic description at the cellular level., *Curr Opin Biotechnol 16*, 336--343.
163. Snoep, J. L., and Westerhoff, H. V. (2004) The Silicon Cell Initiative, *Current Genomics 5*, 687-697.

164. Westerhoff, H. V. (2001) The Silicon Cell, Not Dead but Live!, *Metabolic Engineering 3*, 207-210.
165. Matsushita, K., Nagatani, Y., Shinagawa, E., Adachi, O., and Ameyama, M. (1991) Reconstitution of the ethanol oxidase respiratory chain in membranes of quinoprotein alcohol dehydrogenase-deficient Gluconobacter suboxydans subsp. alpha strains, *J Bacteriol 173*, 3440-3445.
166. Ehlde, M., and Zacchi, G. (1996) Influence of experimental errors on the determination of flux control coefficients from transient metabolite concentrations, *Biochem J 313*, 721-727.
167. Stenseth, N. C., Falck, W., Bjornstad, O. N., and Krebs, C. J. (1997) Population regulation in snowshoe hare and Canadian lynx: Asymmetric food web configurations between hare and lynx, *Proc Nat Acad Sci USA 94*, 5147 - 5152.